NATIONAL
SCIENCE
FOUNDATION

Journal

of the

National Science Foundation
of Sri Lanka

www.nsf.gov.lk

NATIONAL
SCIENCE
FOUNDATION

C O N T E N T S

Cover: Wave flume experiment to evaluate different beach nourishment materials
Wave flume apparatus (a), the stabilized shape after conducting experiment for offshore
sand (b); 100% crushed glass (c); and 25% crushed glass (d) samples
See J.Natn.Sci.Foundation Sri Lanka 2025 53(2): 125 - 138

EDITORIAL

Limitations in the use of AI in research disciplines

Research in any field is an investigation that follows a series of methodical disciplines. These include reviewing existing knowledge and identifying knowledge gaps, designing or structuring the research to address the selected gap, collecting data using appropriate methodologies and adhering to ethical standards where applicable, analyzing the data with suitable tools, and interpreting the results by evaluating relevant arguments and assumptions. This set of methodical disciplines constitutes the first phase of research.

The key outcome of this initial phase should be the generation of new knowledge. As the final step, this knowledge must be published in a standard and structured manner. Even if the initial steps are correctly followed and result in new insights, an investigation is not considered as standard research until it is reported or published in a clear, logical, and standardized way, ensuring that others can examine and verify the findings if necessary.

The standard peer review process is the initial and the most critical step in the standard publication procedure for research. In this step, it is thoroughly checked whether all the required disciplines have been correctly followed and whether the process has led to the generation of new knowledge. In research, the peer review process is critical and essential for two reasons. Firstly, expertise does not make someone immune to errors. Even experts are prone to mistakes due to factors such as miscalculations, misinterpretations, or lapses in attention. Secondly, recognizing a mistake made by someone else–regardless of one's own errors–is a complex human behavior influenced by various factors, including cognitive biases. These two reasons form the foundation of the peer review process.

Artificial Intelligence (AI) is a new and emerging tool that is increasingly used in scholarly work, including research. It is important to examine how extensively AI can be applied within various research disciplines. Although it is not advisable to rely on AI entirely, it can provide significant support in pursuing these primary areas of research, as well as in language checking. The peer review process can also be made significantly easier, as reviewers can use AI to assess the quality and relevance of the same set of research disciplines discussed above.

However, there are certain aspects of the peer review process that AI cannot handle. In addition to considerations of ethics and conflicts of interest, evaluating novelty and assessing significance are critical components of any peer review, which AI cannot adequately perform–because AI relies on pre-existing information. While some AI models can generate novel outputs by recombining, reasoning with, or optimizing existing data in useful ways, the validity of such outputs must still be assessed by humans. For example, in the evaluation process, novelty or originality is expected not only in scientific works but also in creative works, such as the lyrics of a new song. Only humans can truly judge whether the novelty of a given work aligns with scientific standards or creative expectations.

L.P. Jayatissa

RESEARCH ARTICLE

Molecular Genetics

Assessing the impact of salinity stress on Na+, K+, and Ca2+ contents of 125 rice genotypes

NGJ Pradeepika and AL Ranawake*
Department of Agricultural Biology, Faculty of Agriculture, University of Ruhuna, Mapalana, Kamburupitiya, Sri Lanka.

Abstract: The ionic balance of Na^+, K^+, and Ca^{2+} affects salinity tolerance in rice. This study examined the content of Na^+, K^+, and Ca^{2+} in seedling dry matter in 121 traditional rice accessions and four improved rice genatypes under salinity stress and control conditions. The experiment was conducted as a randomized complete block design with four replicates. Seedlings were raised for three days in *Yoshida* solution with an electrical conductivity (EC) of 6 dS/m and then exposed to a EC 12 dS/m salinity level for fourteen days. Salinity tolerance was assessed using a standard visual scoring system. Na^+, K^+, and Ca^{2+} contents were measured using a flame photometer. Salinity tolerance levels were inversely correlated with Na^+, Ca^{2+}, and Na:K ratio, and positively correlated with K^+. Inverse relationships were observed between K^+ and both Na^+ and Ca^{2+}, suggesting antagonism, while a positive correlation existed between Na^+ and Ca^{2+}. Analyzing shoot dry matter, Na^+, K^+, and Ca^{2+} contents in rice help to identify and select salinity-tolerant rice genotypes by prioritizing those with higher K^+ and lower Na^+ and Ca^{2+} levels. The order of Na^+, K^+, and Ca^{2+} in the dry matter of tolerant and moderately tolerant rice genotypes highlights that the ion balance is genotype dependent and not the sole determinant of salinity tolerance in rice. Further research is needed to determine the susceptibility of accessions to salinity stress, focusing on demonstrating decreased Na^+ and Ca^{2+} contents, and increased K^+ content across various stress scenarios and growth phases to understand their potential for salinity tolerance.

Keywords: Na^+, K^+, Ca^{2+} content, salinity tolerance, seedling stage, traditional rice accessions.

INTRODUCTION

Rice as the staple food for half of the world's population, ensures food security, livelihoods, and cultural heritage. It also offers potential solutions to global challenges such as hunger and climate change. Developing salinity tolerance in rice is essential for safeguarding global food security by enabling rice cultivation in saline-affected coastal areas and mitigating the impact of rising sea levels. Salinity stress has been shown to significantly reduce grain yield by 64.52%, primarily affecting seed set, panicle number, and grain quality, with a more pronounced impact in the reproductive stage (Zeng *et al.*, 2023).

It is estimated that one billion hectares of land worldwide are salt affected accounting for 5% of the global land area. Furthermore, the increase in sea level by 12-22 cm in the 20th century and continuing rise by 0.34 cm annually affects rice production in Thailand, Vietnam, China, and Korea (Walthall *et al.*, 2013; Hopmans *et al.*, 2021). Introducing salinity-tolerant genotypes to these affected lands is a sustainable solution to fulfill the demand for rice production. However, the number of genetic variations associated with enhancing salt tolerance in the primary rice crop is limited, and our understanding of the underlying molecular mechanisms

* Corresponding author (lankaranawake@hotmail.com; https://orcid.org/0000-0003-0517-9911)

remains incomplete (Chen *et al.,* 2021; Alfatih *et al.,* 2023).

Sri Lanka has conserved several thousands of traditional rice accessions that are evolutionarily diverse and possess various beneficial traits (Shyamalee and Ranawake, 2024a & b). Selecting for salinity tolerant accessions directly broadens the gene pool for salinity tolerance in rice. Further, research endeavors should prioritize not only exploration of the wide array of genetic resources at our disposal, but also on identifying genetic traits related to salinity tolerance that may have been inadvertently overlooked during the domestication process. This initiative aims to reintroduce these valuable salinity tolerance attributes, especially those found in traditional accessions, into cultivated rice varieties. This knowledge can also be applied to other crops and help scientists to develop strategies for enhancing the resilience of various agricultural species to environmental stresses (Chen *et al.,* 2021).

Exceeding the critical threshold for soil salinity (3.0 dS/m) has adverse effects on various panicle and grain related characteristics in rice (Mumtaz *et al.,* 2018). A soil electrical conductivity (EC) of 6.0 dS/m led to a 50% reduction in rice grain yield, with most rice lands in the region falling into the moderately saline (EC 4-8 dS/m) and highly saline (EC 8-16 dS/m) categories, posing a threat to crop health (Mondal *et al.,* 2001; Djaman *et al.,* 2020). The high concentrations of solutes damage internal membranes, causing failure in osmotic adjustment in the cytoplasm with Na^+ and Cl^- accumulation and storing reactive oxygen species (Kumar *et al.,* 2013). Failure in osmotic adjustment in plants reduces root growth, accelerates leaf drying, and decreases dry matter production, including yield (Fischer, 1996). Different plant parts tolerate osmotic potential differently (Farooq *et al.,* 2021). Furthermore, Na^+ concentration is different within the same plant (Rivelli *et al.,* 2002; de Lacerda *et al.,* 2003).

Salinity creates a series of complex interactions in plant metabolism, defense mechanism and nutrient requirements (Grattan & Grieve, 1999). Na^+ is considered a toxic element for most plants, including rice, when present in excess concentrations in the soil (Gepstein *et al.,* 2005). Additionally, elevated salinity caused by Na^+, reduces transpiration and photosynthesis by closing the stomata (Khan *et al.,* 2023). Stomatal closure increases the leaf temperature, which affects shoot elongation (Rajendran *et al.,* 2009). The toxic concentration of Na^+ is reached before the Cl^- toxicity concentration (Khan *et al*., 2023). Hence, examining Na^+ levels in plants under salinity stress is justifiable when salinity stress is induced using NaCl.

The defense against Na^+ damage in the cell is achieved by minimizing Na^+ entry into the root through the Na^+ transport pathway, maximizing efflux, minimizing xylem loading, accelerating phloem transportation, partitioning Na^+ into different parts of the plants, and ultimately expelling Na^+ out of the leaves (Tester & Davenport, 2003). Accumulation of compatible solutes including proteins is commonly reported in salt-tolerant plants (Tester & Davenport, 2003; *Gao et al*., 2023). Some rice varieties have developed mechanisms to tolerate high levels of accumulated Na^+. These mechanisms involve the selective uptake and compartmentalization of Na^+ in vacuoles thereby reducing its toxic effects in the cytoplasm (Porcel *et al.,* 2016).

A sufficient supply of K^+ can reduce the uptake and accumulation of Na^+ in plant tissues (Gregorio, 1997). Absorption of K^+ while excluding Na^+ to maintain a low Na: K ratio is a strategy for salinity tolerance (Koyama *et al.,* 2001). A high level of K^+ can help counteract the toxic effects of Na: K (Shahzad *et al.,* 2022). Adequate levels of K^+ in plants maintain the correct ion balance and osmotic potential, essential for maintaining cell turgor and overall plant health, especially under saline conditions. Therefore, K^+ content in salinity-sensitive rice genotypes is lower than in salt-tolerant varieties (Asch *et al.,* 2000).

Calcium ions (Ca^{2+}) increases the Ca: Na ratio, ameliorating salinity (Aslam *et al.,* 2003). Plant membrane bound Ca^{2+} is important for cell wall structure, ion transportation and ion exchange (Rengel, 1992; Marschner, 1995). Ca^{2+} competes with Na^+ for binding sites on cell membranes, reducing the influx of Na^+ into plant cells (Rengel, 1992). The opening and closing of stomata in rice plants, which affect water loss and gas exchange, are regulated by Ca^{2+} (Wang *et al.,* 2014). Supplementing Ca^{2+} to salt-stressed plants increases chlorophyll content, reduces H_2O_2 accumulation, and protects against oxidative damage, while also helping to maintain water balance and reduce membrane injury through enhanced antioxidant enzyme activity. Ca^{2+} supplementation is an effective remediation technique for saline affected rice fields (Tahjib-Ul-Arif *et al.,* 2018). Na^+ content and Na-Ca selectivity are useful criteria for evaluating salinity tolerance in rice (Zeng *et al.,* 2003).

Role of Na⁺, K⁺, and Ca²⁺ in salinity stress

Na$^+$, K$^+$, and Ca^{2+} are involved in complex physiological and biochemical processes under salinity stress (Luan *et al.,* 2009; Machado & Serralheiro, 2017). The exclusion of Na$^+$ and absorption of K$^+$ to maintain low Na$^+$ levels in the solute reduces Ca^{2+} availability and transport to growing parts of the plant (Grattan & Grieve, 1999). Conversely, low-K$^+$ or high-Na$^+$ levels induce Ca^{2+} activity that accelerates signaling pathways for salinity tolerance (Luan *et al*., 2009). Reduced Ca^{2+} absorption is essential for salinity tolerance (Läuchli, 1999; Zhu, 2002) and maintaining low cytoplasmic Ca^{2+} activity is also a strategy for salinity tolerance (Läuchli, 1999). Ca^{2+} induces K$^+$ uptake more effectively than Na$^+$ (Hasegawa *et al.,* 2000). Salinity-tolerant genotypes should be able to withstand high Na$^+$ content in the soil and uptake a higher amount of K$^+$ than Na$^+$ (Khan *et al.,* 2023). Different genotypes within a species may exhibit distinct regulatory mechanisms for maintaining Na$^+$, K$^+$, and Ca^{2+} ion balance when subjected to salinity-induced stress conditions. Therefore, a systematic assessment of germplasm to uncover these regulatory pathways is crucial in the context of breeding programs.

Parameters to assess salinity tolerance in rice

A series of studies used different parameters to evaluate salinity tolerance (Zeng *et al.,* 2002). Parameters such as shoot and root length, shoot and root fresh weight or dry weight (Lang *et al.,* 2000; Mahmood *et al.,*2009; Ranawake & Nakamura, 2012; Shyamalee & Ranawake, 2024b), physiological characteristics (Blumwald *et al.,* 2000; Chunthaburee *et al.,* 2015) reproductive stage traits (Counce & Wells, 1990), seedling survival rate (Zeng *et al.,* 2002; Lang *et al.,* 2000), and plant vigour (Yeo *et al.,* 1990) have been used to assess and compare salinity tolerance in rice.

The visible impact of salinity stress on plant growth and health is evaluated by using the visual scoring system (Gregorio *et al.,* 1997). Further, Na$^+$, K$^+$, and Ca^{2+} content have already been confirmed as criteria for salinity tolerance in rice (Gregorio & Senadhira,1993; Ahmad *et al.,* 2007; Khan & Panda, 2008; Luan *et al.,* 2009; Machado & Serralheiro, 2017). This study aims to uncover genotype-specific responses to salinity and the underlying mechanisms governing Na$^+$, K$^+$, and Ca^{2+} under NaCl-induced salinity stress. The objectives were to analyze Na$^+$, K$^+$, and Ca^{2+} accumulation in the seedling dry matter of rice genotypes under salinity stress and to determine their correlation with salinity tolerance levels.

The study included 121 traditional rice accessions with different levels of salinity-tolerance and four improved rice genotypes at the seedling stage (unpublished data). The protocol established by Gregorio *et al.* (1997) was used to assess the level of salinity tolerance in rice genotypes. Analyzing Na$^+$, K$^+$, and Ca^{2+} contents in various rice genotypes under salinity stress are a valuable approach for understanding genotype specific tolerance mechanisms, and guiding breeding efforts to develop more resilient and productive rice varieties for saline environments.

MATERIALS AND METHODS

One hundred and twenty one (121) traditional rice accessions and four improved rice genotypes were collected from the Plant Genetic Resources Center, Gannoruwa, Peradeniya, Sri Lanka (PGRC, 1999) (*Supplementary Table 1*). The study followed a randomized complete block design, with four replicates, with 10 seedlings in each. Rice seeds were germinated in distilled water for 3 ds and then transferred to *Yoshida* solution (Gregorio *et al*., 1997) with an electrical conductivity (EC) of 6 dS/m. The EC of the *Yoshida* solution was adjusted using a calibration curve constructed by dissolving known amounts of NaCl in distilled water. Germinated rice seeds were placed in slits made in styrofoam sheets, which were floated on the *Yoshida* solution in plastic cups. After initial 3-day period in *Yoshida* solution of EC 6 dS/m, the salinity level increased to 12 dS/m and the solution replaced in every 2 ds. The seedlings were then grown in this solution for 14 consecutive days. Preliminary studies were conducted to optimize the experimental conditions using several salinity-susceptible and tolerant rice genotypes.

Visual scoring of salinity tolerance

Plants were evaluated according to visual symptoms described in the following standard evaluation system for salinity tolerance (Gregorio *et al*.,1997):

Score 1: Normal growth, no leaf symptoms (Highly tolerant), Score 3: Nearly normal growth, but leaf tips or few leaves whitish and rolled (Tolerant), Score 5: Growth severely retarded, most leaves rolled, only a few are elongating (Moderately tolerant), Score 7: Complete cessation of growth, most leaves dry, some plants dying (Susceptible), Score 9: Almost all plants are dead or dying (Highly susceptible).

Evaluation of Na⁺, K⁺ and Ca²⁺ content

The seedlings collected after exposing to salinity stress were used to assess the Na^+, K^+ and Ca^{2+} content. The seedlings were quickly rinsed in distilled water to remove external materials and then dried in an oven at 65 °C for 5 ds. Hundred milligrams (100 mg) of dried leaf tissues were measured in three replicates for each rice accession. Leaf samples were digested according to the method described by O'Halloran *et al.*, (1997). The samples were tightly covered with lids, and all vials were packed tightly in a box to keep them on the shaker. The vials were thoroughly shaken on a shaker to suspend all plant materials in the dilute acid for 2 ds at room temperature while agitating occasionally. After 2 days, the samples were filtered to remove all solid materials. Standard solutions were prepared using KCl, NaCl, and $CaCl_2$ as references. A calibration curve was constructed by plotting the absorbance against the concentration of the certified reference solutions. The Na^+, K^+ and Ca^{2+} content in the samples were subsequently determined using this calibration curve, with three replicates, using a flame photometer (Sherwood, 360).

Data analysis

The content of Na^+, K^+, Ca^{2+}, and the Na^+:K^+ ratio of traditional rice accessions under salinity stress and control conditions were analyzed using ANOVA and mean separation was performed using Duncan's multiple range test. Correlation analysis was conducted using SPSS (SPSS, Inc, 2011). Rice accessions were ranked based on their Na^+, K^+, and Ca^{2+} content in the dry matter to compare their ion levels.

RESULTS AND DISCUSSION

Among the 125 rice genotypes visually scored, *Randhunipagal2866* was found to be salinity tolerant while *Suduheenati3397, Bathkiriel3550, Madathawalu3718, Matholuwa3214, Moddaikaruppan3388, Polayal3639, Lumbini3613, Madaelgalle3508, Mudaliwi3672*, and *Sinnakaruppan3391* were moderately salinity tolerant at the seedling stage. All other rice accessions were either susceptible or highly susceptible (*unpublished data*).

Na⁺ reduction and salinity tolerance

Na^+ accumulation was more significant in stressed plants than in plants under controlled cenditions for each rice genotype (Table 1). Since a high concentration of Na^+ can damage shoots and leaves under salinity stress (Lin *et al.*, 2004), reducing Na^+ within the plant is important to develop salinity tolerance. Out of the 125 rice genotypes, 51 (40.15%) rice accessions, with the highest Na^+ accumulation, were found to be salinity susceptible

Table 1: Na^+, K^+, and Ca^{2+} contents (ppm) in shoot dry matter of tolerant and moderately tolerant rice genotypes

TA/MTA	Accession	Na⁺ (C)	Na⁺ (T)	Rank	K⁺ (C)	K⁺ (T)	Rank	Ca²⁺ (C)	Ca²⁺ (T)	Rank	Na⁺/K⁺ (C)	Na⁺/K⁺ (T)
T	*Randhunipagal2866*	17.2	52.15[c]	12	68.2	45[bc]	110	5	8.75[d]	125	0.25	1.16[bcd]
MT	*Suduheenati3397*	26	47.6[c]	6	201.6	44.5[bc]	109	5	8.75[d]	124	0.27	0.61[d]
MT	*Bathkiriel3550*	25	50.75[c]	9	145	68.9[a]	121	5	11[cd]	119	0.17	0.74[cd]
MT	*Madathawalu3718*	17.6	51.1[c]	11	130	49.8[abc]	116	7.5	7.5[d]	126	0.14	1.03[bcd]
MT	*Matholuwa3214*	22	52.2[c]	13	112	37.2[cd]	104	5	15[abc]	99	0.2	1.4[abc]
MT	*Moddaikaruppan3388*	12.8	55.3[bc]	18	108	46.25[bc]	114	7.5	11[cd]	120	0.12	1.2[bcd]
MT	*Polayal3639*	16	56.15[bc]	22	99	59.4[ab]	119	5	11[cd]	117	0.26	1.05[bcd]
MT	*Lumbini3613*	16	76.3[ab]	38	112	49.95[abc]	117	10	17.5[ab]	75	0.14	1.53[abc]
MT	*Madaelgalle3508*	15	79.95[ab]	48	126	38.1[cd]	106	7.5	13[bc]	110	0.12	2.1[ab]
MT	*Mudaliwi3672*	16.8	82.8[ab]	51	115.2	38.2[cd]	107	2.5	13[bc]	108	0.15	2.17[ab]
MT	*Sinnakaruppan3391*	25.2	97[a]	75	129	36.7[d]	101	10	21[a]	44	0.2	2.64[a]

TA: Tolerant accessions, MTA: Moderately tolerant accessions, (C): Control seedling, (T): Seedlings under salinity stress, Rank: Rank of the rice cultivar among 125 rice genotypes when arranged according to the increasing order of Na^+, K^+, Ca^{2+} contents.

The same letters in the same column were not significantly different in the DMRT test at 5% probability level

or highly susceptible. *Madaelgalle3508, Mudaliwi3672,* and *Sinnakaruppan3391* were among the rice genotypes that accumulated a relatively higher amount of Na$^+$ in the shoot dry matter while still being moderately salinity tolerant (Table 1). Further, among the eleven salinity tolerant and moderately salinity tolerant rice accessions, seven rice accessions (*Suduheenati*3397, *Bathkiriel*3550, *Madathawalu*3214, *Randhunipagal*2866, *Matholuwa*3 214, *Moddaikaruppan*3388, and *Polayal*3639) were included among the lowest twenty-two rice accessions with Na$^+$ accumulation. Furthermore, when the rice cultivars were arranged according to increasing order of Na$^+$ accumulation under salinity stress, 85.8% of the studied rice accessions with high values were consistently found to be highly susceptible or susceptible to salinity stress.

Among the tolerant and moderately tolerant rice accessions, (referred to as TMT) *Madaelgalle*3508, *Mudaliwi*3672 and *Sinnakaruppan*3391 were moderately tolerant with high Na$^+$ content in the shoot dry matter (Figure 1). In these accessions, salinity tolerance likely developed in the plant cells by tolerating a higher Na$^+$ level at the initial stages of growth (Cheeseman, 1988; Yeo *et al.,* 1990). Additionally, these three rice accessions may have adopted other salt tolerant mechanisms such as maintaining low Cl$^-$ or Zn$^+$, proline accumulation, or high activity of antioxidant enzymes (Dionisio-Sese & Tobita, 1998; Läuchli, 1999; Zhu, 2002) rather than maintaining a low Na$^+$ content. *Pokkali* is a salinity tolerant rice accession (Gregorio & Senadhira,1993; Waziri *et al.*, 2016), but the four accessions used in the present study recorded Na$^+$ content of 91.85-160 ppm and were not salinity tolerant (*data not shown*).

Figure 1: Differential Na$^+$ content in seedling dry matter of salinity tolerant (*Randhunipagal2866*) and moderately tolerant (all other accessions) rice genotypes under control and salinity-stressed conditions.

K$^+$ accumulation and salinity tolerance

K$^+$ content of stressed seedlings was lower than those of control seedlings in all the studied rice accessions except for *Godawee3919*. Among the eleven salinity-TMT rice accessions all were among the top twenty-six rice accessions with the highest K$^+$ content (Table 1). Previous studies (Gregorio & Senadhira,1993; Chaum *et al.,* 2009; Ahmad *et al.,* 2007; Khan & Panda, 2008; Lokeshkumar *et al.,* 2023) have reported lower K$^+$ content under salinity stress in salinity-tolerant rice accessions. However, *Randhunipagal2866* and *Sinnakruppan3391*

showed insignificant differences in K$^+$ content between the control and salinity-stressed plants (Figure 2). Some highly susceptible rice accessions (26) also had the highest K$^+$ content. While *Godawee3919, Godaheenati3724,* and *Massamba2349* (*Supplementary Table 1*) ranked among the top ten rice accessions with the highest K$^+$ content, they were not among the salinity TMT accessions. Further, these three accessions were not found among the twenty rice genotypes with the lowest Ca^{2+} content. This suggests that relying solely on a genotype-specific pattern of K$^+$ accumulation in rice seedling dry matter under salinity stress is insufficient to confer salinity tolerance.

Figure 2: Differential K$^+$ content in seedling dry matter of salinity tolerant (*Randhunipagal2866*) and moderately tolerant (all other accessions) rice genotypes under control and salinity-stressed conditions.

Na$^+$/K$^+$ ratio and salinity tolerance

The Na$^+$/K$^+$ ratio was higher in all rice genotypes under salinity stress than in control seedlings (Table 1). Among the 125 rice accessions, 88% of salinity susceptible and highly susceptible rice accessions had the highest Na$^+$/K$^+$ ratios. All eleven salinity-TMT rice accessions were among the thirty-seven rice accessions with the lowest Na$^+$/K$^+$ ratios. A reduced Na$^+$/K$^+$ ratio confers salinity tolerance in rice and other crops (Chaum *et al.,* 2009; Lokeshkumar *et al.,* 2023). Maintaining a low Na$^+$/K$^+$ ratio in plants is a mechanism for salinity tolerance (Gregorio, 1997; Asch *et al.,* 2000; Munns, 2005). This has been experimentally proven by demonstrating reduced K$^+$ absorption with the addition of Na$^+$ into the medium (Ahmad *et al.,* 2007). A study reported a negative association between Na$^+$/K$^+$ ratio and salinity tolerance, and a positive association between K$^+$ and Ca^{2+} contents and salinity tolerance, using a plant stimulant to enhance salinity tolerance (Lokeshkumar *et al.,* 2023).

Assalam *et al.* (2003) reported similar results using 1.0 mM Ca^{2+} and higher concentrations of Ca^{2+} in a tissue culture medium. Similar results have also been reported by Goudarzi and Pakniyat (2008). The rice cultivars *Nona Bokra, Pokkali, SR26B* and *Lunishree,* with reduced Na$^+$/K$^+$ ratios, have performed better under salinity stress than the known salinity susceptible rice genotypes, *IR28, IR29, M1-48,* and *Begunbuchi* (Gregorio & Senadhira,1993; Ahmad *et al.,* 2007; Khan & Panda, 2008). Salt tolerance in seedlings increased after application of a plant stimulant to reduce the Na$^+$/K$^+$ balance (Mekawy *et al*., 2024).
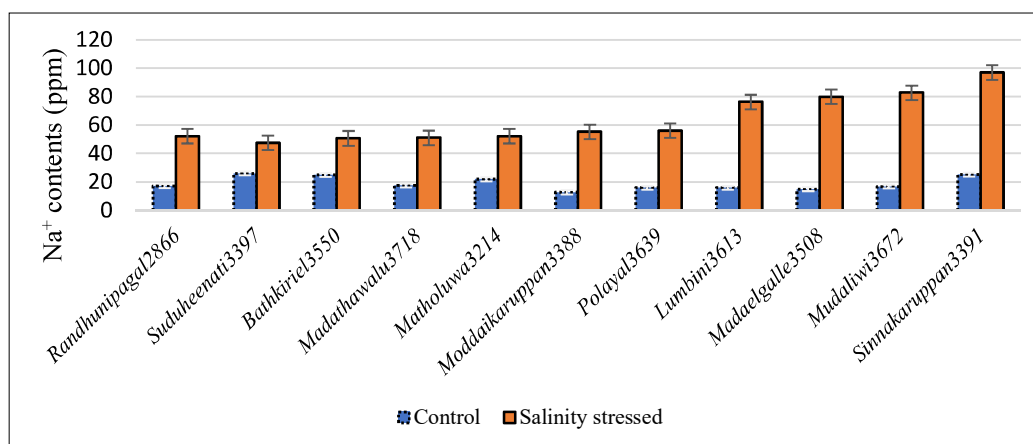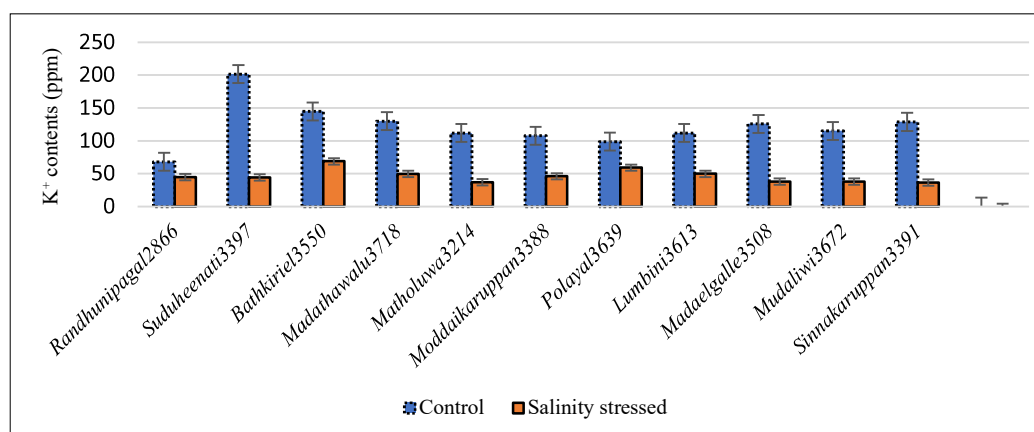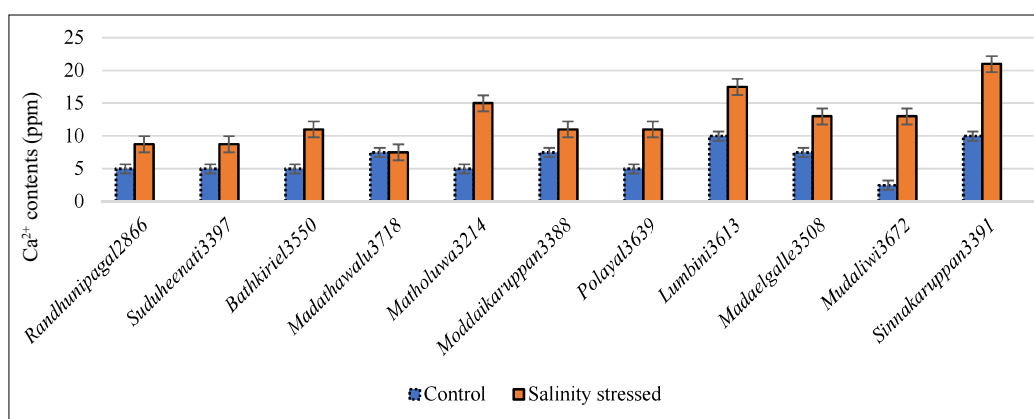

Figure 3: Differential Ca^{2+} content in seedling dry matter of salinity tolerant (*Randhunipagal2866*) and moderately tolerant (all other accessions) rice genotypes under control and salinity-stressed conditions.

Ca²⁺ uptake and salinity tolerance

The Ca^{2+} content increased in all rice genotypes with salinity stress compared to their respective control seedlings (Figure 3). Some rice varieties have developed selective ion transport mechanisms that allow them to preferentially take up Ca^{2+} over Na^+, even under saline conditions. These varieties are better equipped to maintain a healthier sodium-calcium balance and are more salt-tolerant (Song *et al.,* 2006). A similar effect has been reported by Cao *et al*. (2024) and Mahmood *et al*. (2024). Additionally, Orcan and Orcan (2024) demonstrated that the application of $CaCl_2$ resulted in reduced proline content, indicating decreased salinity stress.

Although the lowest Na^+/Ca^{2+} containing rice accessions were not salinity TMT (*Supplementary Table 1*) in the present study, eight salinity TMT accessions, namely *Mudaliwi3672, Madaelgalle3508, Polaya3639l, Bathkiriel3550, Moddaikaruppan3388, Suduheenati3397, Randhunipagal2866,* and *Madathawalu3718,* were among the eighteen rice accessions that recorded the lowest Ca^{2+} accumulation with salinity stress (Table 1).

Na⁺, K⁺, and Ca²⁺

Twenty rice genotypes that recorded the lowest Na^+, Na^+/K^+, and Ca^{2+} contents as well as the highest K^+ content in the 125 rice genotypes studied were closely monitored for salinity tolerance. Interestingly, the group included the salinity-tolerant *Randhunipagal2866*, as well as moderately tolerant accessions *Madathawalu3718*, *suduheenati339*, and *Bathkiriel3550* (Table 1). The Na^+, K^+, and Ca^{2+} contents in the dry matter of these salinity TMT rice accessions were plotted in 2-D and 3-D graphs to clearly display the relative positions of among the recorded maximum and minimum Na^+, K^+, and Ca^{2+} contents in the studied accessions. (*Supplementary Figures 1A and 1B*). Maintaining a low Ca^{2+} activity in the cytoplasm is one of the strategies for salinity tolerance (Läuchli, 1999). Spraying water under NaCl-induced salinity stress has been shown to increase the uptake of Ca^{2+} by rice plants, thereby enhancing their salinity tolerance (Song *et al.* 2006). Under $NaHCO_3$ stress, rapeseed plants experienced a reduction in Ca^{2+} absorption in their stems and leaves, leading to an imbalance of K^+ and Na^+ across different tissues (Cao *et al.*, 2024).

Three other moderately tolerant accessions, *Polayal3639, Moddaikaruppan3388, and Mudaliwi3672*, were not among the twenty genotypes with the lowest Na^+, but they were among the twenty lowest Ca^{2+}, and the highest K^+ containing accessions. The other moderately tolerant *Madaelgalle3508* accession was among the lowest Ca^{2+} containing twenty rice accessions, but not included in any other groups. This suggests that the salinity-mitigating impact of Ca^{2+} is sufficient to confer moderate salinity tolerance in the *Madaelgalle3508* accession, diminishing the harmful effects of NaCl. Moderately tolerant *Sinnakaruppan3391* recorded the highest Ca^{2+} accumulation under salinity stress (Table 1), and was not included in the group of twenty rice accessions with the lowest Na^+ or the highest K^+ content. It is unlikely that the prominent strategy for enhancing the salinity tolerance of *Sinnakaruppan3391* involves the regulation of Na^+, K^+, Na^+/K^+, and Ca^{2+} balance when compared to other potential strategies. Only *Madaelgalle3508* and *Moddaikaruppan3388* were included in the group of twenty rice accessions that recorded the lowest Na^+/K^+ ratio. None of the TMT rice accessions were included in the lowest Na^+/K^+ containing twenty rice accessions though it has been reported that the reduction of Na^+/K^+ or Na^+/Ca^{2+} ratio within the saline solution resulted in a decrease in the concentrations of Na^+ and Cl^- in the shoot (Muhammed *et al.,* 1987).

Not all favorable modes of action of Na^+, K^+, and Ca^{2+} exist in each salinity TMT rice genotype. The interaction between Na^+ and Ca^{2+} uptake is influenced by the genetic makeup of the genotype and specific environmental conditions. Certain rice genotypes may have different strategies for coping with salinity stress, which can impact the balance between Na^+ and Ca^{2+} uptake.

Validation of salinity tolerance in rice accessions at the seedling stage according to correlations of shoot Na⁺, K⁺, and Ca²⁺ content

Salinity tolerance was positively correlated with K^+ content and negatively correlated with Na^+, Na^+/K^+, and Ca^{2+} content. Among Na^+, K^+, and Ca^{2+}, a positive correlation was recorded only between Na^+ and Ca^{2+} (Table 2). Wright *et al.* (1995) reported that Ca^{2+} in the plant increases Na^+ uptake. *Madaelgalle3508, Mudaliwi3672,* and *Sinnakaruppan3391* were moderately tolerant, with the highest recorded Na^+ content among TMT rice genotypes. Interestingly, the same rice accessions recorded the highest Ca^{2+} content (Table 1). This could be because of Na^+ entering nonselective cation channels in plants is strongly influenced by Ca^{2+} (Amtmann & Sanders, 1998). Contrarily, Grattan and Grieve (1999) reported that salinity stress reduces Ca^{2+} availability and mobility when the stress is due to Na^+. However, according to Gupta and Shaw (2021), Ca^{2+}

reduces Na^+ intake when the K^+/Na^+ ratio is higher in salt-tolerant rice compared to salt sensitive varieties. Wu and Wang (2012) concluded that Ca^{2+} regulates K^+/Na^+ in rice influencing selectivity for K^+ over Na^+ and reducing the Na^+ transportation in plants at low salinity. The multifaceted nature of salinity tolerance in plants at the physiological level could exhibit diverse relationship between tolerant traits (Liu *et al.*, 2022).

Table 2:   Correlation of Na^+, K^+ and Ca^{2+}content with other parameters

Traits	r	P
Correlation between seedling shoot Ca^{2+} content and strength of tolerant level[*]	-0.331	0.000
Correlation between seedling Na^+ content and strength tolerant level	-0.267	0.003
Correlation between seedling shoot K^+ content and strength tolerant level	0.480	0.000
Correlation between seedling Na^+/K^+ and strength tolerant level	-0.430	0.000
Correlation between seedling Na^+ and K^+	-0.283	0.001
Correlation between seedling Na^+ and Ca^{2+}	0.624	0.000
Correlation between seedling K^+ and Ca^{2+}	-0.438	0.000

r = Pearson's correlation coefficient, p = Probability level, * Tolerant levels were indicated by an arbitrary scale.

The Na^+/K^+ ratio has an inverse correlation with salt tolerance in rice (Zhu *et al.*, 2001; Gao *et al.*, 2007), with higher ratios observed in salinity-susceptible rice accessions (Goudarzi & Pakniyat, 2008; Zhu *et al.*, 2001; Gao *et al.*, 2007). Salinity-tolerant plants heavily absorb K^+ to maintain a lower Na: K ratio under salinity stress (Ahmad *et al.*, 2007). This is supported by data showing that rice genotypes classified as TMT consistently have low Na^+ content and high K^+ content (Table 1). Ca^{2+} and K^+ show an inverse relationship in absorption (Table 2); Ca^{2+} uptake reduces K^+ uptake, and high K^+ absorption reduces Ca^{2+} uptake (Rengel, 1992). In natural conditions, Ca^{2+} levels in salinized water increase with daily evaporation due to selective precipitation of Ca^{2+} over Na^+ (Grattan & Grieve, 1999). These relationships of Ca^{2+} further extend with N and P (Grattan & Grieve, 1999). When studying germplasm with diverse genetic bases, such as traditional rice accessions, a single parameter may not be effective as different mechanisms of salinity tolerance may prevail. Plant responses to salt stress occur at the organismic, cellular, and molecular levels and are complex including maintaining ionic balance, adjusting osmotic conditions, scavenging reactive oxygen species (ROS), and ensuring nutritional equilibrium (Liu *et al.*, 2022). However, some studies recommend isolated parameters for salinity screening: Mahmood *et al.* (2009) have recommended shoot dry weight as a more reliable parameter than Na^+ content. Reduction of osmotic potential has been found to be the most sensitive parameter to distinguish tolerant plants from susceptible plants (Zhu *et al.*, 2001; Ahmad *et al.*, 2007).

CONCLUSION

Significant relationships were observed among Na^+, K^+, and Ca^{2+} and their impact on salinity tolerance in rice seedlings. Inverse correlations were found between the levels of Na^+, Ca^{2+}, and the Na^+/K^+ ratio with salinity tolerance. Conversely, a positive correlation was found between K^+ content and salinity tolerance in rice at the seedling stage. Na^+ and Ca^{2+} contents were higher, whereas K^+ content was lower in the stressed seedlings compared to the control group. It was evident that rice seedlings tend to accumulate K^+ and exclude Na^+ as a response to salinity stress. Na^+, K^+, and the Na:K ratio were potential parameters in a methodology for screening salinity tolerance in rice seedlings. However, Na^+ and K^+ content alone did not provide a comprehensive assessment of salinity tolerance. This conclusion is supported by the weak inverse correlations between Na^+ content and salinity tolerance (r=-0.267) and Na^+ and K^+ level (r=-0.283). Moreover, Ca^{2+} content was high in stressed seedlings and there was a strong positive correlation between Na^+ and Ca^{2+} contents (r=0.624) in seedlings grown under salinity stress. This suggests that both Ca^{2+} and Na^+ were taken up through physiological processes in response to salinity stress. A negative correlation was observed between Ca^{2+} and K^+ content, highlighting the influence of K^+ on the availability and mobilization of Ca^{2+}. The relationship between any two ions of Na^+, K^+, and Ca^{2+} in dry matter varied among salinity TMT genotypes suggesting genotype-specific ion balancing for salinity tolerance. This study reveals that while Na^+,

K+, Ca2+, and the Na+/K+ ratio are valuable parameters for evaluating salinity tolerance in rice seedlings, a holistic approach considering multiple factors is necessary to accurately assess the tolerance levels of different rice genotypes, as many other metabolic and physiological reactions influence salinity tolerance beyond ion balancing.

Acknowledgement

REFERENCES

Adams, J.F., & Doerge, T.A. (1987). Soil salinity and soil acidity as factors in plant nutrition. In: Boersma, L.L. (Ed.), Future Developments in Soil Science Research. *Soil Science Society of America Journal*, Madison, WI, 193-203. https://doi.org/10.2136/1987

Ahmad, M.S.A., Javed, F., & Ashraf M. (2007). Iso-osmotic effect of NaCl and PEG on growth, cations and free proline accumulation in callus tissue of two indica rice (*Oryza sativa* L.) genotypes. *Journal of Plant Growth Regulation,* 53, 53–63. https://doi.org/10.1007/s10725-007-9204-0

Akbar, M., Yabuno, Y., & Nakao S. (1972). Breeding for saline resistant varieties of rice. I. Variability for salt-tolerance among some rice varieties. *Japanese Journal of Breeding, 22,* 277–284. https://doi.org/10.1270/jsbbs1951.22.277

Alfatih, A., Zhang, J., Song, Y., Jan, S.U., Zhang, Z.S., Xia, J.Q., Zhang, Z.Y., Nazish, T., Wu, J., Zhao, P.X., & Xiang, C.B. (2023). Nitrate-responsive OsMADS27 promotes salt tolerance in rice. *Plant Communications, 4*(2). https://doi.org/10.1016/j.xplc.2022.100458

Amtmann, A. & Sanders, D. (1998). Mechanisms of Na+ uptake by plant cells. *In Advances in Botanical Research*, *29*, 75–112. Academic Press. https://doi.org/10.1016/S0065-2296(08)60310-9

Asch, F., Dingkuln, M., Dörffling, K., & Miezan K. (2000). Leaf K/Na ratio predicts salinity induced yield loss in irrigated rice. *Euphytica, 113*, 109–118. https://doi.org/10.1016/S0065-2296(08)60310-9

Aslam, M., Muhammad, N., Qureshi, R.H., Ahmad, Z., Nawaz, S., & Akhtar, J. (2003). Calcium and salt-tolerance of rice. *Communications in Soil Science and Plant Analysis, 34*(19-20), 3013–3031. https://doi.org/10.52045/jca.v2i1.184

Blumwald, E. (2000). Sodium transport and salt tolerance in plants. *Current Opinion in Cell Biology, 12,* 431–434. https://doi.org/10.1016/S0955-0674(00)00112-5

Bonilla, P., Dvorak, J., Mackill, D., Deal, K., & Gregorio, G. (2002). RLFP and SSLP mapping of salinity tolerance genes in chromosome 1 of rice (*Oryza sativa* L.) using recombinant inbred lines. *Philippine Agricultural Scientist, 85*, 68–76.

Cao, X., Sun, L., Wang, W., & Zhang, F. (2024). Exogenous calcium application mediates K+ and Na+ homeostasis of different salt-tolerant rapeseed varieties under NaHCO3 stress. *Plant Growth Regulation, 102*(2), 367-378. https://doi.org/10.1007/s10725-023-01066-1

Chandran, A.E., Finkler, A., Hait, T.A., Kiere, Y., David, S., Pasmanik-Chor, M., & Shkolnik, D. (2024). Calcium regulation of the Arabidopsis Na+/K+ transporter *HKT1; 1* improves seed germination under salt stress. *Plant Physiology, 194*(3), 1834-1852. https://doi.org/10.1093/plphys/kiad651

Cha-um, S., Trakulyingcharoen, T., Smitamana, P., & Kirdmanee, C. (2009). Salt tolerance in two rice cultivars differing salt tolerant abilities in responses to iso-osmotic stress. *Australian Journal of Crop Science, 3*(4), 221–230.

Cheeseman, J.M. (1988). Mechanisms of Salinity Tolerance in Plants, *Journal of Plant Physiology , 87*,547–550. https://doi.org/10.1104/pp.87.3.547

Chen, T., Shabala, S., Niu, Y., Chen, Z.H., Shabala, L., Meinke, H., Venkataraman, G., Pareek, A., Xu, J., & Zhou, M. (2021). Molecular mechanisms of salinity tolerance in rice. *The Crop Journal, 9*(3), 506–520. https://doi.org/10.1016/j.cj.2021.03.005

Chunthaburee, S., Dongsansuk, A., Sanitchon, J., Pattanagul, W., & Theerakulpisut, P. (2015). Physiological and biochemical parameters for evaluation and clustering of rice cultivars differing in salt tolerance at seedling stage, *Saudi Journal of Biological Sciences, 23*(4), 467–477. https://doi.org/10.1016/j.sjbs.2015.05.013

Counce, P.A., & Wells, B. R. (1990). Rice plant population density effect on early-season nitrogen requirement. *Journal of Production Agriculture, 3*, 390-393. https://doi.org/10.2134/jpa1990.0390

De Lacerda, C.F., Cambraia, J., Oliva, M.A., Ruiz, H.A., & Prisco, J.T. (2003). Solute accumulation and distribution during shoot and leaf development in two sorghum genotypes under salt stress. *Environmental and Experimental Botany, 49*(2), 107–120. https://doi.org/10.1016/S0098-8472(02)00064-3

Dionisio-Sese, M.L., & Tobita, S. (1998). Antioxidant responses of rice seedlings to salinity stress. *Plant Science, 135*, 1-9. https://doi.org/10.1016/S0168-9452(98)00025-9

Farooq, M. Park, J.R., Jang, Y.H., Kim, E.G., & Kim, K.M. (2021). Rice cultivars under salt stress Show differential expression of genes related to the regulation of Na+/K+ balance. *Frontiers in Plant Science, 12*, 680131. https://doi.org/10.3389/fpls.2021.680131

Fischer, K.S. (1996). Improving cereals for the variable rainfed system: from understanding to manipulation. In: Singh, V.P., Singh, R.K., Singh, B.B., Zeigler, R.S. eds. *Physiology of stress tolerance in rice* (pp.1-9). *IRRI*, Manila, the Philippines p1–9.

Flowers, T.J., & Yeo, A.R. (1986). Ion relations of plants under drought and salinity. *Australian Journal of Plant Physiology, 13*, 75-91. https://doi.org/10.1071/PP9860075

Gao, J.P., Chao, D.Y., & Lin, H.X. (2007). Understanding abiotic stress tolerance mechanism: recent studies on stress response in rice. *Journal of Integrative Plant Biology, 49*, 742–750. https://doi.org/10.1111/j.1744-7909.2007.00495.x

Gao, Q., Yin, X., Wang, F., Hu, S., Liu, W., Chen, L., Dai, X., & Liang, M. (2023). OsJRL40, a Jacalin-Related Lectin Gene, Promotes Salt Stress Tolerance in Rice. *International Journal of Molecular Sciences, 248*, 7441. https://doi.org/10.3390/ijms24087441

Gepstein, S., Grover, A. and Blumwald, E., (2005). Producing biopharmaceuticals in the desert: building an abiotic stress tolerance in plants for salt, heat, and drought. *Modern Biopharmaceuticals: Design, Development and Optimization*. 967-994. https://doi.org/10.1071/PP01154

Goudarzi, M., & Pakniyat, H. (2008). Evaluation of wheat cultivars under salinity stress based on some agronomic and physiological traits. *Journal of Agricultural Science,4*, 81–84.

Grattana, S.R., & Grieve, C.M. (1999). Salinity mineral nutrient relations in horticultural crops, *Scientia Horticulturae, 78*, 127–157. https://doi.org/10.1016/S0304-4238(98)00192-7

Gregorio, G.B. (1997). *Tagging salinity tolerance genes in rice using amplified fragment length polymorphism (AFLP)*. [PhD. thesis, University of the Philippines,] Los Baños 118.

Gregorio, G.B., & Senadhira, D. (1993). Genetic analysis of salinity tolerance in rice (*Oryza sativa* L.). *Theoretical and Applied Genetics, 86*, 333–338. https://doi.org/10.1007/BF00222098

Gupta, A. & Shaw, B.P. (2021). Augmenting salt tolerance in rice by regulating uptake and tissue specific accumulation of Na+-through Ca2+-induced alteration of biochemical events. *Plant Biology, 23*, 122-130. https://doi.org/10.1111/plb.13258

Hasegawa, P.M., Bressan, R.A., Zhu, J.K., & Bohnert, H.J. (2000). Plant cellular and molecular responses to high salinity. *Annual Review of Plant Biology, 51*(1), 463–499. https://doi.org/10.1146/annurev.arplant.51.1.463

Hopmans, J.W., Qureshi, A.S., Kisekka, I., Munns, R., Grattan, S.R., Rengasamy, P., Ben-Gal, A., Assouline, S., Javaux, M., Minhas, P.S. & Raats, P.A.C. (2021). Critical knowledge gaps and research priorities in global soil salinity. *Advances in Agronomy, 169*, 1–191. https://doi.org/10.1016/bs.agron.2021.03.001

Khan, A., Khan, A.A., Samreen, S. & Irfan, M. (2023). Assessment of Sodium Chloride (NaCl) Induced Salinity on the Growth and Yield Parameters of *Cichorium intybus* L. *Nature Environment and Pollution Technology, 22*(2). https://doi.org/10.46488/NEPT.2023.v22i02.026

Khan, M.H., & Panda, S.K. (2008). Alterations in root lipid peroxidation and antioxidative responses in two rice cultivars under NaCl-salinity stress. *Acta Physiologiae Plantarum, 30*, 81–89. https://doi.org/10.1007/s11738-007-0093-7

Koyama, M., Levesley, A., Koebner, R., Flowers, T., & Yeo, A. (2001). Quantitative trait loci for component physiological traits determining salt tolerance in rice. *Plant Physiology, 125*, 406–422. https://doi.org/10.1104/pp.125.1.406

Kumar, K., Kumar, M., Kim, S.R., Ryu, H. & Cho, Y.G. (2013). Insights into genomics of salt stress response in rice. *Rice, 6*(1), 1-15. https://doi.org/10.1186/1939-8433-6-27

Lacerda, C.F., Cambraia, J., Oliva, M.A., Ruiz, H.A., Prisco, J.T. (2003). Quantitative trait loci for salt tolerance in rice via molecular markers. *OMon Rice, 8*, 37–48.

Lang, N.T., Yanagihara, S., & Buu, B.C. (2000). Quantitative trait loci for salt tolerance in rice via molecular markers. *Omon Rice, 8*, 37–48.

Läuchli, A. (1999). Salinity-potassium interactions in crop plants. *Frontiers in Potassium Nutrition: New Perspectives on the Effects of Potassium on Physiology of Plants*. D.M. Oosterhuis and G.A. Berkovitz (Eds.). Potash & Phosphate Institute, Norcross, GA, 71-76.

Liu, C., Mao, B., Yuan, D., Chu, C. & Duan, M. (2022). Salt tolerance in rice: Physiological responses and molecular mechanisms. *The Crop Journal, 10*(1), 13-25. https://doi.org/10.1016/j.cj.2021.02.010

Lokeshkumar, B.M., Krishnamurthy, S.L., Rathor, S., Warriach, A.S., Vinaykumar, N.M., Dushyanthakumar, B.M., & Sharma, P.C. (2023). Morphophysiological diversity and haplotype analysis of saltol QTL region in diverse rice landraces for salinity tolerance. *Rice Science, 30*(4), 306-320. https://doi.org/10.1016/j.rsci.2023.02.001

Luan, S., Lan, W. & Lee, S.C. (2009). Potassium nutrition, sodium toxicity, and calcium signaling: connections through the CBL–CIPK network. *Current Opinion in Plant Biology, 12*(3), 339–346. https://doi.org/10.1016/j.pbi.2009.05.003

Machado, R.M.A., & Serralheiro, R.P. (2017). Soil salinity: effect on vegetable crop growth. Management practices to prevent and mitigate soil salinization. *Horticulturae, 3*(2), 30. https://doi.org/10.3390/horticulturae3020030

Mahmood, A., Latif, T., & Khan, M.A. (2009). Effect of salinity on growth, yield and yield components in basmati rice germplasm. *Pakistan Journal of Botany, 41*(6), 3035–3045.

Mahmood, M.Z., Odeibat, H.A., Ahmad, R., Gatasheh, M.K., Shahzad, M., & Abbasi, A.M. (2024). Low apoplastic Na+ and intracellular ionic homeostasis confer salinity tolerance upon Ca2SiO4 chemigation in *Zea mays* L. under salt stress. *Frontiers in Plant Science, 14*, 1268750. https://doi.org/10.3389/fpls.2023.1268750

Mekawy, A.M.M., Assaha, D.V., Li, J. & Ueda, A. (2024). Astaxanthin application enhances salinity tolerance in rice seedlings by abating oxidative stress effects and enhancing Na+/K+ homeostatic balance. *Plant Growth Regulation*, 1-15. https://doi.org/10.1007/s10725-024-01132-2

Muhammed, S., Akbar, M., & Neu, H.U. (1987). Effect of Na/Ca and Na/K ratios in saline culture solution on the growth and mineral nutrition of rice (*Oryza sativa* L.). *Plant Soil, 104*, 57–62. https://doi.org/10.1007/BF02370625

Munns, R. (2005). Genes and salt tolerance: bringing them together. *New Phytologist, 167*, 645–663. https://doi.org/10.1111/j.1469-8137.2005.01487.x

O'Halloran, J. Walsh, A.R., & Fitzpatrick, P.J. (1997). The determination of trace elements in biological and environmental samples using atomic absorption

spectroscopy. In Bioremediation Protocols; Springer: *Berlin/Heidelberg, Germany, 2*, 201–211. https://doi.org/10.1385/0-89603-437-2:201

Orcan, M.Y. & Orcan, P. (2024). Effect of Na, Mg, Ca chloride salts on mineral element, proline and total protein contents in rice (*Oryza sativa* L.) grown *in vitro*. *International Journal of Secondary Metabolite*, *11*(1), 144-156. https://doi.org/10.21448/ijsm.1335099

Porcel, R., Aroca, R., Azcon, R., & Ruiz-Lozano, J.M. (2016). Regulation of cation transporter genes by the arbuscular mycorrhizal symbiosis in rice plants subjected to salinity suggests improved salt tolerance due to reduced Na⁺ root-to-shoot distribution. *Mycorrhiza, 26*, 673–684. https://doi.org/10.1007/s00572-016-0704-5

Rajendran, K., Tester, M., & Roy, S.J. (2009). Quantifying the three main components of salinity tolerance in cereals. *Plant, Cell and Environment*, *32*(3), 237–249. https://doi.org/10.1111/j.1365-3040.2008.01916.x

Ranawake, A.L., & Nakamura, C. (2012). Assessment of salinity tolerance in an inbred population of rice (*Oryza sativa* L.) derived from a *japonica* x *indica* cross, *Tropical Agricultural Research & Extension, 15*(3). https://doi.org/10.4038/tare.v15i3.5250

Reddy, I.N.B.L., Kim, B.K., Yoon, I.S., Kim, K.H. & Kwon, T.R. (2017). Salt tolerance in rice: focus on mechanisms and approaches. *Rice Science*, *24*(3), 123–144. https://doi.org/10.1111/j.1365-3040.1992.tb01004.x

Rengel, Z. (1992). The role of calcium in salt toxicity. *Plant, Cell and Environment, 15*, 625-632. https://doi.org/10.1111/j.1365-3040.1992.tb01004.x

Rivelli, A.R., James, R.A., Munns, R., & Condon, A.G. (2002). Effect of salinity on water relations and growth of wheat genotypes with contrasting sodium uptake, *Functional Plant Biology, 29*, 1065–1074. https://doi.org/10.1071/PP01154

Shahzad, B., Yun, P., Rasouli, F., Shabala, L., Zhou, M., Venkataraman, G., Chen, Z.H. & Shabala, S. (2022). Root K+ homeostasis and signalling as a determinant of salinity stress tolerance in cultivated and wild rice species. *Environmental and Experimental Botany*, *201*, 104944. https://doi.org/10.1016/j.envexpbot.2022.104944

SPSS Inc. (2011). IBM SPSS Software for Windows, Version 20.0.

Song, J.Q., Mei, X.R., & Fujiyama, H. (2006). Adequate internal water status of NaCl-salinized rice shoots enhanced selective calcium and potassium absorption. *Soil Science and Plant Nutrition, 52*(3), 300–304. https://doi.org/10.1111/j.1747-0765.2006.00038.x

Shyamalee, H.A.P.A., & Ranawake, A.L. (2024a). Genetic diversity analysis of traditional and improved rice genotypes in Sri Lanka using SSR markers. *Journal of the National Science Foundation of Sri Lanka*, *52*(2), 215 – 227. http://dx.doi.org/10.4038/jnsfsr.v52i2.11656.

Shyamalee, H.A.P.A., & Ranawake, A.L. (2024b). Screening eighty traditional and improved rice genotypes in Sri Lanka for salinity tolerance at the seedling stage in Yoshida solution. *Journal of the National Science Foundation of Sri*

Lanka, *51*(4), 597 – 614. http://dx.doi.org/10.4038/jnsfsr.v51i4.11500

Tahjib-Ul-Arif, M., Roy, P.R., Al Mamun Sohag, A., Afrin, S., Rady, M.M., & Hossain, M.A. (2018). Exogenous calcium supplementation improves salinity tolerance in BRRI dhan28; a salt-susceptible high-yielding *Oryza sativa* cultivar. *Journal of Crop Science and Biotechnology, 21*, 383–394. https://doi.org/10.1007/s12892-018-0098-0

Tester, M., & Davenport, R. (2003). Na⁺ tolerance and Na+ transport in higher plants. *Annals of Botany, 91*, 503-527. https://doi.org/10.1093/aob/mcg058

Walthall, C. L., Hatfield, J., Backlund, P., Lengnick, L., Marshall, E., & Walsh, M. (2012). Climate Change and Agriculture in the United States: Effects and Adaptation. Washington, DC: United States Department of Agriculture.

Wang, W.H., Chen, J., Liu, T.W., Chen, J., Han, A.D., Simon, M., Dong, X.J., He, J.X., & Zheng, H.L. (2014). Regulation of the calcium-sensing receptor in both stomatal movement and photosynthetic electron transport is crucial for water use efficiency and drought tolerance in Arabidopsis. *Journal of Experimental Botany*, *65*(1), 223-234. https://doi.org/10.1093/jxb/ert362

Waziri, A., Kumar, P., & Purty, R.S. (2016). *Saltol* QTL and their role in salinity tolerance in rice. Austin *Journal of Biotechnology and Bioengineering, 3*(3), 1067.

Wright, G.C., Patten, K.D., & Drew, M.C. (1995). Labeled sodium (²²Na) uptake and translocation in rabbit eye blueberry exposed to sodium chloride and supplemental calcium. *Journal of the American Society for Horticultural Science, 120*, 177–182. https://doi.org/10.21273/JASHS.120.2.177

Wu, G.Q., & Wang, S.M. (2012). Calcium regulates K+/Na+ homeostasis in rice (*Oryza sativa* L.) under saline conditions. *Plant, Soil and Environment*, *58*(3), 121-127. https://doi.org/10.17221/374/2011-PSE

Yeo, A.R., & Flowers, T.J. (1986). Salinity resistance in rice (*Oryza sativa* L.) and a pyramiding approach to breeding varieties for saline soils. *Australian Journal of Plant Physiology, 13*, 161–173. https://doi.org/10.1071/PP9860161

Yeo, A.R., Yeo, M.E., Flowers, S.A. & Flowers, T.J., (1990). Screening of rice (*Oryza sativa* L.) genotypes for physiological characters contributing to salinity resistance, and their relationship to overall performance. *Theoretical and Applied Genetics, 79*, 377–384. https://doi.org/10.1007/BF01186082

Yu, J., Zhu, C., Xuan, W., An, H., Tian, Y., Wang, B., Chi, W., Chen, G., Ge, Y., Li, J. & Dai, Z. (2023). Genome-wide association studies identify OsWRKY53 as a key regulator of salt tolerance in rice. *Nature Communications*, *14*(1), 1–13. https://doi.org/10.1038/s41467-023-39167-0

Zeng, L., Poss, J.A., & Wilson, C. (2003). Evaluation of salt tolerance in rice genotypes by physiological characters. *Euphytica, 129*, 281–292. https://doi.org/10.1023/A:1022248522536

Zheng, C., Liu, C., Liu, L., Tan, Y., Sheng, X., Yu, D., Sun, Z., Sun, X., Chen, J., Yuan, D., & Duan, M. 2023. Effect of salinity stress on rice yield and grain quality: A meta-

analysis. *European Journal of Agronomy, 144*, 126765. https://doi.org/10.1016/j.eja.2023.126765

Zhu, G.Y., Kinet, J.M., & Lutts, S. (2001). Characterization of rice (*Oryza sativa* L.) F3 population selected for salt resistance. Physiological behavior during vegetative growth. *Euphytica, 121*, 251-263. https://doi.org/10.1023/A:1012016431577

Zhu, J.K. (2002). Salt and drought stress signal transduction in plants. *Annual review of plant biology, 53*, 247–273. https://doi.org/10.1146/annurev.arplant.53.091401.143329

Supplementary Table

Supplementary Table 1: Na$^+$, K$^+$, Na:K ratio of control and salinity stressed rice seedlings.

PGRC No.	Name	Na$^+$ (ppm)		K$^+$ (ppm)		Na$^+$/K$^+$		Ca^{2+} (ppm)	
		Control	Treatment	Control	Treatment	Control	Treatment	Control	Treatment
2203	*Dikwee*	16	101.2	128	19.8	0.13	5.11	10	16.25
2340	*Wedaheenati*	18.4	118.9	97.2	30.8	0.19	3.86	10	23
2349	*Massamba*	20	121.5	119.7	71.4	0.17	1.7	10	18.75
2866	***Randhunipagal***	**17.2**	**52.15**	**68.2**	**45**	**0.25**	**1.16**	**5**	**8.75**
3071	*Polayal*	16	134.4	84	28.8	0.19	4.67	10	28
3072	*Thanthiribalan*	17.6	55.5	87	22.8	0.2	2.43	7.5	14
3131	*Dahanala2014*	12.6	91.7	115.6	46.2	0.11	1.98	10	18.75
3132	*Heenati-309*	12	104.5	103.7	33.3	0.12	3.14	10	15
3136	*Pachchaiperumal2462-11*	12.8	90.2	109.8	22.2	0.12	4.06	10	20
3146	*Dewaredderi*	14.4	87.3	95.2	36	0.15	2.43	10	17.5
3158	*KaluBalawee*	16	104	73.4	12.5	0.22	8.32	10	42.5
3160	*Valihandiran*	26.5	121.3	152	30.6	0.17	3.96	10	29
3161	*Heenwee*	20.8	110	100.8	16.5	0.21	6.67	10	26
3170	*Sudubalawee*	19.6	106.75	48	13.5	0.41	7.91	5	42.5
3171	*Suduhetada*	24	112.75	49.4	20.4	0.49	5.53	5	29.25
3183	*Hathiel*	29.6	116.4	98	18.5	0.3	6.29	10	38.75
3191	*Heendikwee*	13.8	96.9	132.6	49.5	0.1	1.96	10	20
3194	*Katharamana*	16.8	90.35	71.4	15.4	0.24	5.87	10	16.5
3195	*Gallkatta*	34	122.2	134.1	15	0.25	8.15	10	38.75
3197	*Nanduheenati*	21.2	165.3	91.8	21.6	0.23	7.65	10	24.25
3200	*Kaluheenati*	19	91.6	63.9	23.55	0.3	3.89	10	20
3202	*Rambuttanwee*	19.2	120.5	119.4	20.1	0.16	6	10	20.25
3214	***Matholuwa***	**22**	**52.2**	**112**	**37.2**	**0.2**	**1.4**	**5**	**15**
3341	*Galpawee*	17.2	76.45	102	20.7	0.17	3.69	5	16.25
3383	*Eatsamba*	36.4	52.5	147.2	13.5	0.25	3.89	12.5	16
3387	*Kahatawee*	19.2	79.2	70.4	21.95	0.27	3.61	10	15
3388	***Moddaikaruppan***	**12.8**	**55.3**	**108**	**46.25**	**0.12**	**1.2**	**7.5**	**11**
3390	*Rathheenati*	15	45.85	108	50.4	0.14	0.91	7.5	13
3391	***Sinnakaruppan***	**25.2**	**97**	**129**	**36.7**	**0.2**	**2.64**	**10**	**21**
3394	*Muthusamba*	15.2	126.8	129	29.5	0.12	4.3	10	25.5
3397	***Suduheenati***	**26**	**47.6**	**97.5**	**78.1**	**0.27**	**0.61**	**5**	**8.75**
3407	*Dewaradderi*	19.8	95.55	131.4	33.25	0.15	2.87	7.5	20
3409	*BG 35-2*	18.4	90.5	100.8	24.3	0.18	3.72	7.5	20
3410	*BG 35-7*	13.2	78.1	139.2	14.5	0.09	5.39	5	24
3415	*BG 34-8*	30	70	100.5	20.45	0.3	3.42	10	16.5
3427	*Nauduwee*	10.8	82.05	126	20.8	0.09	3.94	5	15
3445	*Yakadawee*	8.4	88.4	97.2	17.15	0.09	5.15	5	29
3463	*Karayal*	25.5	57.6	123.2	17.5	0.21	3.29	7.5	15.5
3469	*SuduweeRatnapura*	16	50.8	105	22.5	0.15	2.26	10	17.5
3472	*Masuran*	20	117.7	112.8	14	0.18	8.41	5	22

PGRC No.	Name	Na^+ (ppm)		K^+ (ppm)		Na^+/K^+		Ca^{2+} (ppm)	
		Control	Treatment	Control	Treatment	Control	Treatment	Control	Treatment
3479	*KiriNaran*	20.8	62.5	102.6	45	0.2	1.39	5	17.5
3480	*Karayal*	16.8	124.8	100.8	20.2	0.17	6.18	7.5	18.75
3482	*Akuramboda*	24.5	76.1	149.6	22.8	0.16	3.34	5	13
3486	*Puwakmalatasamba*	19.2	88	133	16.5	0.14	5.33	10	31
3487	*Palasithari601*	20	53.2	99	59.4	0.2	0.9	5	15
3491	*Murungakayan304*	16.8	115.2	120.4	20	0.14	5.76	10	23
3506	*MI329*	23	63	138	13.6	0.17	4.63	10	21.25
3508	***Madaelgalle***	**15**	**79.95**	**126**	**38.1**	**0.12**	**2.1**	**7.5**	**13**
3550	***Bathkiri el***	**25**	**50.75**	**145**	**68.9**	**0.17**	**0.74**	**5**	**11**
3562	*Thunmarhamara*	21	72.3	126	25.8	0.17	2.8	10	20.25
3572	*Sudurusamba*	23.1	110.5	79.2	21.8	0.29	5.07	2.5	16
3573	*Pokkali*	16	91.85	159.6	31.2	0.1	2.94	10	18.5
3579	*kakiriatabalawee*	25	42	107.8	72.05	0.23	0.58	5	11
3591	*Mudukiriel*	26	63.9	133	16.4	0.2	3.9	10	23
3599	*Mahamawee*	24	145.5	57.6	23.35	0.42	6.23	10	24.25
3611	*Balakaharamana*	12	158.4	142.4	21.5	0.08	7.37	7.5	28
3613	***Lumbini***	**16**	**76.3**	**112**	**49.95**	**0.14**	**1.53**	**10**	**17.5**
3616	*Jamiswee*	16	94.6	81	30.45	0.2	3.11	12.5	18
3629	*Ruwanrathran*	18.4	28	98	25.3	0.19	1.11	7.5	16
3634	*Thavalu*	18.4	171.9	117.6	17.5	0.16	9.82	12.5	26.5
3639	***Polayal***	**16**	**56.15**	**61.6**	**53.25**	**0.26**	**1.05**	**5**	**11**
3641	*Heendikwee*	16	128.4	79.5	19.8	0.2	6.48	10	20
3642	*Kahatasamba*	16	66	141.2	15.85	0.11	4.16	7.5	14.5
3644	*Herath*	30	56.7	68	36	0.44	1.58	7.5	11
3645	*Muthumanikkam*	16	109.45	132.6	24.4	0.12	4.49	10	21.25
3646	*Indurukarayal*	27	88.3	67.2	23.85	0.4	3.7	7.5	13
3647	*Kalugires*	23	123.1	134	34	0.17	3.62	10	23
3650	*Madabaru*	22	73	116.2	24.9	0.19	2.93	5	14
3652	*Burumathavalu*	34.8	78.2	126	23.3	0.28	3.36	5	15.5
3656	*Kuruluthudu*	14.4	159.8	103.7	24.5	0.14	6.52	10	28
3662	*Mahasuduwwee*	16.8	90.2	79.2	30	0.21	3.01	5	17.5
3663	*Murunga*	22	74	105.6	14	0.21	5.29	7.5	24
3664	*Tissawee*	21.5	60.7	61.6	22.8	0.35	2.66	7.5	18
3665	*SuduKarayal*	22.2	75.9	79.2	33.35	0.28	2.28	7.5	16.25
3671	*Sudurusamba*	17.6	34.25	123.2	35.6	0.14	0.96	7.5	24
3672	***Mudaliwi***	**16.8**	**82.8**	**115.2**	**38.2**	**0.15**	**2.17**	**2.5**	**13**
3674	*Kirikara*	20	80.85	56.4	18.3	0.35	4.42	10	17.5
3676	*Denawee*	21.2	77.3	120	31.15	0.18	2.48	10	16.25
3679	*Kottakaram*	24	92.5	111.6	19	0.22	4.87	7.5	28
3683	*Mawee*	16.8	47.85	102.6	35	0.16	1.37	10	17.5
3684	*Rathkara*	24	93.4	67.6	27.2	0.36	3.43	10	20
3691	*Gunarathna*	34.3	54.95	92.4	36.5	0.37	1.51	5	12
3692	*Handiran*	12.8	79.2	140	30.4	0.09	2.61	10	13.75
3695	*Kahatasamba*	14	97.35	95	23.8	0.15	4.09	10	17.5

PGRC No.	Name	Na⁺ (ppm)		K⁺ (ppm)		Na⁺/K⁺		Ca²⁺ (ppm)	
		Control	Treatment	Control	Treatment	Control	Treatment	Control	Treatment
3701	*Pokkali*	12	144.75	107.2	15.65	0.11	9.25	12	37.5
3713	*Kalukanda*	19.2	148.75	128	27.6	0.15	5.39	10	26
3718	***MadaThawal***	**17.6**	**51.1**	**130**	**49.8**	**0.14**	**1.03**	**7.5**	**7.5**
3720	*Kirikara*	22.4	39.4	119.7	44.4	0.19	0.89	10	11
3721	*Manamalaya*	28	54	122.1	16.8	0.23	3.21	7.5	18
3724	*GodaHeenati*	11.4	100	136	78.05	0.08	1.28	10	16.5
3725	*Sivuruwee*	27	56	55.8	28.75	0.48	1.95	7.5	10
3726	*Dandumara*	22	126.25	142.4	13	0.15	9.71	10	45
3734	*KanniMurunga*	11.4	115.05	92.4	17.4	0.12	6.61	5	19
3735	*Welihandiran*	13.8	101.2	100.8	31.15	0.14	3.25	10	18.75
3744	*3744*	14.1	78.4	108	33.6	0.13	2.33	2.5	13
3756	*3756*	16	84.5	108	18.6	0.15	4.54	5	16
3881	*Pokkali*	15	134.5	120.4	31.9	0.12	4.22	7.5	26
3882	*Dostaraheenati*	15.2	117.7	114.8	30.15	0.13	3.9	10	23
3919	*Godawee*	12.6	88	39.6	78.2	0.32	1.13	10	15
3922	*Pokkali*	34.4	160	86.4	18.45	0.4	8.67	5	58
3932	*Suduheenati*	26.5	117.3	201.6	44.5	0.13	2.64	5	10
3982	*Kuruwee*	15.2	144	90	37.1	0.17	3.88	10	22.5
4145	*4145*	16.8	107.7	96.2	36.45	0.17	2.95	12.5	23
4159	*Podiwee*	15.2	114.4	67.2	17.2	0.23	6.65	10	23
4178	*Rathumadilla*	13.6	55.3	72	37.8	0.19	1.46	2.5	10
4402	*Haththepasdawasewee*	15.2	99	106.4	21	0.14	4.71	12.5	18.75
4726	*Gonabaru*	24.5	84	127	17.7	0.19	4.75	7.5	16
4732	*Horana wee*	23	107.8	106.4	22.4	0.22	4.81	10	24.25
4753	*Kombila*	21	101.8	134	12.4	0.16	8.21	10	20
4762	*Maharajah*	31.5	67.15	127	15.45	0.25	4.35	7.5	16.25
4770	*Molligoda*	16	119.6	105.6	14.25	0.15	8.39	10	26
4785	*Poovellai*	27.6	144	113.1	36.8	0.24	3.91	12.5	22.5
4809	*Suwandal*	19.6	119	139.2	19.5	0.14	6.1	10	18
4819	*Veliainellu*	13.2	50.4	105.6	45.9	0.13	1.1	10	13.75
4834	*Kallurundoivellai*	17.2	97.75	87	25.05	0.2	3.9	2.5	20
4841	*KoopanSivappu*	27.5	89	129	11.2	0.21	7.95	2.5	31.25
4852	*Nandumawee*	22.5	92.5	129.6	21	0.17	4.4	12.5	18.5
4858	*Potkilivan*	16	76.8	101.2	17	0.16	4.52	2.5	13
4992	*Rathuheenati*	16	89.1	90	31.8	0.18	2.8	10	20
5671	*Suduhandiran*	15	84.5	74.8	23.8	0.2	3.55	10	18
6179	*Gires*	14.4	59.85	177	23.65	0.08	2.53	2.5	12
6249	*6249*	16.8	108.05	144	35.5	0.12	3.04	10	21.25
6863	*Pappaku*	23	108	100.5	21.4	0.23	5.05	2.5	19

* Tolerant or moderately tolerant genotypes were in bold letters.
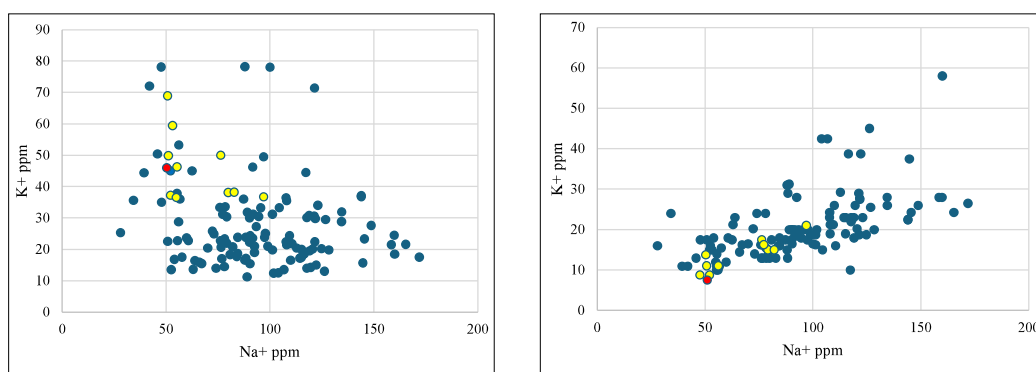
Supplementary figure 1A: Na$^+$, K$^+$ and Ca^{2+} contents of rice accessions under salinity stress. Red: Salinity tolerant *Randunipagal* accession, Yellow: Moderately tolerant rice accessions, Blue: Susceptible or Highly susceptible rice accessions.
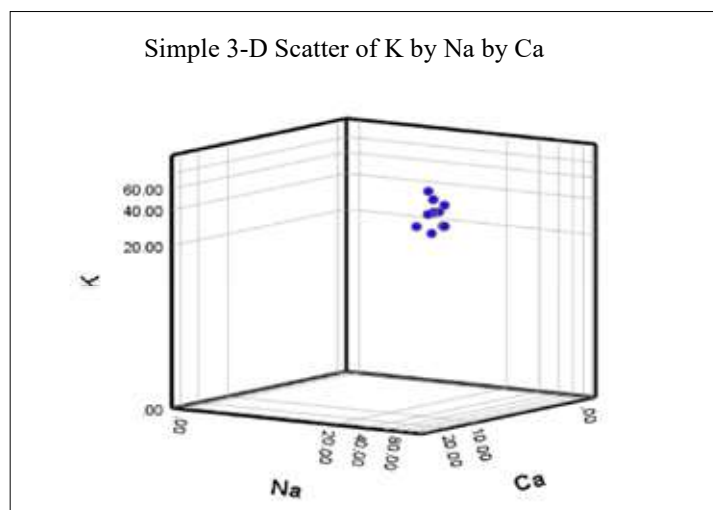
Supplementary figure 1B: Na$^+$, K$^+$ and Ca^{2+} contents of rice salinity tolerant and moderately tolerant rice accessions under salinity stress in 3-D scatter plot.

RESEARCH ARTICLE

Environmental Science

Optimizing beach nourishment composition for coastal protection in Sri Lanka: Insights from flume experiments

NVD Lakshitha, RSM Samarasekara* and HPAM Siriwardana
Department of Civil Engineering, Faculty of Engineering, University of Sri Jayewardenepura, 41, Lumbini Avenue, Rathmalana, Sri Lanka.

Abstract: Beach erosion is a significant threat to Sri Lanka's economically and ecologically valuable coastlines, particularly along the Southwest and Western regions. Traditional beach nourishment methods, such as use offshore sand are common but have limitations in terms of durability and recurring costs. This study investigates the potential benefits of incorporating crushed waste glass into offshore sand to enhance erosion resistance and cost-effectiveness towards beach nourishment. This study evaluated four materials; native sand, offshore sand, river sand, and crushed glass, through controlled hydraulic flume experiments and particle size analysis. Offshore sand was the most susceptibile to erosion with a transported sediment volume of 26%, while crushed glass showed superior stability with only 14% erosion. Blends of offshore sand and crushed glass containing 10–20% crushed glass (CG10–CG20) achieved an optimal balance between durability and material cost. The unique compacting properties and smoother surface texture of crushed glass contributed to reduced sediment mobility under wave action. Furthermore, the study highlighted the environmental benefits of utilising locally available glass waste, promoting sustainable waste management while enhancing coastal resilience. These findings provide practical insights for future beach nourishment projects in Sri Lanka, emphasizing the dual benefits of improved performance and ecological responsibility. Future research should focus on validating these results long-term field settings, assessing ecological impacts, and developing scaling methods for broader coastal management applications.

Keywords: Beach nourishment, coastal protection, crushed-glass, flume experiment, offshore-sand.

INTRODUCTION

Beach nourishment in Sri Lanka

Coastline retreat is an evident sign of the vulnerability of low-lying sandy coasts to erosion and sea level rise (Stronkhorst *et al*., 2018). Various solutions can be implemented to mitigate the effect of beach erosion. Among them, beach nourishment is a popular and non – structural solution (Atkinson *et al*., 2020). The importance of beach nourishment in shore protection projects is growing in parallel with environmental concerns associated with traditional hard coastal engineering projects (Hanson *et al*., 2002), and with the contribution to the tourist industry for beach based activities (Pranzini *et al*., 2018). However, nourishment is not a long-term solution to beach erosion as it requires periodic renourishments to enhance effectiveness (Miller, 2018).

The erosive forces of waves, storms, and rising sea levels do not cease after beach nourishment takes place. Beach nourishment is the process of placing additional sediment to a beach or nearshore area widening the beach, and increasing recreational opportunities while enhancing the local economy (Atkinson & Buldock, 2020). According to Climate-ADAPT (2016), beach nourishment can last anywhere from 2 to 10 years before needing to be repeated due to its temporary nature.

* Corresponding author (samarasekara@sjp.ac.lk; [iD] https://orcid.org/0000-0002-1555-1302)

Typically, offshore sand is use for beach nourishment, but other material alternatives such as pebbles or marble waste can be used based on design requirements.

As an island nation in the Indian Ocean, Sri Lanka relies heavily on the coastline for economic, domestic, recreational, and tourism activities. The West coast area, in particular, is a valuable beach zone, due to its strategic location. This, region has a thriving tourism industry with numerous hotels catering to visitors of all sizes. Moreover, the fishing industry provides livelihood for many of the residents in this area such as the Marawila beach (Samarasekera, 2018).

Hence, the life-style of the residents and industries in this area is heavily dependent on the beach. Therefore, the presence of a wide, nourished beach system that can absorb wave energy, and protect upland areas from flooding, and mitigate erosion is essential for this area . Offshore sand is commonly used for beach nourishment projects worldwide. However, the durability of these projects can vary according to environmental conditions and their locations. Beach nourishment is considered to be very expensive and needs to be periodically repeated in order to sustain the nourished beach (Schirmer, 2017). Thus, it is vital for beach nourishment locations to be accurately identified to ensure long lasting protection of the beaches.

Optimizing beach nourishment in Sri Lanka

Beach nourishment involves depositing additional sediments onto a beach or its adjacent nearshore areas to expand the beach, protect structures, and mitigate coastal erosion. However it necessitates periodic replenishment due to sediment erosion over time (Matthieu A de Schipper, 2018; Staudt *et al*., 2022). It serves several purposes aimed at sustainable coastal management and enhancing coastal community resilience, including erosion control, storm damage reduction, and providing recreational and tourism benefits. By restoring sediment, beach nourishment widens shorelines and acts as a buffer against coastal hazards, protecting infrastructure from wave damage and land loss. Nourished beaches absorb wave energy, reducing the impact on coastal structures and minimizing flooding and property damage during storms. They also offer wider and more attractive recreational spaces, attracting tourists and boosting local economies through increased tourism revenue, visitor spending, and job creation.

Additionally, nourished beaches enhance coastal property values by improving aesthetics, providing better access, and reducing erosion risks. In Sri Lanka, beach nourishment has been carried out in various locations such as Kalido Beach, Mt. Lavinia Beach, Uswatakeiyawa, and Marawila, underscoring the importance of these beaches to the economy through tourism and fishing (Maliq, 2015; Jayathilaka, 2023). Given their critical economic role, comprehensive studies on the beach nourishment practices are imperative (Jayathilaka, 2023).

The research objectives of this study are to determine the current state of upgraded offshore sand globally and assess the feasibility of using crushed glass to enhance offshore sand. Specifically, the study aims to investigate the material composition of river sand, natural beach sand, and offshore sand, and evaluate the erodibility of different nourished sands using hydraulic flume model studies. Additionally, the research seeks to identify the most suitable offshore sand-to-crushed glass ratio, considering beach erodibility.

Factors affecting the durability of beach nourishment

The durability of materials in beach nourishment projects is crucial for effective coastal management and is influenced by factors such as particle size and shape, tidal range, wave energy, climate, and compaction techniques. Larger, well-rounded particles offer better stability and resistance to erosion, while smaller particles are more susceptible. The tidal range affects material exposure, requiring resilience to varying submersion levels. High wave energy and climate change exacerbate erosion, transport sediments, and challenge the durability of the nourishment project (Dette *et al*., 2002). Proper compaction techniques, whether mechanical or natural, enhance stability by reducing pore space and increasing inter-particle contact, minimizing erosion and displacement (CEM, 2012).

Glass as waste material in Sri Lanka

Glass, usually regarded as a completely inert recyclable material, is a significant component of municipal solid waste streams across the world. Recycling glass is highly beneficial since improper disposal is an environmental hazard due to its non-biodegradable nature. Glass waste consists of a variety of items including a diverse collection of bottles, jars, windows, and as packaging materials. It is very tough and waterproof, therefore, it is mostly used for packing food and beverages. Based on 2014 data, Sri Lanka had a total of 309 local authorities, comprising 15 Municipal Councils, 37 Urban Councils, and 257 Pradeshiya Sabhas.

These authorities manage solid waste in various ways. However, according to municipal council databases for solid waste collection in Sri Lanka (2005), glass wastes accounted for 2.03% of the total solid waste collection and currently there is no proper method for collecting and recycling glass waste. Figure 1 illustrates the annual waste composition generated in Sri Lanka (CEA, 2014).
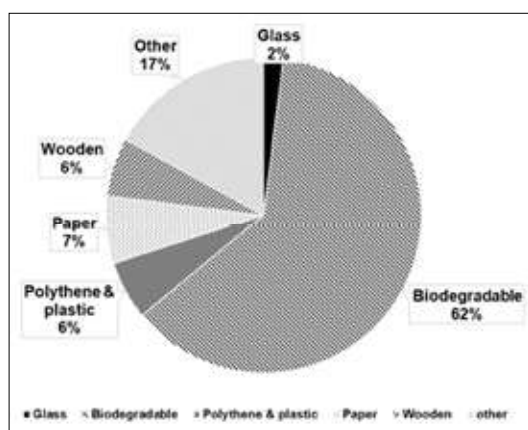

Figure 1: Annual waste composition in Sri Lanka (2014).

Similar studies

Worldwide, only a few similar studies have been conducted. In order for crushed glass to be viable aggregate material for beach nourishment it must be similar in size and appearance to native sand as well as react comparably to the physical forces of waves, currents, and wind. The results of a 1993 study of various physical and engineering properties of glass cullet compared to natural aggregates of comparable grain size (e.g., offshore sand) showed that all the materials tested performed very similarly to each other (Finkl *et al*., 1997). And also a study by Edge (2002) expanded on these findings by comparing the geotechnical properties of crushed glass to those of native sand in physical model experiments by using a 3-D wave basin. The basin was divided into two parts containing either crushed glass or native sand and subjected to regular waves for varying amounts of time (15-120 minutes). Beach profiles (i.e., distance the material traveled) and reflection coefficients for both materials were subsequently determined. The findings showed that crushed glass performed similarly to native sand showing little variation in beach profiles. The wave reflection coefficient for the crushed glass was slightly smaller than that for native sand, which the authors suggested indicated that crushed glass absorbs wave energy better than native sand (Edge *et al*., 2002).

In an effort to minimize negative impacts on coastal macrohabitats, a study was conducted to evaluate the effects of glass cullet on various abiotic factors. These factors were, including moisture content, temperature, and gas exchange, need to be similar to those of native sand to avoid disrupting biological performance. Test containers were filled with 100% native sand (control), 100% glass cullet, and sand/glass mixtures of 75%/25%, 50%/50%, and 25%/75%. After a two-month of period, several parameters were measured, such as water temperature, dissolved oxygen, pH, ammonia, nitrites, nitrates, hydrogen sulfide, and organic phosphate levels. Results showed no significant differences in temperature, dissolved oxygen, and pH among the five series. Although small amounts of hydrogen sulfide precipitate began to form in the absence of wave action, this disappeared once wave simulations were introduced. The study concluded that marine water chemistry was not negatively affected by recycled glass cullet contact (Makowski & Rusenko, 2007). In a separate study focusing on the effect of glass cullet on sea turtle nesting, important abiotic variables such as temperature, moisture content (dew point temperature and relative humidity), and respiratory gas exchange were measured. These variables are crucial for the sex ratios and survivability of sea turtle embryos. Simulated nesting boxes were filled with either 100% native sand (control) or sand/glass mixtures of 75%/25%, 50%/50%, and 25%/75%. Some measurements were taken over two nesting seasons, which were March through May and June through August. Analysis showed that simulated nests containing glass cullet had average temperatures (27.0–31.4°C) within the acceptable incubation range for sea turtles. Moisture content readings showed no significant differences from the beach sand controls. Similarly, high concentrations of oxygen ($> 20.0\%$) were recorded in all experimental nests containing glass cullet, with no significant variations from the beach sand controls (Makowski *et al*., 2008).

MATERIALS AND METHODS

The methodology (see flow diagram Figure 2) involves collecting data from research papers, books, websites, and the Coastal Conservation and Coastal Resource Management Department (CC and CRMD). Samples were collected from the beaches of Kalutara (Kalu river), Panadura, Moratuwa, crushed glass, and offshore sand. Each sample was sieved to obtain the D_{50} value. Design values were calculated using scaling laws (geometric, material property, wave generation). Samples were prepared by varying the proportions of crushed glass and traditional sand to test the hypothesis that incorporating crushed glass improves erosion resistance and durability of beach nourishment materials. Sediment transportation

and other relevant measurements were taken using a flume apparatus. The process was repeated for all samples, and the results were analyzed and compared to draw conclusions.
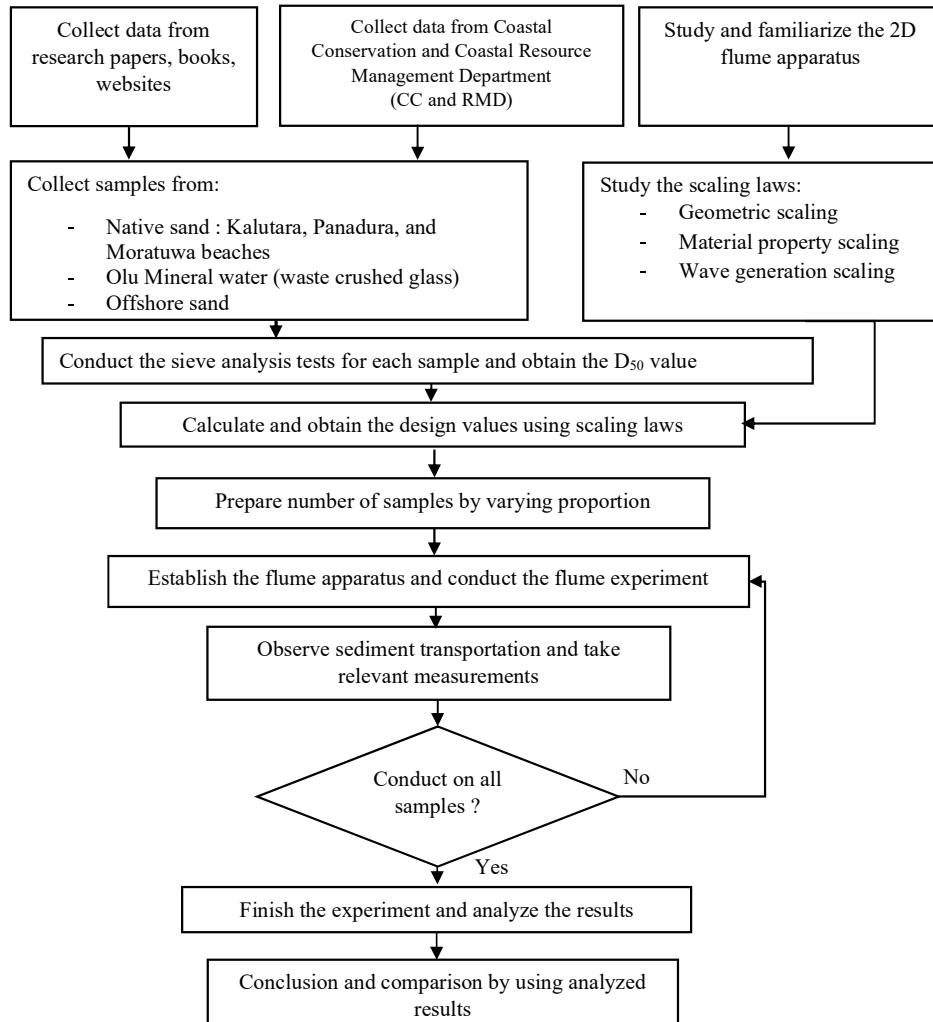
Figure 2: Methodology

Sample collection

The choice and provision of suitable materials for the model experiments affect the accuracy and reliability of the results. The four types of samples collected were:

- Native sand
- Offshore sand
- River sand, and
- Crushed glass

Five native sand samples were collected from the beaches of Kalutara, Moratuwa and Mount Lavinia.

Offshore sand samples were collected from the Muthurajawela offshore sand banks. A large sample of offshore sand was collected from sand banks that belong to "*Sanstha Weli*", after obtaining permission. River sand samples were collected from the banks of the Kalu river.

The crushed glass sample was obtained from, Liquid Island (Pvt) Ltd., Narahenpita. The glass was carefully processed, to ensure that it was crushed to the desired particle size range and free from any contaminants. It was important to select a supplier that consistently supplied crushed glass with the required characteristics for the experiment. Quality control procedures were

implemented to verify the suitability and quality of the acquired crushed glass. Glass bottles were crushed using a crusher at the company location to obtain the crushed glass.

Laboratory experiments

Grain size analysis

A field sample was used to determine the grain size and distribution in the experimental planning. These values were determined empirically after laboratory analysis of sediments collected from the corresponding coastal terrain. The study improved the reliability of the experiment by implementing the right material quality criteria. This implies that results obtained in the laboratory study matched with those observed in the natural beach environment. This enables the tracking of the behavior of the materials within an actual sediment mixture. Each sample of 2 kg was tested using the sieve analysis test with standard sieves, to determine particle size distribution and plotted to calculate the D_{50} value.

Wave flume experiment

The flume experiment is a controlled laboratory investigation used to study fluid flow in an open channel. It includes a water supply system that pumps water into the channel at a controlled rate, an inlet section for smooth flow, and flow control mechanisms such as gates or weirs. For instance, sediment transport studies may involve the addition of sediment particles to the water to observe their movement and deposition patterns. In the study, a wave generation system capable of producing a wide range of wave conditions was utilized. This system allows for the replication of realistic wave processes and the evaluation of beach nourishment materials under different wave scenarios.

Figure 3 shows the wave flume apparatus with a wave paddle and a wave generation control unit. The procedure for operating the wave flume is outlined below. First the apparatus is checked to ensure all the components such as the motor pump, gates etc are functioning properly. Then the required flume area is separated using a gate, which is sealed using modeling clay to ensure it is waterproof.
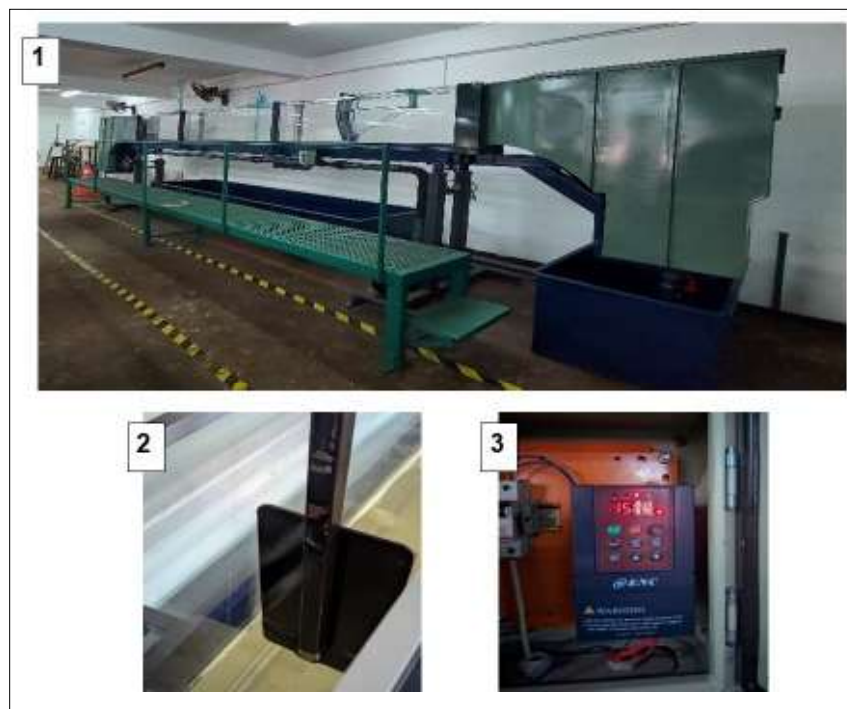

Figure 3: (1): Wave flume apparatus, (2): wave paddle, (3): wave generation control unit, Model: Hydraulic flume: HLE-100-HF-5000/150/500; preparation for experimental setup is described in the text.

Measuring lines are marked using masking tape for reference. Thereafter, the flume is filled with sediment at a 1:5 ratio to establish the desired slope. The inverter is powered on, and the frequency is set to 10 Hz. Water is added to the flume to a level of 20 cm. The inverter is started and the test is run to settle the beach slope. After a few minutes the beach slope is established and it may vary slightly. The experimental duration is set at 15 minutes. The experiments were conducted capturing the initial shape of the beach model and the slope. The inverter is stopped and the experiment results are observed. The shape of the beach (model) and the slope are adjusted as required and the experiment is repeated for two more additional trials per sediment sample. Once a sample is tested the above procedure is repeated for the remaining samples.

Scaling laws

To ensure the accuracy of the experiments, it is crucial to apply scaling laws. Specifically, geometric scaling, wave generation scaling, and material property scaling are fundamental principles that guide the experimental process. By referring to the following equations (Dalrymple, 1991), the deep sea wave length is calculated from equation 1. For shallow depths the condition for wave breaking is given by equation 2.

Deep sea wave length $(L_0) = \frac{gT_0^2}{2\pi}$ ...(1)

Where, L_0 = deep sea wave length in meters; T_0 = wave period; g = 9.81 ms^{-2}

$\frac{d_0}{L_0} = 0.7$ (since, for deep sea $\frac{d_0}{L_0} > 0.5$)   ...(2)

Where, d_0 = depth at wave breaking point

It is assumed that the model flume will be one-twelfth the size of the prototype (scale factor of 1/12), using scaling laws according to Rijn (2011) and Wang *et al.* (1990). The two free parameters were determined from the scales below. Practical standard ranges were n_h = 1 to 50 and n_{d50} = 1 to 5.

Where, n_h = Depth scale and n_{d50} = Sediment size scale.

$\left(\frac{n_l}{n_h}\right) = (n_h)^{0.28}(n_{hd50})^{-0.5}(n_{s-1})^{0.28 \text{ to } 0.5}$ ...(3)

Where, n_{s-1} = relative density scale

Equation 3 provides a relationship of the distortion scale in a physical model accounting for the median sediment size (n_{hd50}), depth scale (n_h) and relative density scale

(n_{s-1}). The range of the distortion scale (n_l/n_h) is between 1 to 2.

$(n_{Tm}) = (n_h)^{0.56}$ ...(4)

Where, n_{TM} = morphological time scale; h_m = model height

Equation 4 gives the relationship between the morphological time scale and model height. For the design, the following standard values were taken by from the above equations.

- $\left(\frac{n_l}{n_h}\right) = 2$

- $n_l = 24$

- $n_h = 12 = \frac{2.5\,m}{h_m}$

- $h_m = 0.208\,m$

Then, by using equation 5, which is given in the flume manual HLE-100-HF-5000/150/500, the number of oscillations of the wave generator is calculated.

$NOC = \left(\frac{1}{T_m \text{ flume}}\right)$ ...(5)

(Flume manual)

Where, NOC – Number of oscillations of wave generator; Tm fulme = Time taken for one complete rotation of the wave paddle

Cost analysis

The unit price of crushed glass in LKR (PGP Glass Ceylon PLC) and the unit price of offshore sand were considered. Equation 6 was generated based on the unit cost of materials.

$C = Px + Q(100 - x)$ ...(6)

C - Unit cost of CG composition
P - Unit cost of crushed glass
Q - Unit cost of offshore sand
x - Percentage of crushed glass in the composition

Where, P = the unit cost of crushed glass is varied with the amount of material, with transportation cost and electricity cost; Q = the unit cost of offshore sand is varied with the amount of material, with transportation cost and environmental concerns.

Table 1: Proportions of glass material and offshore sand in the mixtures. 5CG represents a mixture of 5% crushed glass and 95% of offshore sand

Proportion sample	Crushed glass percentage	Offshore sand percentage
5CG	5 %	95 %
10CG	10 %	90 %
15CG	15 %	85 %
20CG	20 %	80 %
25CG	25 %	75 %

xCG – Mixture of crushed glass and offshore sand, x- percentage of crushed glass

Sample preparation

Five samples of glass material and offshore sand were mixed according to the proportions shown in Table 1. In addition to these mixed samples, one sample each of river sand, native sand, and glass material were prepared (Table 1).

Figure 4 represents the CG proportion of samples prepared and Figure 5 represents the native sand sample, river sand sample, crushed glass sample and offshore sand sample.
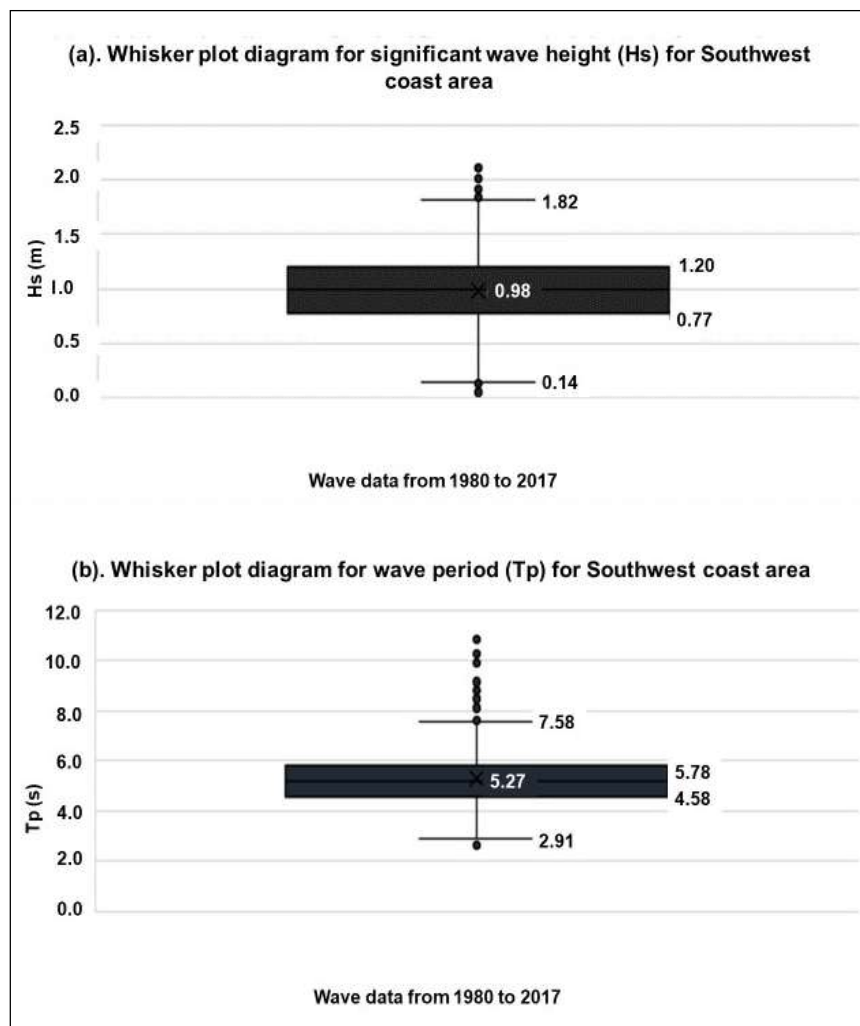

Figure 4: (a) Whisker plot diagram for significant wave height in the Southwest coastal area, and
(b) Whisker plot diagram for wave period in the Southwest coastal area

RESULTS AND DISCUSSION

Design values gained from scaling laws

Figure 6 shows the significant wave heights (Hs) and wave periods in the Southwest coastal area. Chronological data of significant wave height (H_s), and wave peak period (T_p) were collected from 1980 to 2017 (Samarasekara, 2019; Samarasekara *et al*., 2022) and the average 3rd quartile (Q_3) was calculated. These were used as design values.

Furthermore it is shown in Figure 6 (a) the significant wave height (Hs) with a median value of 0.98 m. The interquartile range (IQR) spans from 0.77 to 1.20 m, indicating moderate variability in wave heights. The second plot (b) illustrates the wave period (Tp), with a median of 5.27 seconds. The IQR ranges from 4.58 to 5.78 seconds, highlighting the typical wave period variability. The outliers extend from a maximum of 7.58 seconds to a minimum of 2.91 seconds. The average 3rd quartile (Q_3) obtained through graphs were H_s = 1.20m and T_p = 5.8s.
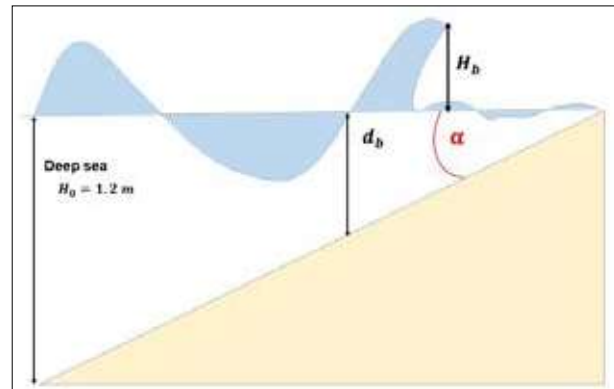
Figure 5: Wave breaking condition and related parameters

Figure 7 represents the conditions of wave breaking and related parameters. It shows that the ratio of wave height to water depth at wave breaking is 0.7 at a shallow depth (Dalrymple, 1991).

$\frac{d_0}{L_0} = 0.7$ (since, for deep sea $\frac{d_0}{L_0} > 0.5$)

Deep sea wave length (L_0) = 53 m (by using equation 1)

Table 2: Depth and height at wave breaking conditions were obtained by referring to wave tables

d_b (m)	L_0 (m)	$\frac{d_0}{L_0}$	$\sqrt{\frac{n_0 C_0}{n_2 C_2}}$	$\frac{d_b}{L_0}$	$\sqrt{\frac{n_0 C_0}{n_1 C_1}}$	H_b (m)	$\frac{H_b}{d_b}$	Condition
1.9	53	0.7	0.9988	0.0358	1.0899	1.31	0.698	$0.698 \leq 0.7$

An iterative method was used to determine the depth and height of wave breaking. Table 2 gives the depth and height measurements at the wave breaking condition, by referring to wave tables. The final comparison is made between H_b/d_b and a threshold value of 0.7, showing that 0.698 is less than or equal to 0.7. This shows that the wave height relative to water depth meets the specified threshold. Therefore, the wave breaking depth and height are 1.9 m and 1.31 m, respectively. The calculated wavelength at the wave breaking point is L = 25 m.

Experimental parameters were determined by using the following scaling laws:

- Water depth (h) = 20 cm
- Water depth at wave breaking (h_m) = 16 cm
- Sediment diameter $(d50_m)$ = Same as samples
- Experimental slope = 1:5

T_m flume = 1.44 s
NOC = 9.5f (Per minute; as flume manual)
f = 4.4 Hz

Since a frequency of 4.4 Hz produced only very small movements in the waves, a frequency of f = 10 Hz was used for all experimental trials to ensure optimum test procedures. By taking f = 10 Hz, the new design resulted in n_T = 2.56 s. This means, relatively fast waves with a higher frequency were considered.

Sediment characteristics analysis

Design values for sediment characteristics, such as grain size distribution, were utilized to create the experimental design. These values were derived from field observations and sediment sampling in the target coastal area. By incorporating the appropriate sediment

characteristics into the experimental setup, the study ensures that the materials used accurately reflect the sediment found in natural beach environments. This enables the evaluation of the materials' behaviour and performance under realistic sediment conditions. To determine the particle size distribution and D_{50} values of the samples, standard sieve analysis test was conducted on the sediment samples collected from the west coast beaches and crashed glass from Liquid Island (Pvt) Ltd. Figure 8 displays the particle size distributions for native sand samples in part (a) and the particle size distribution of offshore sand samples, crushed glass and river sand sample in part (b).
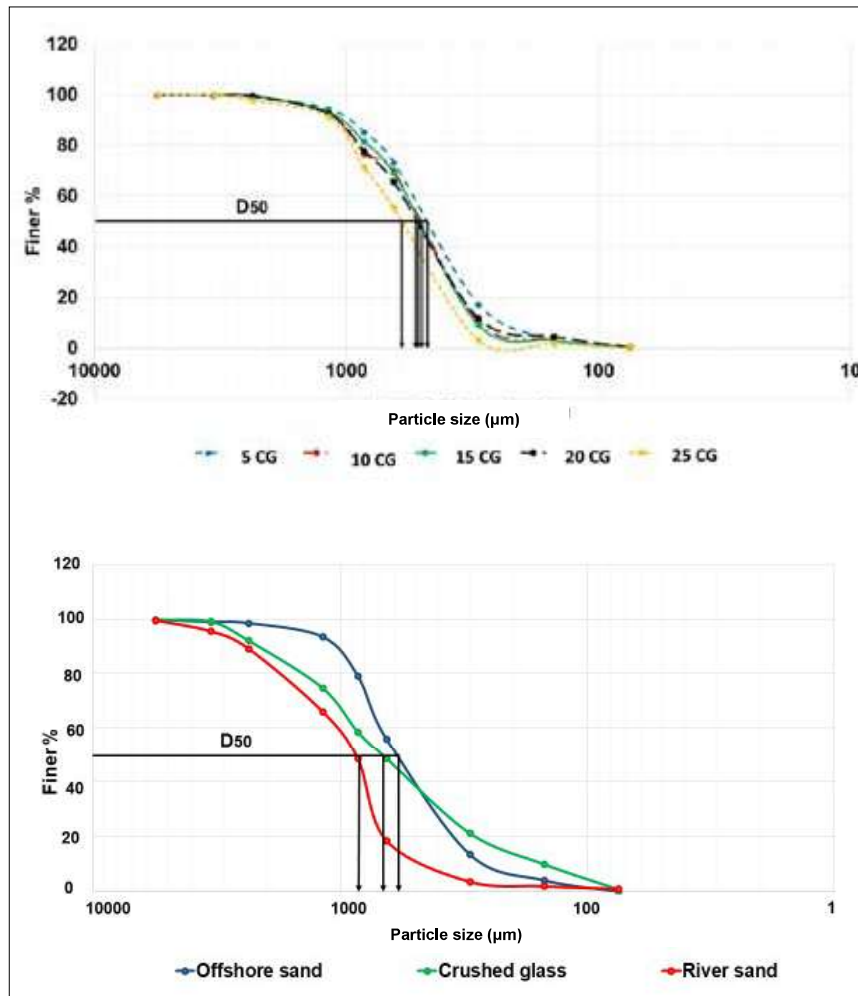
Figure 6: (a) Particle size distribution for five samples of native sand collected from the West coast area, and (b) Particle size distribution for offshore sand, crushed glass and river sand

The five native sand samples in Figure 8-(a), each sorted with D_{50} values ranging from 470 to 598 *μm,* indicate a consistent sedimentary environment characterized by similar energy conditions during deposition. The average D_{50} value was 520.6 *μm*. This offshore sand sample is also well sorted and the curve is much smoother resembling a well-curved S-type graph in Figure 8.b. The D_{50} values for the offshore sand sample was 601 *μm*, for the crushed glass sample was 676 *μm*, and for the river sand sample was 860 *μm*.

Flume experiment analysis and results

Sediments were placed in the flume at a 1:5 ratio to establish the slope. Water was added to a depth of 20 cm, and the inverter was set to 10 Hz. The initial shape of the beach model and slope were documented. The inverter was activated, and the experiment was conducted for 15 minutes.

Figure 9 shows the slope before conducting the experiment and the stabilized shapes or slopes after the experiment. Furthermore, Figure 10 shows that the schematic diagram for water level, initial slope of the beach, stabilized beach and erodible length due to wave. Eroded volume is represented as (A) and remaining volume as (B). The eroded lengths and eroded volumes were calculated in Table 3.

(a) The beach slope before conducting the experiment

(b) The stabilized shape after conducting the experiment for 5CG

(c) The stabilized shape after conducting the experiment for 10CG

(d) The stabilized shape after conducting the experiment for 15CG

(e) The stabilized shape after conducting the experiment for 20CG

(f) The stabilized shape after conducting the experiment for 25CG

(g) The stabilized shape after conducting the experiment for river sand samples

(h) The stabilized shape after conducting the experiment for offshore sand samples

(i) The stabilized shape after conducting the experiment for crushed glass samples

(j) The stabilized shape after conducting the experiment for native sand samples

Figure 7: (a) The beach slope before conducting the experiments (b) to (j). The stabilized shape after conducting the experiment for crushed glass and sand samples.

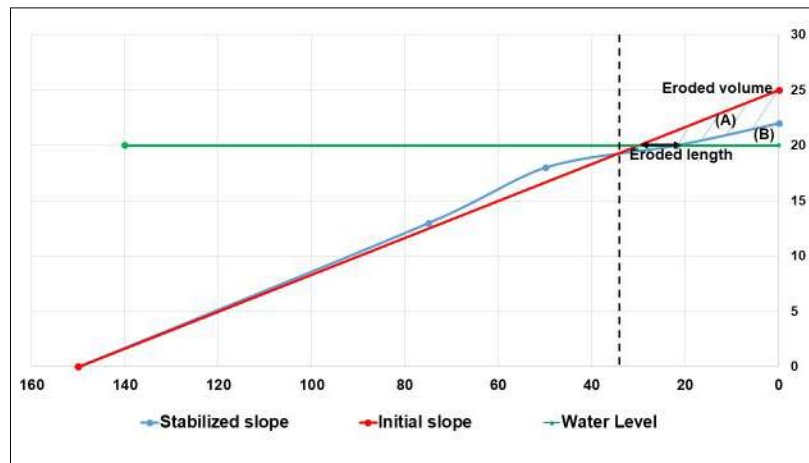**Figure 8:** Schematic diagram for water level, initial slope of the beach, stabilized beach and erodible length due to wave action

Table 3: Average eroded length, average eroded volume, unit cost and percentage of eroded volume for each sample

Sample	Average eroded length (cm)	Average eroded volume (A-cm^3)	Unit cost (LKR/m^3)	Percentage of eroded volume (A%-cm^3)
5CG	7.4	581	18575	27
10CG	7.0	526	18650	24
15CG	6.2	461	18725	22
20CG	5.0	392	18800	18
25CG	4.4	358	18875	16
River sand	6.2	525	23750	24
Offshore sand	7.4	570	18500	26
Crushed glass	3.6	302	20000	14
Native sand	6.3	471	-	22

Table 3 gives the average eroded length in cm, average eroded volume in cm^3, unit cost in LKR/m^3 and percentage of eroded volume in cm^3. The correlation coefficient (r) was -0.99, indicating a very strong inverse relationship. The coefficient of determination (R^2) was 0.976, demonstrating that 97.6% of the variability in the measured value is explained by the percentage of crushed glass. The p-value was 0.0016, confirming that the relationship is statistically significant ($p < 0.05$). This suggests that as the proportion of crushed glass content increases, the measured property decreases consistently and predictably. Overall, there is a statistically significant, strong negative linear relationship between the percentage of crushed glass and the measured value.

Sieve analysis and flume tests were conducted to evaluate the properties of the materials. The sieve analysis determined the particle size distribution and D_{50} value of each sample. Flume experiments simulated wave conditions to observe the behavior of different sand and crushed glass mixtures. These experiments provided insights into the stability and erodibility of the nourishment materials. The sieve analysis revealed that native sand and offshore sand had a higher percentage of finer particles compared to river sand and crushed glass. The D_{50} values for each sample were calculated, providing a basis for comparing the suitability of the different materials for beach nourishment. (Figure 8). Larger, well-rounded particles generally offer better

stability and resistance to erosion compared to smaller particles. The crushed glass used in this study had a varied particle size distribution but was primarily larger than the fine particles in natural sands. This contributed to the increased erosion resistance observed in the flume experiments. (CEM, 2012)

Proper compaction of nourishment materials is crucial for stability. The study ensured consistent compaction techniques across all samples, which helped isolate the effects of material composition on erosion resistance. The crushed glass mixtures benefited from the inherent density and interlocking properties of glass particles, enhancing stability.

The flume experiments revealed that mixtures containing crushed glass displayed different erosion patterns compared to those with only natural sand. The following trends were observed:

- **Native sand**: Showed moderate erosion, with an average eroded length of 6.3 cm and an average eroded volume of 471 cm³. The eroded volume percentage was 22% (Table 3)
- **Offshore sand**: Demonstrated similar erosion characteristics to native sand, with an average eroded length of 7.4 cm and an average eroded volume of 570 cm³ having 26% eroded volume (Table 3)
- **River sand**: The erosion resistance compared to offshore sand was lower, with an average eroded length of 6.2 cm and an average eroded volume of 525 cm³. Furthermore, the eroded volume percentage was 24%. (Table 3)
- **Crushed glass:** Showed minimal erosion, with an average eroded length of 3.6 cm and an average eroded volume of 302 cm³. This had the lowest eroded percentage of 14% (Table 3)
- **Crushed glass and offshore sand mixtures**: The erosion resistance increased with higher percentages of crushed glass. For instance, the 25% crushed glass mixture (25CG) had the lowest average eroded length of 4.4 cm and an average eroded volume of 358 cm³. The percentage of eroded volume varied from 16% (for CG25) to 27% (for CG5). (Table 3)

Additionally, Table 3 illustrates the relationship between the unit cost of CG compositions and the eroded volume of relevant compositions. It shows a linear increase from CG5 to CG25, with costs ranging from 18,575 LKR/m³ to 18,875 LKR/m³. This suggests that higher CG compositions incur higher unit costs. The eroded volume decreases from 581 cm³ for CG5 to 358

cm³ for CG25. This indicates that higher CG compositions result in lesser erosion, suggesting better durability. The trade-off between cost and durability, shows that higher CG compositions are more expensive, but offer better resistance to erosion (Table 3). The decreasing eroded volume trend underscores the improved performance of higher CG compositions in minimizing erosion, despite their increased cost. This information is critical for decision-making in optimizing beach nourishment compositions for coastal protection.

Environmental and economic considerations

Incorporating crushed glass in beach nourishment projects not only addresses the issue of coastal erosion but also provides an environmentally friendly solution for managing glass waste. Glass is a non-biodegradable material that poses environmental hazards if not properly managed. Utilizing it in coastal protection projects aligns with sustainable waste management practices (Griggs, 2023). Economically, crushed glass can be a cost-effective alternative to traditional sand sources, especially in regions where sand mining is restricted or expensive. The availability of waste glass in urban areas of Sri Lanka makes it a viable option for large-scale beach nourishment projects.

Challenges in using crushed glass

Using crushed glass for beach nourishment in Sri Lanka poses several challenges. Environmental concerns include potential habitat disruption and the risk of chemical leaching (Kenoin, 1997). Logistical issues involve the collection, processing, and transportation of glass, which can be costly and complex since currently there is no proper method to collect waste glass in the country. Economically, the high initial costs and the need for a sustainable market are significant hurdles. Social acceptance and regulatory compliance are also critical, as public perception and legal standards must be addressed. Additionally, technical challenges such as performance monitoring and adaptation to local conditions must be overcome to ensure the effectiveness and safety of using crushed glass in coastal protection efforts because of the lack of technology in Sri Lanka (Saja *et al*., 2022).

Future availability of crushed glass

Sri Lanka generates approximately 7000 MT of solid waste per day. Of this, glass waste accounts for 2.03% (i.e., around 140 MT) and annually is about 50,000 MT – 55,000 MT (Darmasiri, 2019).

Study limitations

The study has several notable limitations, as sample collection was geographically restricted to specific beaches, potentially overlooking broader sediment variability across Sri Lanka's coastline. The data used for scaling laws was limited to the Southwest coastal area. Further, laboratory experiments were conducted under controlled conditions, which might not fully represent the complex and dynamic nature of actual coastal environments. The study utilized a single wave generation system, limiting the scope of wave conditions tested and there was no measurement gauge to measure the wave conditions generated. It also focused on a limited set of materials and short-term observations, without addressing long-term erosion effects or comprehensive economic and ecological impacts.

CONCLUSION

The inclusion of crushed glass in beach nourishment compositions presents a promising approach to enhancing coastal protection in Sri Lanka. The study demonstrates that crushed glass can enhance the erosion resistance of nourishment materials, providing a viable alternative to traditional sand sources. Based on these findings, offshore sand appears to have the least performance in terms of sediment transport and potential durability among the materials. However, the results suggest that mixtures with higher percentages of crushed glass exhibit superior erosion resistance compared to traditional sand materials. These findings have significant implications for future coastal management strategies, offering a sustainable and cost-effective solution to combat coastal erosion while addressing waste management challenges. The integration of crushed glass in beach nourishment compositions offers a sustainable and effective solution for coastal protection in Sri Lanka. Referring to Table 3, the best optimized beach nourishment composition for coastal protection in Sri Lanka is between CG10 and CG20. Therefore, by adopting innovative and environmentally friendly approaches, Sri Lanka can strengthen its coastal defenses and ensure the long-term resilience of its coastal ecosystems and communities. The promising results of this study open several avenues for future research. Long-term monitoring of beach nourishment projects using crushed glass will be essential to assess durability and ecological impacts over time. Collaboration with international researchers and institutions can also provide valuable insights and facilitate the exchange of best practices in coastal management. Future research should focus on long-term field studies to validate laboratory findings and assess ecological impacts. Additionally, exploring optimal crushed glass and sand proportions for different coastal settings can further refine and maximize benefits. Finally, expanding geographic sampling and wave condition testing will strengthen understanding and application of crushed glass in diverse coastal environments.

Acknowledgement

REFERENCES

Atkinson, A. L., and Baldock, T. E. (2020). Laboratory investigation of nourishment options to mitigate sea level rise induced erosion. *Coastal Engineering*, *161*, 103769. https://doi.org/10.1016/ j. coastaleng.2020.103769

Beach nourishment (U.S. National Park Service). (2020). Nps. gov. https://www.nps.gov/articles/beachnourishment.htm

Central Environmental Authority. (2014). Annual report 2014. Central Environmental Authority of Sri Lanka. https://www.parliament.lk/uploads/documents/paperspresented/annual-report-central-environmental-authority-2014.pdf

Dalrymple, R. W. (1991). Coastal sedimentary environments (2nd ed.). Springer-Verlag.

de Oliveira, V. N., Gitirana, G. F. N., Jr., dos Anjos Mascarenha, M. M., Sales, M. M., Varrone, L. F. R., & da Luz, M. P. (2021). An enhanced flume testing procedure for the study of rill erosion. *Water*, *13*(21), Article 2956. https://doi.org/10.3390/w13212956

de Schipper, M. A., Luijendijk, A. P., van der Molen, J., Stive, M. J. F., & Ranasinghe, R. (2018). A field-scale experiment on the effects of a mega-nourishment on coastal safety. *Coastal Engineering*, *136*, 99–110. https://doi.org/10.1016/j.coastaleng.2018.02.005

Dette, H. H., Larson, M., Murphy, J., Newe, J., Peters, K., Reniers, A., and Steetzel, H. (2002). Application of prototype flume tests for beach nourishment assessment. *Coastal Engineering*, *47*(2), 137–177. https://doi.org/10.1016/s0378-3839(02)00124-2

Dharmasiri, M. L. (2019). Waste management in Sri Lanka: Challenges and opportunities. *Sri Lanka Journal of Advanced Social Studies*, *9*(1), 72–85. https://doi.org/10.4038/sljass.v9i1.7149

Edge, B. L., Cruz-Castro, O., and Magoon, O. T. (2002). Recycled glass for beach nourishment. In Proceedings of the 28th International Conference on Coastal Engineering (pp. 3630–3641). World Scientific.

Finkl, C. W., and Kerwin, L. (1997). Emergency beach fill

from glass cullet: An environmentally green management technique for mitigating erosional 'hot spots' in Florida. Proceedings of the 10th Annual National Conference on Beach Preservation Technology, 304–319.

Griggs, G. (2023, March 26). 'Recycling' glass back to sand for beaches? Coastal Care. https://coastalcare.org/2023/03/recycling-glass-back-to-sand-for-beachnourishment/

Guimarães, A., Coelho, C., Veloso-Gomes, F., & Silva, P. A. (2021). 3D physical modeling of an artificial beach nourishment: Laboratory procedures and nourishment performance. *Journal of Marine Science and Engineering*, *9*(6), 613. https://doi.org/10.3390/jmse9060613

Hanson, H., Brampton, A., Capobianco, M., Dette, H. H., Hamm, L., Laustrup, C., Lechuga, A., and Spanhoff, R. (2002). Beach nourishment projects, practices, and objectives—a European overview. *Coastal Engineering*, *47*(2), 81–111.

Jayathilaka, R., Ratnayake, N. P., Wijayaratna, N., & Arulananthan, K. (2023). A review of coastal erosion mitigation measures on Sri Lanka's western coast, an island nation in the Indian Ocean: Current gaps and future directions. *Ocean & Coastal Management*, *242*, Article 106653. https://doi.org/10.1016/j.ocecoaman.2023.106653

Jayathilake, D. (2020). Mount Lavinia beach nourishment project successful – DG Coastal Conservation Dept. https://www.defence.lk/Article/view_article/1679

Kerwin, L. (1997). Potential applications for recycled glass in beach management: Emergency stabilization of "hot spots" in Broward County, Florida (Master's thesis). Florida Atlantic University.

Makowski, C., and Rusenko, K. (2007). Recycled glass cullet as an alternative beach fill material: Results of biological and chemical analyses. *Journal of Coastal Research*, *23*(3), 545–552.

Makowski, C., Finkl, C. W., and Rusenko, K. (2013). Suitability of recycled glass cullet as artificial dune fill along coastal environments. *Journal of Coastal Research*, *29*(4), 772–782.

Makowski, C., Rusenko, K., and Kruempel, C. J. (2008). Abiotic suitability of recycled glass cullet as an alternative sea turtle nesting substrate. *Journal of Coastal Research*, *24*(3), 771–779.

Maliq, R. (2015). Beach nourishment in Sri Lanka. Rukshan Maliq's Blog. https://rukshanmaliq.blogspot.com/2015/01/beach-nourishment-in-sri-lanka.html

Miller, B. (2018). 20 beach renourishment pros and cons. Green Garage. https://greengarageblog.org/20-beach-renourishment-pros-and-cons

Pagán, J. I., *et al*. (2021). Classification of sediment quality according to its behavior in the accelerated particle wear test (APW). *Sustainability*, *13*(5), 2633. https://doi.org/10.3390/su13052633

Pan, S. (2011). Modelling beach nourishment under macro-tide conditions. *Journal of Coastal Research*, (64), 6.

Pranzini, E., Anfuso, G., and Muñoz-Perez, J. J. (2018). A probabilistic approach to borrow sediment selection in beach nourishment projects. *Coastal Engineering*, *139*,

32–35.

Saja, A. M. A., Zimar, A. M. Z., and Junaideen, S. M. (2021). Municipal solid waste management practices and challenges in the southeastern coastal cities of Sri Lanka. *Sustainability*, *13*(8), 4556. https://doi. org/10.3390/su13084556

Samarasekara, R. S. M. (2019). Evaluation of coastal erosion processes and management in a developing country: A case study in Marawila Beach, Sri Lanka (Unpublished master's thesis). The University of Tokyo.

Samarasekara, R. S. M., Gijsman, R., Ganal, C., Mielck, F., Wolbring, J., Hass, H. C., Goseberg, N., Schüttrumpf, H., Schlurmann, T., & Schimmels, S. (2022). The sustainability of beach nourishments: A review of nourishment and environmental monitoring practice [Preprint]. OSF. https://doi.org/10.31223/osf.io/knrvw

Samarasekara, R. S. M., Sasaki, J., Jayaratne, R., Suzuki, T., Ranawaka, R. A. S., & Pathmasiri, S. D. (2018). Historical changes in the shoreline and management of Marawila Beach, Sri Lanka, from 1980 to 2017. *Ocean & Coastal Management*, *165*, 370–384. https://doi.org/10.1016/j.ocecoaman.2018.09.012

Schirmer, M. (2017). The sustainability of beach nourishments: A review of nourishment and environmental monitoring practice. *Journal of Coastal Conservation*, *21*(5), 873–884.

Staudt, F., Gijsman, R., Ganal, C., Mielck, F., Wolbring, J., Hass, H. C., Goseberg, N., Schüttrumpf, H., Schlurmann, T., & Schimmels, S. (2021). The sustainability of beach nourishments: A review of nourishment and environmental monitoring practice. *Journal of Coastal Conservation*, *25*(2), Article 34. https://doi.org/10.1007/s11852-021-00801-y

Staudt, F., Gijsman, R., Ganal, C., Mielck, F., Wolbring, J., Hass, H. C., Goseberg, N., Schüttrumpf, H., Schlurmann, T., & Schimmels, S. (2022). The sustainability of beach nourishments: A review of nourishment and environmental monitoring practice [Preprint]. OSF. https://doi.org/10.31223/osf.io/knrvw

Stronkhorst, J., Huisman, B., Giardino, A., Santinelli, G., & Mulder, J. (2018). Sand nourishment strategies to mitigate coastal erosion and sea level rise at the coasts of Holland (The Netherlands) and Aveiro (Portugal) in the 21st century. *Ocean & Coastal Management*, *156*, 266–278. https://doi.org/10.1016/j.ocecoaman.2017.11.017

The Coastal Engineering Manual. (2006). U.S. Army Corps of Engineers.

U.S. Army Corps of Engineers. (2012). Coastal engineering manual (EM 1110-2-1100). U.S. Army Engineer Research and Development Center.

van Rijn, L. C., Tonnon, P. K., Sánchez-Arcilla, A., Cáceres, I., & Grüne, J. (2011). Scaling laws for beach and dune erosion processes. *Coastal Engineering*, *58*(7), 623–636. https://doi.org/10.1016/j.coastaleng.2011.01.008

Wang, H., Toue, T., and Dette, H. (1990). Movable bed modeling criteria for beach profile response. In Proceedings of the 22nd ICCE (Vol. 3, pp. 2566 2579). Delft, The Netherlands.

RESEARCH ARTICLE

Ordered Random Variables

On recursive computation for the moments of generalized order statistics for the Kumaraswamy family of distributions with characterizations

SH Shahbaz* and **MQ Shahbaz**
Department of Statistics, Faculty of Science, King Abdulaziz University, Jeddah, Saudi Arabia.

Abstract: The generalized order statistics (GOS) is a unified model for random variables that are arranged in increasing order of magnitude. Several other models for increasingly arranged random variables appear as special cases of *GOS*. The distributional properties of generalized order statistics for specific baseline distributions have been studied by various authors. One specific domain of study in the context of generalized order statistics is to develop some recursive formulae to obtain moments of the distribution of generalized order statistics for any baseline distribution. The relations for the moments of generalized order statistics for families of distributions have not been explored much. This paper is based on some recursive relations to compute the single and joint moments of generalized order statistics for the Kumaraswamy family of distributions. These relations are useful to recursively compute the single and joint moments of generalized order statistics for any member of the Kumaraswamy family of distributions. We illustrate the results with examples using different baseline distributions. Additionally, we present some characterization results using single and joint moments of GOS.

Keywords: Characterizations, generalized order statistics, Kumaraswamy family of distributions, recurrence relations.

INTRODUCTION

In some practical situations, the data being studied is double-bounded, so a suitable double-bounded distribution is needed. Several such distributions are available in the literature. The beta distribution is one such distribution that can be used to model this type of data.

For a continuous random variable w, the probability density and cumulative distribution function of the beta distribution are

$$g(w) = \frac{1}{B(a,b)} w^{a-1} (1-w)^{b-1} ; \ 0 < w < 1 , \ (a,b) > 0$$

and

$$G(w) = I_x(a,b) = \frac{B_x(a,b)}{B(a,b)} = \frac{1}{B(a,b)} \int_0^x v^{a-1}(1-v)^{b-1} dv,$$

where a and b are the shape parameters, $B(a,b)$, $B_x(a,b)$, and $I_x(a,b)$ are, the complete beta function, the incomplete beta function, and the incomplete beta function ratio, respectively, that are defined as

$$B(a,b) = \int_0^1 v^{a-1} (1-v)^{b-1} du ; \ B_x(a,b) =$$

$$\int_0^x v^{a-1} (1-v)^{b-1} du ; \ I_x(a,b) = \frac{B_x(a,b)}{B(a,b)} .$$

One disadvantage of the beta distribution is that its cumulative distribution function (cdf) $G(w)$ is not in the compact form. A simple, yet powerful, alternative to the

* Corresponding author (mkmohamad@kau.edu.sa; https://orcid.org/0000-0002-0695-1216)

beta distribution for modeling of [0,1] bounded data is the Kumaraswamy distribution (Kumaraswamy, 1980). The probability density and cumulative distribution functions of the Kumaraswamy distribution are

$$g(w;a,b) = abw^{a-1}(1-w^a)^{b-1} \; ; \; 0 < w < 1 \; ; \; a,b > 0$$

...(1)

and $G(w) = 1 - (1-w^a)^b \; ; \; 0 < z < 1 \; ; \; a,b > 0$,

...(2)

respectively. The Kumaraswamy distribution has extensive applications in various domains of life, including hydrology. The distribution has also been used as an alternative to the beta distribution as its cumulative distribution function (cdf) is in a compact form (Jones, 2009).

The generalized order statistics (GOS) (Kamps, 1995) and the dual generalized order statistics (DGOS) (Burkschat *et al*., 2003) are two unified models to study the distributional properties arranged in increasing or decreasing order. The probability density function (pdf) of a single GOS and the joint pdf of two GOS for a sample of size *n* is are (Kamps, 1995)

$$f_{r:n,m,k}(w) =$$

$$\frac{C_{r-1}}{(r-1)!} f(w)[\bar{F}(w)]^{\gamma_r-1} \tau_m^{r-1}[F(w)]; w \in \mathbb{R},$$

...(3)

and

$$f_{r,s:n,m,k}(w_1, w_2) =$$

$$\frac{C_{s-1}}{(r-1)!(s-r-1)!} f(w_1) f(w_2) \left[\bar{F}(w_1) \right]^m \tau_m^{r-1} \left[F(w_1) \right]$$

$$\times \left[\bar{F}(w_2) \right]^{\gamma_s-1} \left[\varphi_m\{F(w_1)\} - \varphi_m\{F(w_2)\} \right]^{s-r-1}$$

$$-\infty < w_1 < w_2 < \infty$$

...(4)

respectively, where $\bar{F}(w) = 1 - F(w)$,

$\gamma_r = k + (n-r)(m+1)$, $C_{r-1} = \prod_{j=1}^r \gamma_j$

and

$$\varphi_m(v) = \begin{cases} -(1-v)^{m+1}/(m+1) & ; \; m \neq -1 \\ -\ln(1-v) & ; \; m = -1. \end{cases} ;$$

$$\tau_m(v) = \begin{cases} \left[1 - (1-v)^{m+1} \right]/(m+1); & m \neq -1 \\ -\ln(1-v) & m = -1. \end{cases}$$

Various distributional methods for modeling random variables arranged in ascending order appear as a special case of GOS. The ordinary order statistics appear as a special case when $m = 0$ and $k = 1$. The *k*th upper records appear as a special case when $m = -1$. Several textbooks, such as Ahsanullah and Nevzorov (2001) and Shahbaz *et al*. (2016), provide detailed discussions on GOS. Much of the research in this area focuses on deriving formulas for the recursive calculation of GOS moments for various baseline distributions. In addition, some authors have used GOS moments to obtain characterization results.

The recurrence relations for moments of GOS for the exponential distribution (Ahsanullah, 2000) and Rayleigh distribution (Mohsin *et al*., 2010) are some useful illustrations of the recurrence relations for moments of GOS. The development of the recurrence relations for moments of DGOS has also been an area of interest. Some examples of recurrence relations for the moments of dependent generalized order statistics for well-known distributions, such as the power function distribution, are given by Pawlas and Szynal (2001) and Athar and Faizan (2011). Kumar (2011) also provided recurrence relations for the moments of GOS from the Kumaraswamy distribution, along with some characterizations. In addition, a general formula showing the relationship between single and joint moments of GOS is available in Athar and Islam (2004), which is useful for developing recurrence relations for specific cases.

MATERIALS AND METHODS

The Kumaraswamy distribution has been used as a baseline distribution to propose a new family of distributions, known as the Kumaraswamy family of distributions (Cordeiro & Castro, 2011). The cdf and probability density function (pdf) of the Kumaraswamy generated (*Kum–G*) family of distributions are

$$F_G(w) = 1 - [1 - H^a(w; \xi)]^b; w \in \mathbb{R}$$

...(5)

and

$$f_G(w) = abh(w;\xi)[H(x;\xi)]^{a-1}[1 - H^a(w;\xi)]^{b-1};$$

$$w \in \mathbb{R}, \qquad\qquad ...(6)$$

respectively, where $H(w;\xi)$ and $h(w;\xi)$ are the *cdf* and *pdf* of any baseline distribution, and ξ is the vector of parameters of the baseline distribution $H(x;\xi)$. It is to be noted that the *exponentiated–G* family of distributions; (Gupta *et al*., 1998; Nadarajah & Kotz, 2006), appears as a special case of the *Kum–G* family of distributions for $b = 1$.

The Kum–G family of distributions has gained the interest of many researchers, leading to the development of several new distributions based on different baseline distributions. A Kumaraswamy inverse Weibull distribution has been proposed by using the inverse Weibull distribution as a baseline distribution in (3) (Shahbaz *et al*., 2012). A Kumaraswamy power function distribution has been proposed by using the power function baseline distribution in the *Kum–G* family of distributions (Abdul-Moniem, 2017), whereas a Kumaraswamy log-logistic distribution has been proposed by using the log-logistic distribution in (3) (de Santana *et al*., 2012).

In this paper, some recurrence relations for moments of GOS for the *Kum–G* family of distributions have been obtained. These relations are obtained in the following sections.

Recurrence relation for the single moments

This section deals with the recurrence relation for single moments of GOS for the Kumaraswamy family of distributions. The recurrence relation is obtained by first noting the following relation between the density and distribution function of the *Kum–G* family of distributions

$$\bar{F}(w) = \frac{1}{ab}r_H^{-1}(w)\left[H^{-a}(w) - 1\right]f(w) \qquad ...(7)$$

where $r_H(w) = h(w)/H(w)$ is the reversed hazard rate function of the baseline distribution $H(w)$. The relation (7) is useful in deriving a recurrence relation for moments of GOS for the Kumaraswamy family of distributions. The recurrence relation for single moments of GOS for the *Kum–G* distribution is derived in the following theorem.

Theorem–1: The single moments of GOS for the *Kum–G* family of distributions are related as

$$E\left(W_{r:n,m,k}^p\right) - E\left(W_{r-1:n,m,k}^p\right) =$$

$$\frac{p}{ab\gamma_r}\left[E\left\{\Phi\left(W_{r:n,m,k}\right)\right\} - E\left\{\Delta\left(W_{r:n,m,k}\right)\right\}\right], \qquad ...(8)$$

where $\quad \Phi(w) = w^{p-1}r_H^{-1}(w)H^{-a}(w) \quad$ and $\quad \Delta(w) = w^{p-1}r_H^{-1}(w)$.

Proof: Consider the following relation for the single moments of GOS for any parent distribution, (Athar & Islam, 2004),

$$E\left(W_{r:n,m,k}^p\right) - E\left(W_{r-1:n,m,k}^p\right) = \frac{pC_{r-1}}{\gamma_r(r-1)!}\int_{-\infty}^{\infty} w^{p-1}\left[\bar{F}(w)\right]^{\gamma_r}\tau_m^{r-1}\left[F(w)\right]dw \quad \text{or}$$

$$E\left(W_{r:n,m,k}^p\right) - E\left(W_{r-1:n,m,k}^p\right) = \frac{pC_{r-1}}{\gamma_r(r-1)!}\int_{-\infty}^{\infty} w^{p-1}\bar{F}(w)\left[\bar{F}(w)\right]^{\gamma_r-1}\tau_m^{r-1}\left[F(w)\right]dw. \qquad ...(9)$$

Now, using (7) in (9), we have

$$E\left(W_{r:n,m,k}^p\right) - E\left(W_{r-1:n,m,k}^p\right) = \frac{pC_{r-1}}{ab\gamma_r(r-1)!}\int_{-\infty}^{\infty} w^{p-1}\left[r_H^{-1}(w)\left\{H^{-a}(w) - 1\right\}\right]f(w)$$

$$\times\left[\bar{F}(w)\right]^{\gamma_r-1}\tau_m^{r-1}\left[F(w)\right]dw$$

or $\quad E\left(W_{r:n,m,k}^{p}\right) - E\left(W_{r-1:n,m,k}^{p}\right) = \dfrac{pC_{r-1}}{ab\gamma_{r}\left(r-1\right)!}\displaystyle\int_{-\infty}^{\infty}\left[w^{p-1}r_{H}^{-1}\left(w\right)H^{-a}\left(w\right)\right]f\left(w\right)\left[\overline{F}\left(w\right)\right]^{\gamma_{r}-1}$

$$\times \tau_{m}^{r-1}\left[F\left(w\right)\right]dw - \dfrac{pC_{r-1}}{ab\gamma_{r}\left(r-1\right)!}\int_{-\infty}^{\infty}\left[w^{p-1}r_{H}^{-1}\left(w\right)\right]f\left(w\right)\left[\overline{F}\left(w\right)\right]^{\gamma_{r}-1}\tau_{m}^{r-1}\left[F\left(w\right)\right]dw$$

or $\quad E\left(W_{r:n,m,k}^{p}\right) - E\left(W_{r-1:n,m,k}^{p}\right) = \dfrac{p}{ab\gamma_{r}}\left[E\left\{\Phi\left(W_{r:n,m,k}\right)\right\} - E\left\{\Delta\left(W_{r:n,m,k}\right)\right\}\right]\quad,$

where $\Phi\left(w\right) = w^{p-1}r_{H}^{-1}\left(w\right)H^{-a}\left(w\right)$ and $\Delta\left(w\right) = w^{p-1}r_{H}^{-1}\left(w\right)$, then the theorem is complete.

Since the exponentiated–*G* family of distributions appears as a special case of the *Kum–G* family of distributions for *b* = 1, the recurrence relation for single moments of GOS for the *exponentiated–G* family of distributions can be readily written from (8). The recurrence relations for single moments of special cases of GOS can also be easily written from (8). For example, the recurrence relation for single moments of upper record values is obtained by using *m* = –1 in (8) and is given as

$$E\left(W_{K(r)}^{p}\right) - E\left(W_{K(r-1)}^{p}\right) =$$

$$\dfrac{p}{abk}\left[E\left\{\Phi\left(W_{K(r)}\right)\right\} - E\left\{\Delta\left(W_{K(r)}\right)\right\}\right]$$

$$\dots(10)$$

The relation (8) can be used to obtain the recurrence relation for other special cases.

Recurrence relation for the joint moments

In this section, we have obtained the recurrence relation for the joint moments of GOS for the *Kum–G* family of distributions. The recurrence relation is obtained in the following theorem.

Theorem–2: The joint moments of GOS for the *Kum–G* family of distributions are related as

$$E\left(W_{r:n,m,k}^{p_{1}}W_{s:n,m,k}^{p_{2}}\right) - E\left(W_{r:n,m,k}^{p_{1}}X_{s-1:n,m,k}^{p_{2}}\right) =$$

$$\dfrac{p_{2}}{ab\gamma_{s}}\left[E\left\{\Phi\left(W_{r:n,m,k}W_{s:n,m,k}\right)\right\}\right.$$

$$\left. - E\left\{\Delta\left(W_{r:n,m,k}W_{s:n,m,k}\right)\right\}\right],$$

$$\dots(11)$$

where

$$\Phi\left(W_{r:n,m,k}W_{s:n,m,k}\right) = w_{1}^{p_{1}}w_{2}^{p_{2}-1}r_{H}^{-1}\left(w_{2}\right)H^{-a}\left(w_{2}\right) \text{ and } \Delta\left(W_{r:n,m,k}W_{s:n,m,k}\right) = x_{1}^{p_{1}}x_{2}^{p_{2}-1}r_{H}^{-1}\left(w_{2}\right).$$

Proof: Consider the following relation (Athar and Islam, 2004) for the joint moments of *GOS* for any parent distribution

$$E\left(W_{r:n,m,k}^{p_{1}}W_{s:n,m,k}^{p_{2}}\right) - E\left(W_{r:n,m,k}^{p_{1}}W_{s-1:n,m,k}^{p_{2}}\right) = \dfrac{p_{2}C_{s-1}}{\gamma_{s}\left(r-1\right)!\left(s-r-1\right)!}\int_{-\infty}^{\infty}\int_{w_{1}}^{\infty}w_{1}^{p_{1}}w_{2}^{p_{2}-1}f\left(w_{1}\right)\left[\overline{F}\left(w_{1}\right)\right]^{m}$$

$$\times \tau_{m}^{r-1}\left[F\left(w_{1}\right)\right]\left[\varphi_{m}\left\{F\left(w_{2}\right)\right\} - \varphi_{m}\left\{F\left(w_{1}\right)\right\}\right]^{s-r-1}\left[\overline{F}\left(w_{2}\right)\right]^{\gamma_{s}}dw_{2}dw_{1},$$

$$E\left(W_{r:n,m,k}^{p_{1}}W_{s:n,m,k}^{p_{2}}\right) - E\left(W_{r:n,m,k}^{p_{1}}W_{s-1:n,m,k}^{p_{2}}\right) = \dfrac{p_{2}C_{s-1}}{\gamma_{s}\left(r-1\right)!\left(s-r-1\right)!}\int_{-\infty}^{\infty}\int_{w_{1}}^{\infty}w_{1}^{p_{1}}w_{2}^{p_{2}-1}f\left(w_{1}\right)$$

or $\qquad\qquad \times \left[\overline{F}\left(w_{1}\right)\right]^{m}\tau_{m}^{r-1}\left[F\left(w_{1}\right)\right]\left[\varphi_{m}\left\{F\left(w_{2}\right)\right\} - \varphi_{m}\left\{F\left(w_{1}\right)\right\}\right]^{s-r-1}\times\overline{F}\left(w_{2}\right)\left[\overline{F}\left(w_{2}\right)\right]^{\gamma_{s}-1}dw_{2}dw_{1}.\qquad \dots(12)$

Now, using (7) in (12), we have

$$E\left(W_{r:n,m,k}^{P_1}W_{s:n,m,k}^{P_2}\right)-E\left(W_{r:n,m,k}^{P_1}W_{s-1:n,m,k}^{P_2}\right)=\frac{qC_{s-1}}{ab\gamma_s\left(r-1\right)!\left(s-r-1\right)!}\int_{-\infty}^{\infty}\int_{w_1}^{\infty}w_1^{P_1}w_2^{P_2-1}\left[r_H^{-1}\left(w_2\right)\right.$$

$$\times\left\{H^{-a}\left(w_2\right)-1\right\}\right]f\left(w_1\right)f\left(w_2\right)\left[\bar{F}\left(w_1\right)\right]^m\tau_m^{r-1}\left[F\left(w_1\right)\right]$$

$$\times\left[\varphi_m\left\{F\left(w_2\right)\right\}-\varphi_m\left\{F\left(w_1\right)\right\}\right]^{s-r-1s-r-1}\left[\bar{F}\left(w_2\right)\right]^{\gamma_s-1}dw_2dw_1.$$

$$E\left(W_{r:n,m,k}^{P_1}W_{s:n,m,k}^{P_2}\right)-E\left(W_{r:n,m,k}^{P_1}W_{s-1:n,m,k}^{P_2}\right)=\frac{p_2C_{s-1}}{ab\gamma_s\left(r-1\right)!\left(s-r-1\right)!}\int_{-\infty}^{\infty}\int_{w_1}^{\infty}\left[w_1^{P}w_2^{P_2-1}r_H^{-1}\left(w_2\right)H^{-a}\left(w_2\right)\right]$$

$$\times f\left(w_1\right)f\left(w_2\right)\left[\bar{F}\left(w_1\right)\right]^m\tau_m^{r-1}\left[F\left(w_1\right)\right]\left[\varphi_m\left\{F\left(w_2\right)\right\}-\varphi_m\left\{F\left(w_1\right)\right\}\right]^{s-r-1s-r-1}$$

or
$$\times\left[\bar{F}\left(w_2\right)\right]^{\gamma_s-1}dw_2dw_1-\frac{p_2C_{s-1}}{ab\gamma_s\left(r-1\right)!\left(s-r-1\right)!}\int_{-\infty}^{\infty}\int_{w_1}^{\infty}\left[w_1^{P}w_2^{P_2-1}r_H^{-1}\left(w_2\right)\right]$$

$$\times f\left(w_1\right)f\left(w_2\right)\left[\bar{F}\left(w_1\right)\right]^m\tau_m^{r-1}\left[F\left(w_1\right)\right]\left[\varphi_m\left\{F\left(w_2\right)\right\}-\varphi_m\left\{F\left(w_1\right)\right\}\right]^{s-r-1s-r-1}$$

$$\times\left[\bar{F}\left(w_2\right)\right]^{\gamma_s-1}dw_2dw_1$$

or $\qquad E\left(W_{r:n,m,k}^{P_1}W_{s:n,m,k}^{P_2}\right)-E\left(W_{r:n,m,k}^{P_1}W_{s-1:n,m,k}^{P_2}\right)=\frac{p_2}{ab\gamma_s}\left[E\left\{\Phi\left(W_{r:n,m,k}W_{s:n,m,k}\right)\right\}-E\left\{\Delta\left(W_{r:n,m,k}W_{s:n,m,k}\right)\right\}\right],$

where $\Phi\left(W_{r:n,m,k}W_{s:n,m,k}\right)=w_1^{P_1}w_2^{P_2-1}r_H^{-1}\left(w_2\right)H^{-a}\left(w_2\right)$ and $\Delta\left(W_{r:n,m,k}W_{s:n,m,k}\right)=w_1^{P_1}w_2^{P_2-1}r_H^{-1}\left(w_2\right)$, then the theorem is complete.

The recurrence relation for the joint moments of GOS for the *exponentiated–G* family of distributions can be readily obtained from (11) by using $b = 1$.

Examples

The recurrence relations for single and joint moments of *GOS* for some members of the *Kum–G* family of distributions have been derived in this section.

Kumaraswamy power function distribution

The Kumaraswamy power function distribution (Abdul-Moniem, 2017) is obtained by using the following cdf $H(w)=\left(\frac{w}{\lambda}\right)^{\theta}$ and pdf $h(w)=\frac{\theta}{\lambda}\left(\frac{w}{\lambda}\right)^{\theta-1}$ in (3) and (4), where $0<w<\lambda,\theta\geq1,\lambda>0.$

Also, for the power function distribution, we have $r_H\left(w\right)=h\left(w\right)/H\left(w\right)=\theta/w$. Now, the recurrence relations for single and joint moments of *GOS* for the Kumaraswamy power function distribution can be obtained by using (8) and (11). For this, we first see that for the power function distribution, we have

$$\Phi\left(w\right)=w^{p-1}r_H^{-1}\left(w\right)H^{-a}\left(w\right)=\lambda^{a\theta}w^{p-a\theta}/\theta$$

and $\Delta\left(w\right)=w^{p-1}r_H^{-1}\left(w\right)=w^p/\theta.$

Using the above expressions in (8), the recurrence relation for single moments of GOS for the Kumaraswamy power function distribution is obtained as

$$E\left(W_{r:n,m,k}^{p}\right)-E\left(W_{r-1:n,m,k}^{p}\right)=$$

$$\frac{p}{ab\gamma_r}\left[\frac{\lambda^{a\theta}}{\theta}E\left(W_{r:n,m,k}^{p-a\theta}\right)-\frac{1}{\theta}E\left(W_{r:n,m,k}^{p}\right)\right]$$

or $\mu_{r:n,m,k}^{p}-\mu_{r-1:n,m,k}^{p}=\frac{p}{ab\theta\gamma_r}\left(\lambda^{a\theta}\mu_{r:n,m,k}^{p-a\theta}-\mu_{r:n,m,k}^{p}\right)$

or $\mu_{r:n,m,k}^{p}=\frac{1}{ab\theta\gamma_r+p}\left(p\lambda^{a\theta}\mu_{r:n,m,k}^{p-a\theta}+ab\theta\gamma_r\mu_{r-1:n,m,k}^{p}\right),$

$$...(13)$$

where $\mu_{r:n,m,k}^{p}=E\left(W_{r:n,m,k}^{p}\right)$, etc.

Again, for the power function distribution, we have

$$\Phi\left(W_{r:n,m,k}W_{s:n,m,k}\right)=w_1^{P_1}w_2^{P_2-1}r_H^{-1}\left(w_2\right)H^{-a}\left(w_2\right)$$

$$=\lambda^{a\theta}w_1^{p}w_2^{q-a\theta}/\theta$$

and $\Delta\left(W_{r:n,m,k}W_{s:n,m,k}\right) = w_1^{P_1} w_2^{P_2-1} r_H^{-1}\left(w_2\right) = w_1^{P_1} w_2^{P_2}\big/\theta$.

Using the above expressions in (11), the recurrence relation for the joint moments of GOS for the Kumaraswamy power function distribution is obtained as

$$E\left(W_{r:n,m,k}^{P_1} W_{s:n,m,k}^{P_2}\right) - E\left(W_{r:n,m,k}^{P_1} W_{s-1:n,m,k}^{P_2}\right) =$$

$$\frac{p_2}{ab\theta\gamma_s}\left[\lambda^{a\theta} E\left(W_{r:n,m,k}^{P_1} W_{s:n,m,k}^{P_2-a\theta}\right) - E\left(W_{r:n,m,k}^{P_1} W_{s:n,m,k}^{P_2}\right)\right]$$

or $\mu_{r,s:n,m,k}^{P_1,P_2} - \mu_{r,s-1:n,m,k}^{P_1,P_2} = \frac{p_2}{ab\theta\gamma_s}\left(\lambda^{a\theta}\mu_{r,s:n,m,k}^{p,q-a\theta} - \mu_{r,s:n,m,k}^{p,q}\right)$

or $\mu_{r,s:n,m,k}^{P_1,q_2} = \frac{1}{ab\theta\gamma_s + p_2}\left(p_2\lambda^{a\theta}\mu_{r,s:n,m,k}^{P_1,P_2-a\theta} + ab\theta\gamma_s\mu_{r,s-1:n,m,k}^{P_1,P_2}\right),$

...(14)

where $\mu_{r,s:n,m,k}^{P_1,P_2} = E\left(W_{r:n,m,k}^{P_1} W_{s:n,m,k}^{P_2}\right)$, etc. The relations (13) and (14) are the same as obtained earlier (Khan *et al.*, 2018).

Kumaraswamy reflected exponential distribution

The Kumaraswamy reflected exponential distribution is obtained by using the following cdf and pdf in (3) and (4)

$$H\left(w\right) = \exp\left(\frac{w}{\theta}\right) \,\&\, h\left(w\right) = \frac{1}{\theta}\exp\left(\frac{w}{\theta}\right); \, w < 0 \,, \, \theta > 0\,.$$

Also, for the reflected exponential distribution, we have $r_H\left(w\right) = h\left(w\right)\big/H\left(w\right) = 1\big/\theta$. Now, the recurrence relations for single and joint moments of GOS for the Kumaraswamy reflected exponential distribution can be obtained by using (8) and (11). For this, we first see that for the reflected exponential distribution, we have

$$\Phi\left(w\right) = w^{p-1} r_H^{-1}\left(w\right) H^{-a}\left(w\right) = \theta w^{p-1}\exp\left(-\frac{aw}{\theta}\right)$$

$$= \theta\sum_{j=0}^{\infty}\frac{\left(-1\right)^j a^j}{j!\theta^j} w^{p+j-1}$$

and $\Delta\left(w\right) = w^{p-1} r_H^{-1}\left(w\right) = \theta w^{p-1}$.

Using the above expressions in (8), the recurrence relation for single moments of GOS for the Kumaraswamy reflected exponential distribution is now obtained as

$$E\left(W_{r:n,m,k}^{p}\right) - E\left(W_{r-1:n,m,k}^{p}\right) = \cdot$$

$$\frac{p\theta}{ab\gamma_r}\left[\sum_{j=0}^{\infty}\frac{\left(-1\right)^j a^j}{j!\theta^j} E\left(W^{p+j-1}\right) - E\left(W_{r:n,m,k}^{p-1}\right)\right]$$

or

$$\mu_{r:n,m,k}^{p} - \mu_{r-1:n,m,k}^{p} = \frac{p\theta}{ab\gamma_r}\left[\sum_{j=0}^{\infty}\frac{\left(-1\right)^j a^j}{j!\theta^j}\mu_{r:n,m,k}^{p+j-1} - \mu_{r:n,m,k}^{p-1}\right].$$

...(15)

Again, for the reflected exponential distribution, we have

$$\Phi\left(W_{r:n,m,k}W_{s:n,m,k}\right) = w_1^{P_1} w_2^{P_2-1} r_H^{-1}\left(w_2\right) H^{-a}\left(w_2\right)$$

$$= \theta w_1^{P_1} w_2^{P_2-1}\exp\left(-\frac{aw_2}{\theta}\right)$$

$$= \theta\sum_{j=0}^{\infty}\frac{\left(-1\right)^j a^j}{j!\theta^j} w_1^{P_1} w_2^{P_2+j-1}$$

and

$$\Delta\left(W_{r:n,m,k}W_{s:n,m,k}\right) = w_1^{P_1} w_2^{P_2-1} r_H^{-1}\left(w_2\right) = \theta w_1^{P_1} w_2^{P_2-1}\,.$$

Using the above expressions (11), the recurrence relation for the joint moments of GOS for the Kumaraswamy reflected exponential distribution is obtained as

$$E\left(W_{r:n,m,k}^{P_1} W_{s:n,m,k}^{P_2}\right) - E\left(W_{r:n,m,k}^{P_1} W_{s-1:n,m,k}^{P_2}\right) =$$

$$\frac{p_2\theta}{ab\gamma_s}\left[\sum_{j=0}^{\infty}\frac{\left(-1\right)^j a^j}{j!\theta^j} E\left(W_{r:n,m,k}^{P_1} W_{s:n,m,k}^{P_2+j-1}\right)\right.$$

$$\left. - E\left(W_{r:n,m,k}^{P_1} W_{s:n,m,k}^{P_2-1}\right)\right],$$

or

$$\mu_{r,s:n,m,k}^{P_1,P_2} - \mu_{r,s-1:n,m,k}^{P_1,P_2} =$$

$$\frac{p_2\theta}{ab\gamma_s}\left[\sum_{j=0}^{\infty}\frac{\left(-1\right)^j a^j}{j!\theta^j}\mu_{r,s:n,m,k}^{P_1,P_2+j-1} - \mu_{r,s:n,m,k}^{P_1,P_2-1}\right].$$

...(16)

The recurrence relations for single and joint moments of *GOS* for the exponentiated reflected exponential distribution can be easily obtained from (15) and (16) by using $b = 1$.

Kumaraswamy inverse Weibull distribution

The Kumaraswamy inverse Weibull distribution (Shahbaz *et al.*, 2012) is obtained by using the following cdf and pdf in (3) and (4)

$$H(w) = \exp\left(-\alpha w^{-\beta}\right) \ \& \ h(w) = \alpha\beta w^{-(\beta+1)}\exp\left(-\alpha w^{-\beta}\right)$$

$$w, \alpha, \beta > 0 \ .$$

Also, for the inverse Weibull distribution, we have $r_H(w) = h(w)/H(w) = \alpha\beta w^{-(\beta+1)}$. Now, the recurrence relations for single and joint moments of GOS for the Kumaraswamy inverse Weibull distribution can be obtained by using (8) and (11). For this, we first see that for the inverse Weibull distribution, we have

$$\Phi(w) = w^{p-1}r_H^{-1}(w)H^{-a}(w) = \frac{1}{\alpha\beta}w^{p+\beta}\exp\left(a\alpha w^{-\beta}\right)$$

$$= \frac{1}{\alpha\beta}\sum_{j=0}^{\infty}\frac{a^j\alpha^j}{j!}w^{p-\beta(j-1)}$$

and $\quad \Delta(w) = w^{p-1}r_H^{-1}(w) = w^{p+\beta}/\alpha\beta .$

Using the above formulae in (8), the recurrence relation for single moments of GOS for the Kumaraswamy inverse Weibull distribution is obtained as

$$E\left(W_{r:n,m,k}^{p}\right) - E\left(W_{r-1:n,m,k}^{p}\right) =$$

$$\frac{p}{ab\alpha\beta\gamma_r}\left[\sum_{j=0}^{\infty}\frac{a^j\alpha^j}{j!}E\left(W^{p-\beta(j-1)}\right) - E\left(W_{r:n,m,k}^{p+\beta}\right)\right]$$

or $\quad \mu_{r:n,m,k}^{p} - \mu_{r-1:n,m,k}^{p} =$

$$\frac{p}{ab\alpha\beta\gamma_r}\left[\sum_{j=0}^{\infty}\frac{a^j\alpha^j}{j!}\mu_{r:n,m,k}^{p-\beta(j-1)} - \mu_{r:n,m,k}^{p+\beta}\right]$$

or $\mu_{r:n,m,k}^{p+\beta} =$

$$\sum_{j=0}^{\infty}\frac{a^j\alpha^j}{j!}\mu_{r:n,m,k}^{p-\beta(j-1)} - \frac{ab\alpha\beta\gamma_r}{p}\left(\mu_{r:n,m,k}^{p} - \mu_{r-1:n,m,k}^{p}\right).$$

$$...(17)$$

Again, for the inverse Weibull distribution, we have

$$\Phi\left(W_{r:n,m,k}W_{s:n,m,k}\right) = w_1^{p_1}w_2^{p_2-1}r_H^{-1}(w_2)H^{-a}(w_2)$$

$$= \frac{1}{\alpha\beta}w_1^{p_1}w_2^{p_2+\beta}\exp\left(-a\alpha w_2^{-\beta}\right)$$

and

$$\Delta\left(W_{r:n,m,k}W_{s:n,m,k}\right) = w_1^{p_1}w_2^{p_2-1}r_H^{-1}(w_2) = w_1^{p_1}w_2^{p_2+\beta}/\alpha\beta .$$

Using the above expressions in (11), the recurrence relation for the joint moments of GOS for the Kumaraswamy reflected exponential distribution is obtained as

$$E\left(W_{r:n,m,k}^{p_1}W_{s:n,m,k}^{p_2}\right) - E\left(W_{r:n,m,k}^{p_1}W_{s-1:n,m,k}^{p_2}\right) =$$

$$\frac{p_2}{ab\alpha\beta\gamma_s}\left[\sum_{j=0}^{\infty}\frac{a^j\alpha^j}{j!}E\left\{W_{r:n,m,k}^{p_1}W_{s:n,m,k}^{p_2-\beta(j-1)}\right\} - E\left(W_{r:n,m,k}^{p_1}W_{s:n,m,k}^{p_2+\beta}\right)\right]$$

or $\mu_{r,s:n,m,k}^{p_1,p_2} - \mu_{r,s-1:n,m,k}^{p_1,p_2} =$

$$\frac{p_2}{ab\alpha\beta\gamma_s}\left[\sum_{j=0}^{\infty}\frac{a^j\alpha^j}{j!}\mu_{r,s:n,m,k}^{p_1,p_2-\beta(j-1)} - \mu_{r,s:n,m,k}^{p_1,p_2+\beta}\right]$$

or $\quad \mu_{r,s:n,m,k}^{p_1,p_2+\beta} =$

$$\sum_{j=0}^{\infty}\frac{a^j\alpha^j}{j!}\mu_{r,s:n,m,k}^{p_1,p_2-\beta(j-1)} - \frac{ab\alpha\beta\gamma_s}{p_2}\left(\mu_{r,s:n,m,k}^{p_1,p_2} - \mu_{r,s-1:n,m,k}^{p_1,p_2}\right).$$

$$...(18)$$

The relations (17) and (18) are useful to derive the relations for single and joint moments of GOS for the Kumaraswamy inverse exponential and Kumaraswamy inverse Rayleigh distributions. For example, using $\beta = 2$ in (17) and (18), the relations for single and joint moments of GOS for the inverse Rayleigh distribution are obtained.

Kumaraswamy log-logistic distribution

The Kumaraswamy log-logistic distribution (de Santana *et al.*, 2012) is obtained by using the following cdf and pdf of the log-logistic distribution in (3) and (4)

$$H(w) = w^{\theta}\left(1+w^{\theta}\right)^{-1} \ \& \ h(w) = \theta w^{\theta-1}\left(1+w^{\theta}\right)^{-2} ; x, \theta > 0 .$$

The relations for single and joint moments of *GOS* for the Kumaraswamy log-logistic distribution can be obtained by using (8) and (11). For this, we first see that for the log-logistic distribution, we have

$$\Phi(w) = w^{p-1}r_H^{-1}(w)H^{-a}(w) = \frac{1}{\theta}w^{p-a\theta}\left(1+w^{\theta}\right)^{a+1}$$

$$= \frac{1}{\theta}\sum_{j=0}^{\infty}\frac{\Gamma(a+2)}{j!\Gamma(a-j+2)}w^{p-\theta(j-1)}$$

and $\Delta(w) = w^{p-1}r_H^{-1}(w) = \left(w^p + w^{p+\theta}\right)/\theta .$

Using the above formulae in (8), the recurrence relation for single moments of GOS for the Kumaraswamy log-logistic distribution is obtained as

$$E\left(W_{r:n,m,k}^{p}\right) - E\left(W_{r-1:n,m,k}^{p}\right) = \frac{p}{ab\theta\gamma_{r}}\left[\sum_{j=0}^{\infty}\frac{\Gamma(a+2)}{j!\Gamma(a-j+2)}E\left(W_{r:n,m,k}^{p-\theta(j-1)}\right) - \left\{E\left(W_{r:n,m,k}^{p}\right) + E\left(W_{r:n,m,k}^{p+\theta}\right)\right\}\right]$$

or $\quad ab\theta\gamma_{r}\mu_{r:n,m,k}^{p} - ab\theta\gamma_{r}\mu_{r-1:n,m,k}^{p} = p\sum_{j=0}^{\infty}\frac{\Gamma(a+2)}{j!\Gamma(a-j+2)}\mu_{r-1:n,m,k}^{p-\theta(j-1)} - p\mu_{r:n,m,k}^{p} - p\mu_{r:n,m,k}^{p+\theta}$

or $\quad \mu_{r:n,m,k}^{p+\theta} = \sum_{j=0}^{\infty}\frac{\Gamma(a+2)}{j!\Gamma(a-j+2)}\mu_{r-1:n,m,k}^{p-\theta(j-1)} - \left(\frac{ab\theta\gamma_{r}}{p}+1\right)\mu_{r:n,m,k}^{p} + \frac{ab\theta\gamma_{r}}{p}\mu_{r-1:n,m,k}^{p}.$ \hfill ...(19)

Again, for the log-logistic distribution, we have

$$\Phi\left(W_{r:n,m,k}W_{s:n,m,k}\right) = w_{1}^{p_{1}}w_{2}^{p_{2}-1}r_{H}^{-1}(w_{2})H^{-a}(w_{2}) = \frac{1}{\theta}w_{1}^{p_{1}}w_{2}^{p_{2}-a\theta}\left(1+w_{2}^{\theta}\right)^{a+1} = \frac{1}{\theta}\sum_{j=0}^{\infty}\frac{\Gamma(a+2)}{j!\Gamma(a-j+2)}w_{1}^{p_{1}}w_{2}^{p_{2}-\theta(j-1)}$$

and $\Delta\left(W_{r:n,m,k}W_{s:n,m,k}\right) = w_{1}^{p_{1}}w_{2}^{p_{2}-1}r_{H}^{-1}(w_{2}) = \left(w_{1}^{p_{1}}w_{2}^{p_{2}} + w_{1}^{p_{1}}w_{2}^{p_{2}+\theta}\right)\big/\theta.$

Using the above expressions in (11), the relation for the joint moments of GOS for the Kumaraswamy reflected exponential distribution is obtained as

$$E\left(W_{r:n,m,k}^{p_{1}}W_{s:n,m,k}^{p_{2}}\right) - E\left(W_{r:n,m,k}^{p_{1}}W_{s-1:n,m,k}^{p_{2}}\right) = \frac{p_{2}}{ab\theta\gamma_{s}}\left[\sum_{j=0}^{\infty}\frac{\Gamma(a+2)}{j!\Gamma(a-j+2)}E\left(W_{r:n,m,k}^{p_{1}}W_{s:n,m,k}^{p_{2}-\theta(j-1)}\right)\right.$$
$$\left. - \left\{E\left(W_{r:n,m,k}^{p_{1}}W_{s:n,m,k}^{p_{2}}\right) + E\left(W_{r:n,m,k}^{p_{1}}W_{s:n,m,k}^{p_{2}+\theta}\right)\right\}\right]$$

or $ab\theta\gamma_{s}\mu_{r,s:n,m,k}^{p_{1},p_{2}} - ab\theta\gamma_{s}\mu_{r,s-1:n,m,k}^{p_{1},p_{2}} = p_{2}\sum_{j=0}^{\infty}\frac{\Gamma(a+2)}{j!\Gamma(a-j+2)}\mu_{r,s:n,m,k}^{p_{1},p_{2}-\theta(j-1)} - q\mu_{r,s:n,m,k}^{p_{1},p_{2}} - q\mu_{r,s:n,m,k}^{p_{1},p_{2}+\theta}$

or $\mu_{r,s:n,m,k}^{p_{1},p_{2}+\theta} = \sum_{j=0}^{\infty}\frac{\Gamma(a+2)}{j!\Gamma(a-j+2)}\mu_{r,s:n,m,k}^{p_{1},p_{2}-\theta(j-1)} - \left(\frac{ab\theta\gamma_{s}}{p_{2}}+1\right)\mu_{r,s:n,m,k}^{p_{1},p_{2}} + \frac{ab\theta\gamma_{s}}{p_{2}}\mu_{r,s-1:n,m,k}^{p_{1},p_{2}}.$ \hfill ...(20)

The relations (19) and (20) can be used to obtain the recurrence relations for single and joint moments for the special cases of GOS for the Kumaraswamy log-logistic distributions.

Kumaraswamy pareto distribution

The Kumaraswamy Pareto distribution (Bourguignon *et al.*, 2012) is obtained by using the following cdf and pdf of the Pareto distribution in (3) and (4)

$$H(w) = 1 - \left(\frac{\beta}{w}\right)^{k} \quad \& \quad h(w) = \frac{k\beta^{k}}{w^{k+1}}\ ;\ w \geq \beta\ ,\ \beta, k > 0.$$

The recurrence relations for single and joint moments of GOS for the Kumaraswamy Pareto distribution can be obtained by using (8) and (11). For this, we first see that for the Pareto distribution, we have

$$\Phi(w) = w^{p-1}r_{H}^{-1}(w)H^{-a}(w) = \frac{1}{k\beta^{k}}w^{p+k}\left[1-(w/\beta)^{-k}\right]^{-(a-1)} = \frac{1}{k\beta^{k}}\sum_{j=0}^{\infty}(-1)^{j}\beta^{kj}\frac{\Gamma(a+r-1)}{r!\Gamma(a-1)}w^{p-k(j-1)}$$

and $\Delta(w) = w^{p-1} r_H^{-1}(w) = \dfrac{w^{p+k}}{k\beta^k}\left[1-(w/\beta)^{-k}\right] = \dfrac{1}{k\beta^k}\left(w^{p+k} - \beta^k w^p\right).$

Using the above expressions in (8), the relation for the single moments of GOS for the Kumaraswamy log-logistic distribution is obtained as

$$E\left(W_{r:n,m,k}^p\right) - E\left(W_{r-1:n,m,k}^p\right) = \frac{p}{abk\beta^k \gamma_r}\left[\sum_{j=0}^{\infty}(-1)^j \beta^{kj}\frac{\Gamma(a+r-1)}{r!\Gamma(a-1)}E\left(W_{r:n,m,k}^{p-k(j-1)}\right) - \left\{E\left(W_{r:n,m,k}^{p+k}\right) - \beta^k E\left(W_{r:n,m,k}^p\right)\right\}\right]$$

or $abk\beta^k \gamma_r \mu_{r:n,m,k}^p - abk\beta^k \gamma_r \mu_{r-1:n,m,k}^p = p\sum_{j=0}^{\infty}(-1)^j \beta^{kj}\dfrac{\Gamma(a+r-1)}{r!\Gamma(a-1)}\mu_{r-1:n,m,k}^{p-k(j-1)} - p\mu_{r:n,m,k}^{p+k} + p\beta^k \mu_{r:n,m,k}^p$

or $\mu_{r:n,m,k}^{p+k} = \sum_{j=0}^{\infty}(-1)^j \beta^{kj}\dfrac{\Gamma(a+r-1)}{r!\Gamma(a-1)}\mu_{r-1:n,m,k}^{p-k(j-1)} + \dfrac{\beta^k(p-abk\gamma_r)}{p}\mu_{r:n,m,k}^p + \dfrac{abk\beta^k \gamma_r}{p}\mu_{r-1:n,m,k}^p.$ ...(21)

Again, for the log-logistic distribution, we have

$$\Phi\left(W_{r:n,m,k}W_{s:n,m,k}\right) = w_1^{p_1} w_2^{p_2-1} r_H^{-1}(w_2) H^{-a}(w_2) = \frac{1}{k\beta^k} w_1^{p_1} w_2^{p_2+k}\left[1-(w_2/\beta)^{-k}\right]^{-(a-1)}$$

$$= \frac{1}{k\beta^k}\sum_{j=0}^{\infty}(-1)^j \beta^{kj}\frac{\Gamma(a+r-1)}{r!\Gamma(a-1)}w_1^{p_1} w_2^{p_2-k(j-1)}$$

and $\Delta\left(W_{r:n,m,k}W_{s:n,m,k}\right) = w_1^{p_1} w_2^{p_2-1} r_H^{-1}(w_2) = \dfrac{1}{k\beta^k}\left(w_1^{p_1} w_2^{p_2+k} - \beta^k w_1^{p_1} w_2^{p_2}\right).$

Using the above formulae in (11), the relation for the joint moments of GOS for the Kumaraswamy log-logistic distribution is obtained as

$$E\left(W_{r:n,m,k}^{p_1}W_{s:n,m,k}^{p_2}\right) - E\left(W_{r:n,m,k}^{p_1}W_{s-1:n,m,k}^{p_2}\right) = \frac{p_2}{abk\beta^k \gamma_s}\left[\sum_{j=0}^{\infty}(-1)^j \beta^{kj}\frac{\Gamma(a+r-1)}{r!\Gamma(a-1)}E\left(W_{r:n,m,k}^{p_1}W_{s:n,m,k}^{p_2-k(j-1)}\right)\right.$$
$$\left. - \left\{E\left(W_{r:n,m,k}^{p_1}W_{s:n,m,k}^{p_2+k}\right) - \beta^h E\left(W_{r:n,m,k}^{p_1}W_{s:n,m,k}^{p_2}\right)\right\}\right]$$

or $abk\beta^k \gamma_s \mu_{r,s:n,m,k}^{p_1,p_2} - abk\beta^k \gamma_s \mu_{r,s-1:n,m,k}^{p_1,p_2} = q\sum_{j=0}^{\infty}(-1)^j \beta^{kj}\dfrac{\Gamma(a+r-1)}{r!\Gamma(a-1)}\mu_{r,s:n,m,k}^{p_1,p_2-k(j-1)} - q\mu_{r,s:n,m,k}^{p_1,p_2+k} + q\beta^k \mu_{r,s:n,m,k}^{p_1,p_2}$

or $\mu_{r,s:n,m,k}^{p_1,p_2+k} = \sum_{j=0}^{\infty}(-1)^j \beta^{kj}\dfrac{\Gamma(a+r-1)}{r!\Gamma(a-1)}\mu_{r,s:n,m,k}^{p_1,p_2-k(j-1)} + \dfrac{\beta^k(q-abk\gamma_s)}{q}\mu_{r,s:n,m,k}^{p_1,p_2} + \dfrac{abk\beta^k \gamma_s}{q}\mu_{r,s-1:n,m,k}^{p_1,p_2}.$ ...(22)

The relations for single and joint moments of GOS for the log-logistic distribution can be easily obtained from (21) and (22) by setting $a = b = 1$.

CHARACTERIZATION RESULTS

In this section, we have given some characterization results for the *Kum–G* family of distributions based on single and joint moments of GOS. These results are given in the following Theorems.

Theorem 3: For a random variable *X* to have density and distribution functions as given in (5) and (6), respectively, it is necessary and sufficient that the single moments of its *GOS* are related as

$$E\left(W_{r:n,m,k}^{p}\right) - E\left(W_{r-1:n,m,k}^{p}\right) = \frac{p}{ab\gamma_r}\left[E\left\{\Phi\left(W_{r:n,m,k}\right)\right\}\right.$$

$$\left. - E\left\{\Delta\left(W_{r:n,m,k}\right)\right\}\right],$$

where $\Phi(x) = x^{p-1} r_G^{-1}(x) G^{-a}(x)$ and $\Delta(x) = x^{p-1} r_G^{-1}(x)$.

Proof: The necessity follows immediately from Theorem 1. Now, to prove the sufficiency, we consider (9) as

$$\frac{pC_{r-1}}{\gamma_r(r-1)!}\int_{-\infty}^{\infty} w^{p-1}\left\{\overline{F}(w)\right\}^{\gamma_r}\tau_m^{r-1}\left[F(w)\right]dw$$

$$= \frac{pC_{r-1}}{\gamma_r(r-1)!}\int_{c}^{\infty} w^{p-1}\left\{\overline{F}(w)\right\}^{\gamma_r-1}\tau_m^{r-1}\left\{F(w)\right\}$$

$$\times \left[\frac{1}{ab}r_H^{-1}(w)\left\{H^{-a}(w)-1\right\}f(w)\right]dw$$

or

$$\frac{pC_{r-1}}{\gamma_r(r-1)!}\int_{-\infty}^{\infty} w^{p-1}\left\{\overline{F}(w)\right\}^{\gamma_r-1}\tau_m^{r-1}\left[F(w)\right]$$

$$\left[\overline{F}(w) - \frac{1}{ab}r_H^{-1}(w)\left\{H^{-a}(w)-1\right\}f(w)\right]dw = 0$$

Using the above expression alongside (7), we have

$$\frac{p_2 C_{s-1}}{\gamma_s(r-1)!(s-r-1)!}\int_{c}^{\infty}\int_{w_1}^{\infty} w_1^{p_1} w_2^{p_2-1} f(w_1)\left[\overline{F}(w_1)\right]^m \tau_m^{r-1}\left[F(w)\right]\left[\varphi_m\left\{F(w_2)\right\} - \varphi_m\left\{F(w_1)\right\}\right]^{s-r-1}$$

$$\times \left[\overline{F}(w_2)\right]^{\gamma_s} dw_2 dw_1 = \frac{p_2 C_{s-1}}{\gamma_s(r-1)!(s-r-1)!}\int_{c}^{\infty}\int_{w_1}^{\infty} w_1^{p_1} w_2^{p_2-1} f(w_1)\left[\overline{F}(w_1)\right]^m \tau_m^{r-1}\left[F(w)\right]$$

$$\times \left[\varphi_m\left\{F(w_2)\right\} - \varphi_m\left\{F(w_1)\right\}\right]^{s-r-1}\left[\overline{F}(w_2)\right]^{\gamma_s-1}\left[\frac{1}{ab}r_H^{-1}(w_2)\left\{H^{-a}(w_2)-1\right\}f(w_2)\right]dw_2 dw_1$$

Applying the *Müntz–Száz* theorem to the above equation (Hwang and Lin, 1984), we have

$$\overline{F}(w) = \frac{1}{ab}r_H^{-1}(w)\left[H^{-a}(w)-1\right]f(w),$$

which is the relationship between the density and distribution function of the Kumaraswamy family of distributions and the theorem is complete.

Theorem 4: For a random variable *X* to have density and distribution functions as given in (5) and (6), respectively, it is necessary and sufficient that the joint moments of its GOS are related as

$$E\left(W_{r:n,m,k}^{p_1} W_{s:n,m,k}^{p_2}\right) - E\left(W_{r:n,m,k}^{p_1} W_{s-1:n,m,k}^{p_2}\right) =$$

$$\frac{p_2}{ab\gamma_s}\left[E\left\{\Phi\left(W_{r:n,m,k} W_{s:n,m,k}\right)\right\} - E\left\{\Delta\left(W_{r:n,m,k} W_{s:n,m,k}\right)\right\}\right],$$

where $\Phi\left(W_{r:n,m,k} W_{s:n,m,k}\right) = w_1^{p_1} w_2^{p_2-1} r_H^{-1}(w_2) H^{-a}(w_2)$

and $\Delta\left(W_{r:n,m,k} W_{s:n,m,k}\right) = w_1^{p_1} w_2^{p_2-1} r_H^{-1}(w_2)$.

Proof: The necessity follows immediately from Theorem 2. Now, to prove the sufficiency, we consider (12) as

$$E\left(W_{r:n,m,k}^{p_1} W_{s:n,m,k}^{p_2}\right) - E\left(W_{r:n,m,k}^{p_1} W_{s-1:n,m,k}^{p_2}\right) =$$

$$\frac{p_2 C_{s-1}}{\gamma_s(r-1)!(s-r-1)!}\int_{-\infty}^{\infty}\int_{w_1}^{\infty} w_1^{p_1} w_2^{p_2-1} f(w_1)\left[\overline{F}(w_1)\right]^m$$

$$\times \tau_m^{r-1}\left[F(x_1)\right]\left[\varphi_m\left\{F(w_2)\right\} - \varphi_m\left\{F(w_1)\right\}\right]^{s-r-1}$$

$$\overline{F}(w_2)\left[\overline{F}(w_2)\right]^{\gamma_s-1} dw_2 dw_1.$$

or

$$\frac{p_2 C_{s-1}}{\gamma_s (r-1)!(s-r-1)!} \int_c^\infty \int_{w_1}^\infty w_1^{p_1} w_2^{p_2-1} f(w_1) \left[\overline{F}(w_1)\right]^m \tau_m^{r-1} \left[F(w_1)\right] \left[\varphi_m\left\{F(w_2)\right\} - \varphi_m\left\{F(w_1)\right\}\right]^{s-r-1}$$

$$\times \left[\overline{F}(w_2)\right]^{\gamma_s-1} \left[\overline{F}(w_2) - \frac{1}{ab} r_H^{-1}(w_2) \left\{H^{-a}(w_2) - 1\right\} f(w_2)\right] dw_2 dw_1 = 0.$$

Applying the *Müntz–Száz* theorem to the above equation (Hwang and Lin, 1984), we have

$$\overline{F}(w_2) = \frac{1}{ab} r_H^{-1}(w_2) \left[H^{-a}(w_2) - 1\right] f(w_2),$$

which is (7) and hence the theorem.

CONCLUSION

In this paper, we have derived some recurrence relations for the single and joint moments of GOS for the Kumaraswamy (*Kum–G*) family of distributions. The relations derived are useful to obtain the relations for single and joint moments of GOS for any member of the *Kum–G* family of distributions. The obtained relations are also helpful in deriving the relations for single and joint moments of the special cases of GOS. The applicability of the derived relations is illustrated with the help of some example distributions, including Kumaraswamy power function, Kumaraswamy reflected exponential, Kumaraswamy inverse Weibull, Kumaraswamy log-logistic, etc. The recurrence relations are also used to characterize the *Kum–G* family of distributions.

REFERENCES

Abdul-Moniem, I, B. (2017). The Kumaraswamy power function distribution, *Journal of Statistics Applications & Probability*, *6*(1), 81–90. DOI: https://doi:10.18576/jsap/060107

Ahsanullah, M. (2000). Generalized order statistics from exponential distribution, *Journal of Statistical Planning and Inference*, *85*(1), 85–91. DOI: https://doi.org/10.1016/S0378-3758(99)00068-3

Ahsanullah, M., & Nevzorov, V. B. (2001). *Ordered Random Variables*, Nova Science Publishers, USA.

Athar H., & Faizan M. (2011). Moments of lower generalized order statistics for power function distribution and a characterization, *International Journal of Statistical Sciences*, *11*, 125–134.

Athar, H., & Islam, H. M. (2004). Recurrence relations between single and product moments of generalized order statistics from a general class of distributions. *Metron*, *62*(3), 327-337.

Bourguignon, M., Silva, R. B., Zea, L. M., & Cordeiro, G. M. (2013). The Kumaraswamy Pareto distribution, *Journal of Statistical Theory and Applications*, *12*(2), 129–144. DOI: https://doi.org/10.2991/jsta.2013.12.2.1

Burkschat M., Cramer E., & Kamps, U. (2003). Dual generalized order statistics. *Metron*, *61*(1), 13–26.

Cordeiro, G. M., & de Castro, M. (2011). A new family of generalized distributions, *Journal of Statistical Computation and Simulation*, *81*(7), 883–891. DOI: https://doi.org/10.1080/00949650903530745

de Santana, T. V. F, Ortega, E. M. M., & Cordeiro, G. M. (2012). The Kumaraswamy log-logistic distribution, *Journal of Statistical Theory and Applications*, *11*(3), 265–291.

Gupta, R. C., Gupta, P. L., & Gupta, R. D. (1998). Modeling failure time data by Lehman alternatives, *Commutations in Statistic–Theory and Methods*, *27*(4), 887–904. DOI: https://doi.org/10.1080/03610929808832134

Hwang, J. S., & Lin, G. D. (1984). Extensions of *Müntz–Száz* theorems and application. *Analysis*, *4*(2), 143–160. DOI: https://doi.org/10.1524/anly.1984.4.12.143

Jones, M. C. (2009). Kumaraswamy's distribution: A beta-type distribution with some tractability advantages, *Statistical Methodology*, *6*(1), 70–81. DOI: https://doi.org/10.1016/j.stamet.2008.04.001

Kamps, U. (1995). A concept of generalized order statistics, *Journal of Statistical Planning and Inference*, *48*(1), 1–23. DOI: https://doi.org/10.1016/0378-3758(94)00147-N

Kotb, M. S., El-Din M. M. M., & Newer H. A. (2013). Recurrence relations for single and product moments of lower generalized order statistics from a general class of distributions and its characterizations, *International Journal of Pure and Applied Mathematics*, *87*(2), 229–247. DOI: https://doi.org/10.12732/ijpam.v87i2.4

Khan, M. J. S., Kumar, S., & Kumar, A. (2018). Relations for moments of Kumaraswamy power function distribution based on ordered random variables and characterization, *International Journal of Advanced Research in Science Engineering and Technology*, *5*(2), 5250–5257.

Kumar, D. (2011). Generalized Order Statistics from Kumaraswamy Distribution and its Characterization, *Tamsui Oxford Journal of Information and Mathematical Sciences*, *27*(3), 463-476.

Kumaraswamy, P. (1980). A generalized probability density function for double-bounded random processes.

Journal of Hydrology, *46*(1), 79-88. DOI: https://doi.org/10.1016/0022-1694(80)90036-0

Mohsin, M., Shahbaz, M. Q., & Kibria, G. (2010). Recurrence relations for moments of generalized order statistics for Rayleigh distribution, *Applied Mathematics and Information Sciences*, *4*(3), 273–279.

Nadarajah, S., & Kotz, S. (2006). Exponentiated type distributions, *Acta Applicandae Mathematica*, *92*(2), 97–111. DOI: https://doi.org/10.1007/s10440-006-9055-0

Pawlas, P., & Szynal, D. (2001). Recurrence relations for single and product moment of lower generalized order statistics from Inverse Weibull distribution, *Demonstratio Mathematics*, *34*(2), 353-358. DOI: https://doi.org/10.1515/dema-2001-0214

Shahbaz, M. Q., Ahsanullah, M., Hanif Shahbaz, S., & Al-Zahrani, B. (2016). *Ordered Random Variables: Theory and Applications*, Atlantis Studies in Probability and Statistics, Springer. DOI: https://doi.org/10.2991/978-94-6239-225-0

Shahbaz, M. Q., Shahbaz, S., & Butt, N. S. (2012) The Kumaraswamy Inverse Weibull distribution, *Pakistan Journal of Statistics and Operation Research*, *8*(3), 479-489. DOI: https://doi.org/10.18187/pjsor.v8i3.520

Mathematical Subject Classification: 62G30, 62E10, 60E05

RESEARCH ARTICLE

Environmental Science

Impact of probiotics mixture as a water additive on water quality, growth performance and survival of *Catla catla* fry

AKMMK Meddage[1,2], PM Manage[1,2*] and PM Withanage[3]

[1] *Department of Zoology, University of Sri Jayewardenepura, Nugegoda, Sri Lanka.*
[2] *Centre for Water Quality and Algae Research, Department of Zoology, University of Sri Jayewardenepura, Nugegoda, Sri Lanka.*
[3] *Fish Nutrition Research Development and Training Section, Udawalawe, Sri Lanka.*

Abstract: The main objective of this study was to assess the impact of a commercial probiotic as a water additive on the survival, growth performance, and water quality of *C. catla.* A field trial was conducted for 66 days. About 360 *C. catla* fry (0.25 ± 0.01 g) were distributed randomly among 12 quadruplicate-designed cemented tanks, each containing 30 healthy fish in 0.15 m^3 of water. Control tanks were not treated with probiotics while the treatment tanks received 0.012 g m^{-2} $week^{-1}$ and 0.03 g m^{-2} $week^{-1}$ of the probiotic. Principal Component Analysis was carried out to identify key water quality factors. One-way ANOVA followed by Tukey's test was used to compare statistical differences. The results showed that adding probiotics significantly decreased ammonia concentration ($p < 0.05$). No significant differences were found in water temperature, total dissolved solids, pH, and electrical conductivity between treatments and control. The fish in tanks treated with probiotics showed a substantial increase in survival rate ($p < 0.05$), with the highest value of 92 ± 1.5%. The survival of *C. catla* fry was enhanced when a high dosage of 0.03 g m^{-2} $week^{-1}$ was administered. Despite the positive impact on survival, probiotic treatment did not influence the overall growth performance.
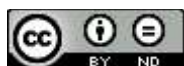
Keywords: Aquaculture, survival, *Catla catla*, probiotics as a water additive, water quality improvement

INTRODUCTION

Aquaculture has emerged as one of the fastest-growing industries, accounting for around 50 % of the food fish production (Rathnachandra *et al.*, 2024; Samarawardane *et al.*, 2021). However, the intensification of aquaculture practices has led to significant challenges, including the decline of the survival of the host species, disease outbreaks, poor water quality, and the excessive use of antibiotics, which contribute to the development of antibiotic-resistant bacteria (Manage, 2018). The aquaculture systems generate wastewater containing significant components such as ammonia, phosphate, and suspended particles. Phosphorus and nitrogen are two excretory products of farmed fish, which greatly affect the quality of water and harm fish health (Yang *et al.*, 2021; Zabidi *et al.*, 2021; Ali *et al.*, 2021). These compounds affect the survival of the culture organism, ultimately leading to significant decline of production as well (Ali *et al.*, 2021). Various biological, physical, and chemical approaches have been developed and used subsequently to manage water pollution in aquaculture (Dawood & Koshio, 2016; El-Saadony *et al.,* 2021; Hai, 2015). Nevertheless, the accumulation of these harmful chemicals in living organisms over time and their potential risks when consumed by humans are noteworthy issues (Jahangiri, 2018). As a result of the detrimental impact of chemicals and antibiotics on the environment, which leads to the prevalence of mutagenic microbial strains and negatively affects fish health, it is no longer advisable to use them for disease control (Jahangiri, 2018; Manage, 2018). Hence, using environmentally

friendly feed additives, such as microbial supplements, to enhance aquaculture-related species' physiology, growth performance, and immune responses has garnered significant interest recently (Jahangiri, 2018; Mishra & Sharma, 2021). The role of probiotics in fish reproduction is a new area of research (Jahangiri, 2018; Nayak, 2020; Olmos-soto, 2015). Probiotic supplementation refers to the use of microorganisms in the aquaculture industry and has become a practical and extensively used method in aquaculture (El-Saadony *et al.*, 2021; Pandiyan *et al.*, 2013).

Sri Lanka has limited but stable fish production with an expanding aquaculture sector for finfish (Athukorala, 2008). The focus has been on initiating small-scale fish farming to assist local communities with income and food supply (Hansika *et al.*, 2024). In Sri Lanka, the inland fisheries sector contributes around 0.2% to the Gross Domestic Production (GDP), showing a 70% growth in inland fishing contribution (Hansika *et al.*, 2024; Rathnachandra *et al.*, 2024). Further, it is responsible for about 20% of the total fish production in the country (Adikari *et al.*, 2017). The sector provides direct and indirect employment for a considerable number of people. During the last few years, the demand for cultured

Carp species has significantly increased owing to their substantial market value (Adikari *et al.*, 2017). Besides, the cultivation of *C. catla* and its demand in Sri Lanka has significantly increased due to it being a delicious and cost-effective protein source, and its appearance (Athukorala, 2008). Nevertheless, the Carp Breeding Centre of the National Aquaculture Development Authority (NAQDA) in Udawalawe (Figure 2) has detected an issue related to their *C. catla* farming. This problem may involved in the production decline and the spread of diseases.

The Udawalawe Reservoir serves as the primary water source for this centre (Figure 1), playing a crucial role in meeting the region's water demands (Athukorala, 2008). However, the reservoir is subjected to various forms of pollution, primarily driven by rapid urbanization. These factors may contribute to increased mortality rates among *C. catla* fry. Inadequate water quality management could negatively impact the survival rate of *C. catla* during the transition stage from fry to fingerling. Therefore, the present experiment was undertaken to find an efficient, environmentally friendly method to increase the survival rate of *C. catla* and improve the water quality parameters in the rearing water.
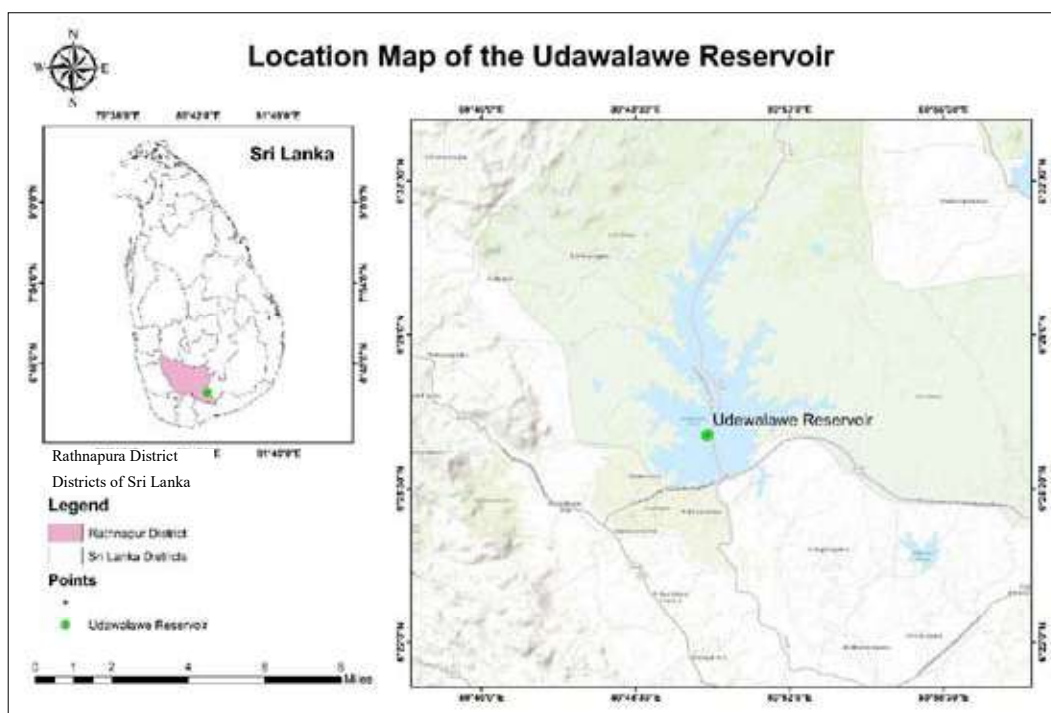

Figure 1: The location map of the Reservoir, Udawalawe Sri Lanka, was generated using ArcMap 10.8. The map highlights the reservoir's role in providing water supply to nearby regions and shows the area's distribution of water bodies.

This study selected a commercially available probiotic supplement, and it was employed to ascertain the effect of probiotics administered to the closed system. Besides, there have been limited investigations on the direct application of multi-strain probiotics in fish farming, as commercial probiotic products are predominantly employed as a supplement in fish feed to enhance fish growth (Ali *et al.*, 2021; El-kady *et al.*, 2022; Hassan *et al.*, 2022; Jahangiri, 2018). Therefore, the administration method of probiotics in aquaculture plays a crucial role in determining their favourable performance (Jahangiri, 2018). Hence, the objective of this study was to evaluate the current methods of probiotic delivery through water in finfish aquaculture. The primary goal of this study was to assess the impact of directly introducing a commercially available probiotic mixture on *C. catla* fish water quality, growth performance, and survival. To the best of the author's knowledge, this is the first study done to assess how multi-strain probiotics enhance *C. catla* survival in Sri Lanka.
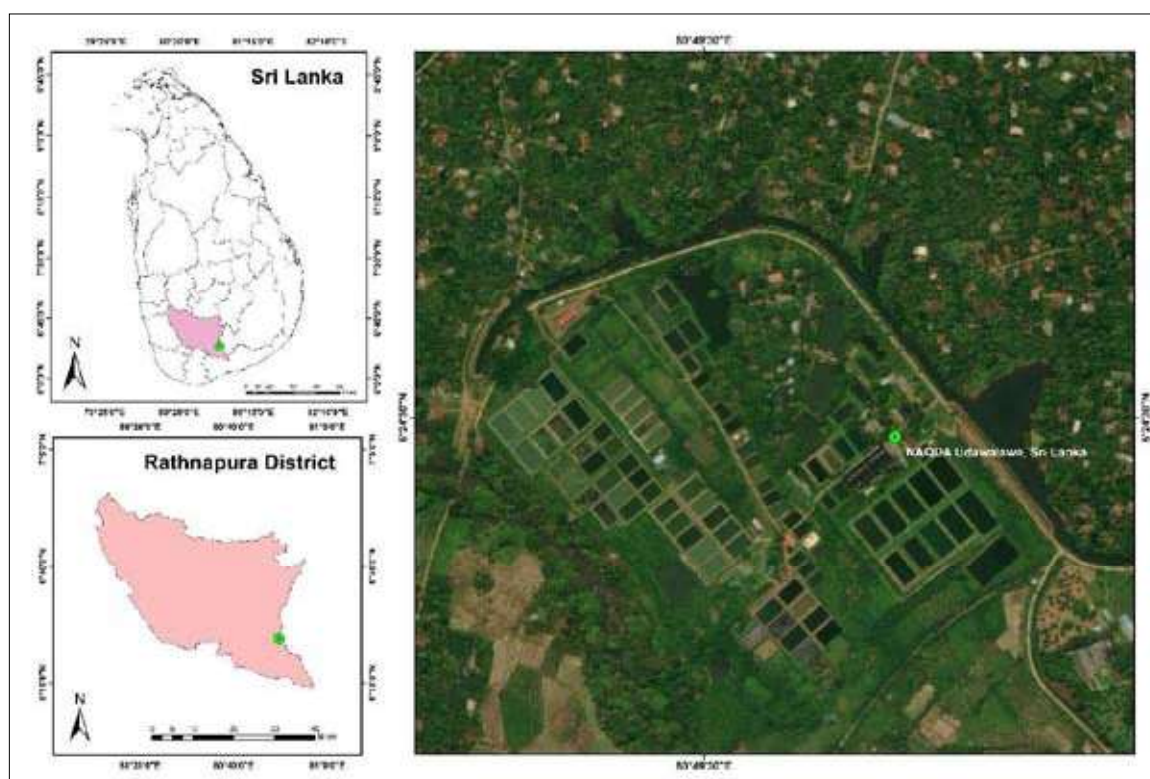

Figure 2: The location map of the Carp Breeding Centre of NAQDA in Udawalawe, Sri Lanka generated using ArcMap 10.8. The map illustrates the location of the Centre and surrounding water bodies. It also highlights the water supply, which is sourced from the Udawalawe Reservoir

MATERIALS AND METHODS

Study site and experimental fish

C. catla fry were obtained from the NAQDA Carp Breeding Centre, Udawalawe, Sri Lanka (6°24'29.1 "N, 80°49'39.8"E), as illustrated in Figure 2. The experiments were also carried out at this Centre and Centre for Water Quality and Algae Research of the University of Sri Jayewardenepura, Sri Lanka.

Experimental set-up

The experiment employed 12 rectangular cement tanks (0.58 × 0.69 × 0.26 m) each with 0.15 m³ capacity. The tanks were continuously aerated for 66 ds. Each tank was stocked with 30 fry with an average body weight (BW) of 0.25 ± 0.01 g, standard length of 3.15 ± 0.04 cm and total length of 3.97 ± 0.05 cm.

Each treatment was done in quadruplicate. A commercially available probiotic was purchased at

the local market. Fry were acclimated to experimental conditions for 14 ds following the procedure described by Das *et al*. (2021).

Experimental design

Cemented tanks were used for the experiment. The control tanks (TC - TC_{-1}, TC_{-2}, TC_{-3}, and TC_{-4}) received only commercial feed. C. *calta* fried in treatment tanks (T_1 - T_{1-1}, T_{1-2}, T_{1-3}, and T_{1-4}) were fed commercial feed supplemented with probiotics at the manufacturer-recommended dose (0.012 g m^{-2} week^{-1}). Another set of treatment tanks (T_2 - T_{2-1}, T_{2-2}, T_{2-3} and T_{2-4}) received commercial feed with a higher probiotic dose (0.030 g m^{-2} week^{-1}).

The commercial probiotic and the use of it as a water additive

According to the manufacturer, the powdered probiotic used for the present study contains spore-forming *Bacillus* spp. (1.0 × 10^9 CFU g^{-1}), *B. subtilis* (1.0 × 10^9 CFU g^{-1}), and *B. licheniformis* (1.0 × 10^9 CFU g^{-1}), and non-spore-forming *Nitrosomonas* sp. (0.25 × 10^9 CFU g^{-1}) and *Pediococcus acidilactici* (1.0 × 10^9 CFU g^{-1}) bacteria. The probiotic was directly added to the rearing water following the manufacturer's instructions. The water in the experimental tanks (T_1 & T_2) were treated with the probiotic at a rate of 0.012 g m^{-2} (lower dose for T_1) and 0.03 g m^{-2} (higher dose for T_2) weekly, while the water in the control tanks (Tc) received no probiotic.

Feeding protocol

Following Withanage (2022), C. *catla* fries in each tank (experimental and control) were fed a recommended commercial feed 3 times a day at 9.00 am, 12.00 noon, and 4.00 pm. According to Withanage (2022), the daily feed ration was adjusted biweekly based on the live body weight of C. *catla* fry, starting from 12.0% of body weight initially; this was then adjusted to 8% and 6% (Mohanty, 2003; Biswas *et al*., 2006). The water volumes (water levels) in the control and treatment tanks were maintained constant for the experimental period; the water lost through evaporation was refilled every 2 ds to maintain a constant water level in each tank (Yang *et al*., 2021).

Fish performance and feed utilizations

The growth of C. *catla* fry was assessed biweekly for 66 ds. Random fish samples were collected from each tank; excess water was removed using clean tissue paper, and the weight of each fish was recorded using an electronic balance (OHASU Adventure AR 2130, USA). After recording each fish's standard length (SL) and total length (TL) separately, each was released back to the relevant tank very carefully. Following Banu *et al*. (2020), conventional methods were employed to compare growth performance under different treatments. (Hossain *et al*., 2017; Banu *et al*., 2020).

To determine the growth performance of C. *catla*, the following parameters, *viz*., weight gain rate (WGR%), final body weight (FBW), condition factor (k), average daily gain (ADG), length gain rate (LGR), specific growth rate (SGR), survival rate (SR%), length gain (LG), feed conservation ratio (FCR), and feed conservation efficiency (FCE) were measured based on the following equations (Froese *et al*., 2013; M. Y. Hossain *et al*., 2015; Shah *et al*., 2021; Tabassum *et al*., 2021):

$$\text{Condition factor (k)} = \frac{\text{Body weight in gm}}{(\text{Body length in cm})^3} \times 100$$

$$\text{ADG} = \frac{(\text{Mean final fish weight} - \text{Mean initial fish weight})}{\text{Time (final time} - \text{initial time)}}$$

$$\text{SGR(\%)} = \frac{(\ln W_t - \ln W_1)}{(\text{Final Time} - \text{Initial Time})} \times 100$$

$$\text{FCR} = \frac{\text{Feed (g) consumed by the fish}}{\text{Weight (g) grain of the fish (Final weight} - \text{Initial weight)}}$$

$$\text{Survival rate (\%)} = \frac{\text{No of actual fish survived}}{\text{No actual fish stocked}} \times 100$$

$$\text{Weight gain (WG, g/fish)} = W_t - W_0$$

Where W_0 = initial mean weight of fish in grams.
W_t = the final mean weight of fish in grams.

$$\text{Length gain Rate} = \frac{L_t - L_0}{L_0} \times 100$$

Where L_0 = initial mean length of fish in cm.
L_t = Final length of fish in cm.

$$\text{Weight gain (\%)} = \frac{\text{mean final weight} - \text{mean initial weight}}{\text{mean initial weight}} \times 100$$

Total feed intake (g) = Total food consumed (g) in each group.

Length-Weight Relationship (LWR) and condition factors of *C. catla* were calculated using the following formula.

The relationship between weight (W) and length (L) in fish has the form:

$W = aL^b$

Where a = scaling coefficient for the weight at the length of the fish species.
b = shape parameter for the body form of the fish species.

When the above model is logarithmically transformed

In (W) = In (a) + b In (L) or Y = A + b X

Where ln(a) is the intercept and (b) is the slope or regression coefficient of the graph of Ln W against Ln L

The above relationship is linear and was used to calculate ordinary linear regression using Microsoft Excel (Kadhar *et al.*, 2014).

Monitoring water quality

The physicochemical parameters of each tank's culture water (pH, DO, TDS, and EC) were recorded daily at 10:00 hrs. using a multiparameter (Thermo Scientific –Star A221). Nitrate and ammonia were measured using APHA Standard Methods (APHA, 2017).

Statistical analysis

One-way analysis of variance (ANOVA) was used to determine the significant variation between the different tested groups, followed by the Tukey HSD test. Statistical significance was settled at a probability value of $p < 0.05$. Principal Component Analysis (PCA) was applied to reduce the dimensionality of the data set and to analyze the water quality indicators, including pH, TDS, Temperature, EC, DO, NO_3^-, and NH_4^+, of all treatment samples. The first four principal components (PCs) were selected based on their eigenvalues above the threshold of unity, which is a widely used standard. Four PCs were obtained by extracting the correlation matrix. Statistical analysis was performed using Minitab version 21 for Windows.

RESULTS AND DISCUSSION

Growth performance and survival

At the end of the study, the survival of *C. catla* fry showed a significant difference between the control and treatment groups *(p < 0.05).* The results indicated that treatments T_2 and T_1 exhibited the highest survival rates (Figure 3) compared to all other treatments, while the control group showed a slightly lower survival rate *(p < 0.05)*. However, during the initial trial stage, statistical analysis indicated no significant differences in fish weight between the treatment and control tanks *(p > 0.05*, Table 1). The growth performance parameters FCR, SGR, FBW, ADG, k, FL, BWG, and TL did not show significant differences *(p >0.05)*.

The T_2 group exhibited the highest survival rate (Figure 3) of 92 ± 1.5%, followed by the T_1 group, with a rate of 87 ± 0.4%, and the T_C group, with a rate of 80 ± 0.3%. Furthermore, the (mean) survivability rate of *C. catla* was significantly increased in the T_2 (95.5 ± 0.2%) treatment as compared to the T_1 (93.02 ± 0.3%) and T_C (90.00 ± 0.1%) treatments.

The logarithmic analysis of the length-weight relationship (LWR) and determination coefficient values (R2) are shown in Figures 4, 5, and 6. The experiment revealed a significant positive correlation between length and weight with r (102) = 0.71, *p < 0.001*. Additionally, Figures 4, 5 and 6 demonstrate substantial and strong positive correlation *(p < 0.05)* between length and weight across all experimental groups, with correlation coefficients of 0.712, 0.862, and 0.855 for TC, T1, and T2 treatments, respectively (Table 1). Moreover, no significant changes were recorded in the average growth quality parameters *(p > 0.05)*.

Table 1:   Growth performance and biometric indices of *C. catla* fry Mean ± SE).

Parameters	T_C Control	T_1 Treatment	T_2 Treatment	P value
Initial body weight (g)	0.25 ± 0.00[a]	0.25 ± 0.00[a]	0.26 ± 0.00[a]	0.109
Final body weight (g)	0.84 ± 0.04[a]	0.87 ± 0.03[a]	0.92 ± 0.03[a]	0.193
Average daily weight gain (g)	0.009 ± 0.00[a]	0.009 ± 0.00[a]	0.009 ± 0.00[a]	0.957
Body weight gain (g)	0.38 ± 0.10[a]	0.39 ± 0.13[a]	0.40 ± 0.14[a]	0.996
SGR (%)	2.29 ± 0.15[a]	2.27 ± 0.23[a]	2.21 ± 0.26[a]	0.969
Weight gain rate (%)	149.9 ± 40.2[a]	153.3 ± 51.8[a]	151.9 ± 54.0[a]	0.997
FCR	1.49 ± 0.33[a]	1.47 ± 0.41[a]	1.57 ± 0.50[a]	0.985
Final Total length (cm)	3.97 ± 0.05[a]	4.03 ± 0.05[a]	4.03 ± 0.05[a]	0.700
Final Standard length (cm)	3.15 ± 0.04[a]	3.24 ± 0.04[a]	3.24 ± 0.04[a]	0.307
Condition factor (k)	1.06 ± 0.06[a]	1.02 ± 0.02[a]	1.02 ± 0.02[a]	0.731
Total feed intake (g)	62.95 ± 4.09[a]	60.57 ± 5.33[a]	65.57 ± 7.15[a]	0.841
Weekly survival rate (%)	90.00 ± 1.66[b]	93.02 ± 1.18[ab]	95.50 ± 5.52[a]	0.010

The different superscript letters in the same row indicate significant differences ($p < 0.05$).
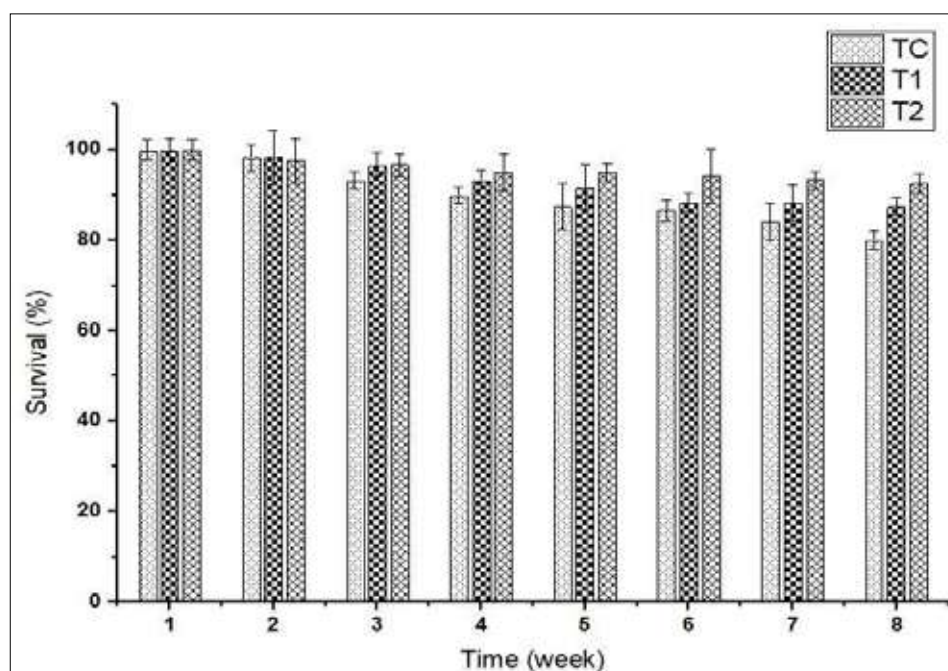

Figure 3:   The survival rate among treatments (Initially, treatment T_1, T_2, and control tanks showed similar survival percentages. At the end of the study, control tanks showed the lowest survival and probiotic-treated tanks showed the highest survival compared to control tanks).
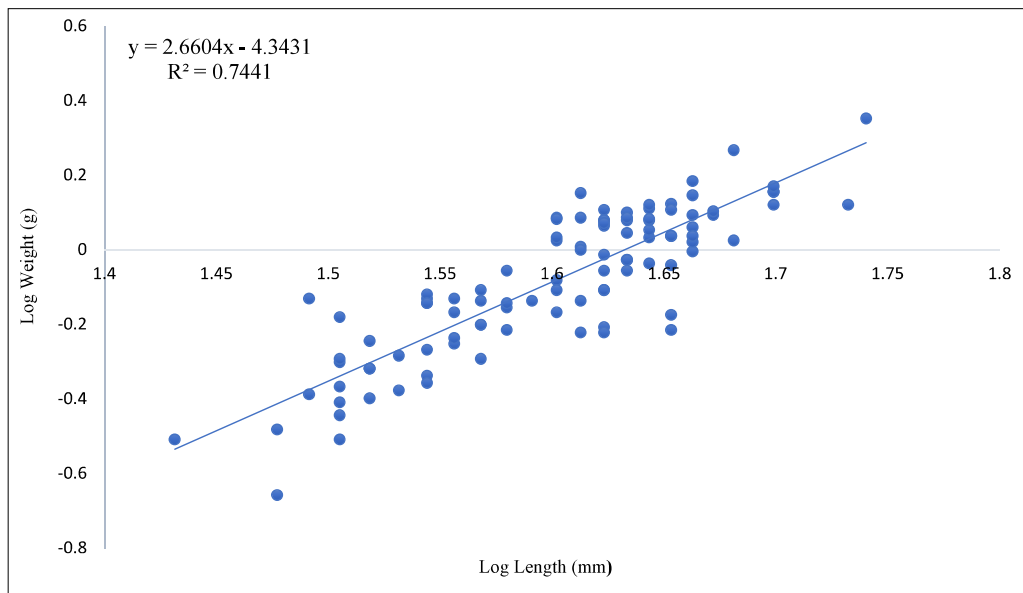
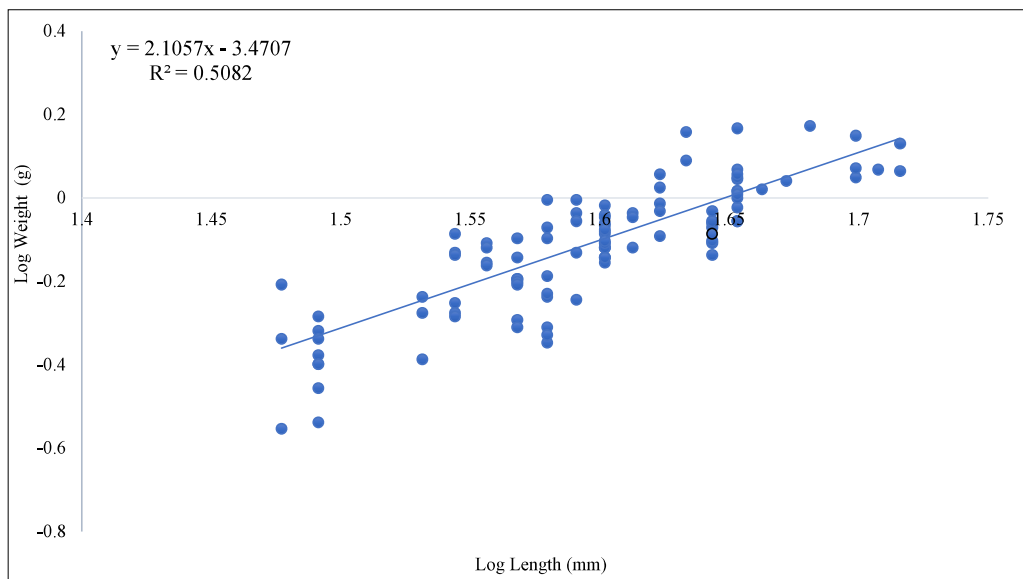**Figure 4:**   Length-weight relationship of *C. catla* supplement probiotic in T_1 tanks.

Figure 5:   Length-weight relationship of *C. catla* supplement probiotic in T_C tanks.
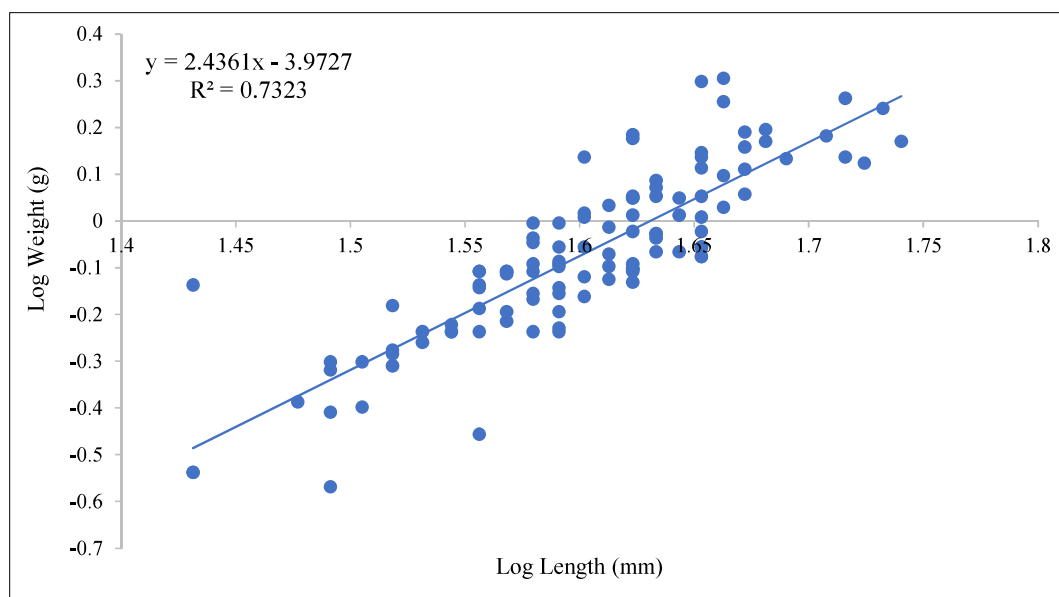
Figure 6:   Length-weight relationship of *C. catla* supplement probiotic in T$_2$ tanks.

Water quality

PCA was employed to analyze the water quality indicators, including pH, TDS, Temperature, EC, DO, NO$_3^-$, and NH$_4^+$, of all treatment samples. The first four components were selected based on their eigenvalues above the threshold of unity, a widely used standard. Four PCs were obtained by extracting the correlation matrix. These PCs represent the processes that influence the chemical composition of water and account for approximately 84.0% of the total variance in the sample. The details can be found in Table 2. The PC variance is as follows: 34.9% for PC1, 21.4% for PC2, 14.6% for PC3, and 13.1% for PC4. All PCs that had eigenvalues larger than 0.9 were kept in this investigation. The first principal component strongly relates to two of the original variables. The physicochemical attributes exhibited minimal positive loadings to the factor (PC1) in the data sets. PCA assesses the availability of either a positive or negative correlation. A value close to 1 suggests a strong correlation between the parameter and the PC. The number exceeding 0.75 signifies a strong association. The study revealed a strong correlation among values ranging from 0.5 to 0.74. The first principal component positively correlates with rising TDS and EC scores. This indicates that these two criteria exhibit a correlation. The variables exhibit a positively correlated pattern, whereby the increase of one corresponds to the increase of others. Table 2 demonstrates that TDS and EC have strong positive loadings on PC 1, while DO and pH significantly contribute to PC2. In addition, NH$_4^+$ exhibits the most significant favourable loading on PC3, while temperature and NO$_3^-$ display the most excellent favourable loading on PC4.

Additionally, it has been shown that the first principal component exhibits the highest correlation with the TDS. With a correlation coefficient 0.553, this primary component predominantly indicates the TDS. Parameters with high values typically indicate a significant amount of TDS available for treatment. The second principal component is positively correlated with none of the variables but negatively correlated with pH and DO. The data set showed a strong positive correlation (0.898) between the factor PC3 and the physicochemical feature of NH$_4^+$.

Additionally, the biplot derived from the PCA analysis illustrates the connections between different treatment groups in the two-dimensional space defined by the first two components. Principal component 1 has similar heavy loadings for NO$_3^-$, NH$_4^+$, DO, temperature, TDS, EC, and pH. The biplot reveals that the ammonia, TDS, EC, and nitrate water quality parameters indicate higher levels of differences from the origin than the pH, temperature, and DO parameters.

Table 2: PCA loadings and percentage of variance were explained for water quality parameters in the study on the impact of a probiotic mixture on *C. catla*.

Parameter	PC1	PC2	PC3	PC4
PH	0.126	-0.588	0.252	0.449
TDS	0.553	0.287	0.040	-0.085
Temperature	0.337	-0.380	-0.028	-0.568
DO	0.398	-0.518	-0.101	0.059
EC	0.545	0.320	-0.016	-0.109
NO_3^-	0.307	0.181	-0.342	0.663
NH_4^+	0.121	0.156	0.898	0.117
Eigenvalue	2.4449	1.4997	1.0225	0.9197
% Cumulative variance	34.9	56.4	71.0	84.1
% variance explained	34.9	21.4	14.6	13.1

Table 3: Effect of the probiotic supplement on water quality in *C. catla* tanks (Mean±SE).

Parameters	T_C Control	T_1 Treatment	T_2 Treatment	p value
pH	6.81 ± 0.07^a	6.74 ± 0.07^a	6.63 ± 0.07^a	0.261
Temperature (ºC)	24.99 ± 0.16^a	25.16 ± 0.15^a	25.09 ± 0.15^a	0.761
TDS (mg L^{-1})	71.77 ± 4.27^a	74.43 ± 2.90^a	74.65 ± 3.50^a	0.821
DO (mg L^{-1})	6.19 ± 0.14^b	6.69 ± 0.09^b	6.85 ± 0.12^a	0.010
EC (µS cm^{-1})	146.34 ± 7.43^a	159.97 ± 7.24^a	148.03 ± 7.81^a	0.194
TAN (mg L^{-1})	0.083 ± 0.07^a	0.052 ± 0.04^b	0.064 ± 0.05^b	0.006
NO_3^--N (mg L^{-1})	1.76 ± 0.18^b	2.56 ± 0.34^a	2.54 ± 0.32^a	0.006

The different superscript letters in the same row indicate different subsets identified by analysis of variance (ANOVA) followed by Tukey post-hoc multiple comparisons of significant differences among groups. Means ± SE in the same row superscripted with varying lowercase letters are significantly ($p < 0.05$) different.

The water quality parameters of the control and treatment tanks are given in Table 3. The control tanks had the lowest average DO levels (6.19 ± 0.14 mg L-1), while the T2 had the highest average DO levels (6.85 ± 0.12 mg L-1). The DO level at the treatment tanks was significantly higher than that of the control ($p < 0.05$). After two weeks, the tanks treated with probiotics exhibited notably elevated concentrations of DO, and this increase persisted over time (Figure 08). No statistically significant difference ($p > 0.05$) in the mean values for pH, temperature, TDS, and EC was observed between the treatment and control groups. Nevertheless, the transparency levels of the groups treated with probiotics (T_1 and T_2) remained consistently low. The concentrations of ammonia differed significantly between the two treatment groups that received probiotics and the control group ($p < 0.05$). The control groups (Tc) had the highest average TAN concentration of 0.083 ± 0.01 mg L^{-1}, while the treatments with probiotics had the lowest average TAN concentrations ($T_1 = 0.052 \pm 0.04$ mg L^{-1} and $T_2 = 0.064 \pm 0.05$ mg L^{-1}, $p < 0.05$). In addition, NO_3^- concentrations in the T_1 and T_2 treatments were significantly higher compared to the control Tc groups ($p < 0.05$). The concentration of NO_3^- increased as the culture age progressed in all treatments (Figure 09), ranging from 1.76 to 2.54 mg L^{-1}. In addition, probiotic supplement-treated T_2 groups had the highest mean NO_3^- (2.56 ± 0.34 mg L^{-1}), whereas control treatments had the lowest mean NO_3^- (1.76 ± 0.18 mg L^{-1}). The water temperature in the treatment and control groups varied between 24.99 ºC and

25.16 ºC. The temperature exhibited uniform fluctuations throughout the entire duration of the experiment. The pH remained consistent and within acceptable limits throughout the study. Nevertheless, the result indicated a diminished concentration of water colour in the groups that received probiotic treatment (T_1 and T_2). A statistically significant difference ($p < 0.05$) was found in the concentration of TAN between the two groups treated with probiotics and the control group (Figure 07).

In addition, the control group Tc had the highest average TAN concentration of 0.083 ± 0.007 mg L^{-1}. In contrast, the probiotic treatments ($p < 0.05$, $T_2 = 0.064 \pm 0.005$ mg L^{-1} and $T_1 = 0.052 \pm 0.004$ mg L^{-1}) had the lowest average TAN concentration. The nitrate concentration in the T_1 (2.56 ± 0.34 mg L^{-1}) and T_2 (2.54 ± 0.32 mg L^{-1}) groups were significantly higher (p = 0.006, $p < 0.05$) compared to the control Tc groups.
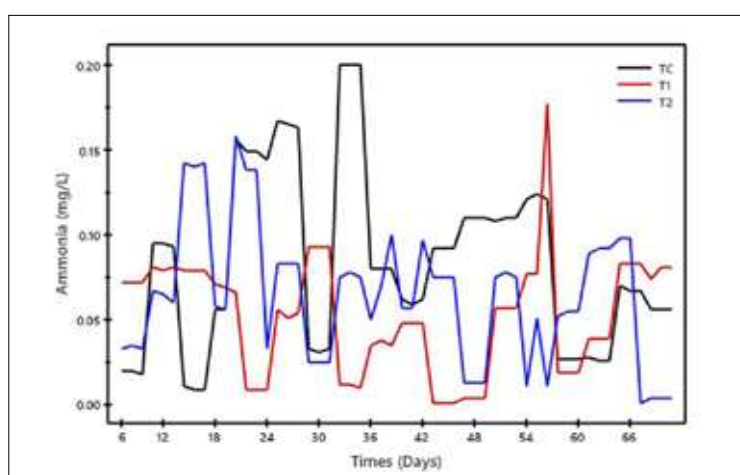

Figure 7: Variation of Ammonia (NH_4^+) concentration during the experimental period.
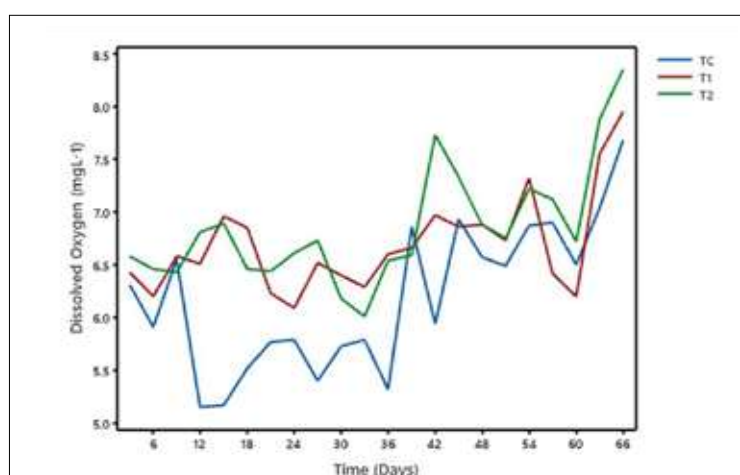

Figure 8: Variation of dissolved oxygen (DO) concentration during the experimental period.
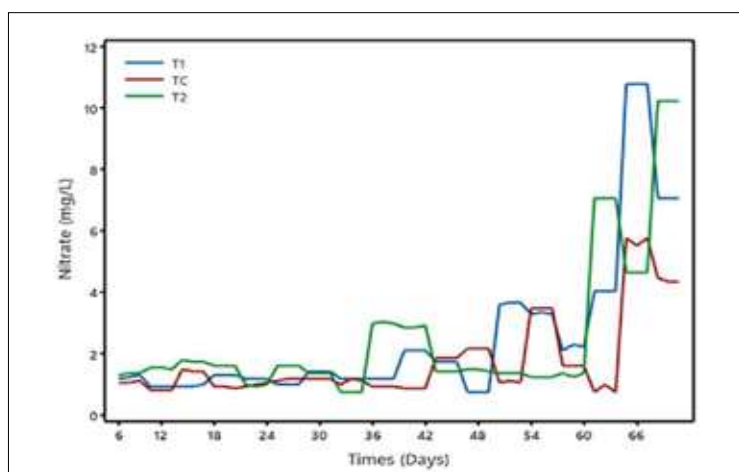
Figure 09: Variation of Nitrate (NO$_3^-$) concentration during the experimental period.

The study findings showed that probiotic direct supplementation significantly impacted the water quality parameters in the rearing water. The probiotic-treated tanks showed significantly greater dissolved oxygen levels than the control groups. Therefore, providing probiotic supplements containing *Bacillus* sp. can increase DO concentration in aquaculture (Mishra & Sharma, 2021; Nayak, 2020; Olmos, 2014). According to some earlier studies, adding *Bacillus* sp. improved the dissolved oxygen concentrations in waterways (Sahu *et al.*, 2008; Shah *et al.*, 2021; Tabassum *et al.*, 2021). The bacterial spores, such as *B. subtilis*, *B. licheniformis*, *P. acidilactici*, *Bacillus* sp. coagulants, *Nitrosomonas* sp., and *Nitrobacter* sp., were consistent in the bacterial mixture used in this experiment. These specific bacteria are referred to as probiotic bacteria from the genera *Pseudomonas* sp., *Rhodopseudomonas* sp., *Bacillus* sp., *Nitrosomonas* sp., and *Nitrobacter* sp. as potential bioremediation for aquaculture waste (Shah *et al.*, 2021; Tabassum *et al.*, 2021). These bacterial species inhibit pathogenic activities and expedite the aquaculture water degradation, which was undetectable in the present research.

The study showed a significant difference in TAN and NO$_3^-$ concentrations between the treatment and control groups. Tanks treated with probiotics had lower TAN concentrations. Previous research has recently shown how *Bacillus* sp. can survive in aerobic, anaerobic, and facultative aerobic environments; this unique characteristic permits a change in the metabolism of nitrogen species, boosting the nitrification and denitrification processes (Kumar *et al.*, 2015; Wang *et al.*, 2008). This could be due to the probiotic bacteria's ability for bioremediation and the approach to using probiotic supplements (Jahangiri, 2018; Samarawardane *et al.*, 2021). When the bacteria are present in tanks, they efficiently transform the organic matter into simple, non-toxic substances, which the bacteria need to initiate their metabolism, having the organic matter in the environment as the sole carbon source (Zhou *et al.*, 2009). This might account for probiotic-treated tanks having lower ammonia concentrations than control tanks. In addition, *Nitrobacter* sp. and *Nitrosomonas* sp. were used as probiotics and effectively broke down organic matter in water. This may also be the reason for the low NH$_4^+$ levels and high-water transparency in probiotic-treated tanks. However, the average TDS, pH, EC, and temperature values were not affected by the addition of probiotics to rearing water and were within acceptable levels. Similar results have been reported by Zhou *et al.* (2009) and Yang *et al.* (2021) also. Probiotic tank treatments might be a valuable approach in rearing *Catla catla* fry. More comparison studies are needed to determine the impact of probiotic supplements on the water quality of tanks used for livestock farming.

Growth performance and feed utilization

The results of this study revealed that the direct addition of the probiotic combination to the culture water had no impact on the growth parameters. This might be because the fish may not have taken in enough probiotics through this method of administration to stimulate their digestive mechanisms effectively (El-kady *et al.*, 2022). Similar trends were found (Hassan *et al.*, 2022; Jahangiri,

2018). Nevertheless, *C. catla* survival in ponds treated with probiotics was significantly higher than in control ponds. Previous studies have demonstrated that probiotic administration significantly increases host species survival rates (Tabassum *et al.*, 2021). When added directly to the water, the optimal dosage of probiotics should be determined based on the weight of the fish being treated and the volume of water (Hai, 2015). It is crucial to utilize probiotics properly since the manufacturer-recommended dosage also significantly increases the host species survival. The capacity of a species to fight invasions decides how long it can survive (El-Kady *et al.*, 2022). Probiotic supplementation has improved survival rates, particularly in earlier studies (Dawood & Koshio, 2016; Jahangiri, 2018). This could be caused by the administration method of the probiotic supplement.

Length-weight relationships (LWRs) and condition factors are generally used to evaluate the health and growth of fish (Froese *et al.*, 2013; Hossain *et al.*, 2015). The LWR of each fish is influenced by its behaviour, maturity, sex, and diet (Kadhar *et al.*, 2014; Bag *et al.*, 2016). In this study, all groups including those who received probiotics displayed excellent growth. LWRs are important for comparing life histories of fish and play a significant role in fisheries management (Froese *et al.*, 2013). LWRs are important for conservation and to prevent the exploitation of young fish and reduce the impact on spawning stocks (Tabassum *et al.*, 2021). Present study found no relationship between probiotic administration and LWR of *Catla catla* fry. Thus, the findings indicated that addition of probiotics into water improved only a few water quality parameters and had no effect on the growth of the *Catla catla* fry. Their survival rates also increased probably due to changing of the water quality to desirable ranges. However, more studies on the direct administration of probiotics is needed to develop effective and affordable therapies for the species used in aquaculture.

CONCLUSION

Findings of this study revealed that probiotic supplementation added to culture water could significantly reduce the NH_4^+ concentration in the water while increasing the survival rate of young *C. catla* fry. However, this method of administration did not enhance their growth performance of *C. catla*. Therefore, it is recommended that more comprehensive studies be conducted on applying probiotics as a water additive.

Acknowledgement

Ethics Statement

The researchers adhered to all institutional and national guidelines for the care and use of laboratory animals.

REFERENCES

Adikari, A., Sundarabarathy, T. V., Herath, H., Nayananjalie, W. A. D., & Adikari, A. (2017). Formulating artificial feeds for Indian carp (*Catla catla*) fry using aquatic plants (*Ipomoea aquatica* and *Hydrilla verticillata*). *International Journal of Scientific Research Publications, 7*(7), 83–89. https://www.ijsrp.org/research-paper-0717.php?rp=P676566

Athukorala, D. A. (2008). Reproductive biology of *Catla catla* in the Udawalawe Reservoir, Sri Lanka. *Sri Lanka Journal of Aquatic Sciences, 13*(1), 47-58.

American Public Health Association. (2017). *Standard methods for the examination of water and wastewater* (23rd ed.). Washington, DC: American Public Health Association.

Ali, H., Rahman, M. M., Jaman, A., Eltholth, M., & Murray, F. J. (2021). Assessment of the efficacy of prophylactic health products on water quality and shrimp (*Penaeus monodon*) performance at the nursery phase. *Aquaculture Nutrition, 27*(4), 1173–1180. https://doi.org/10.1111/anu.13257

Bag, N., Moulick, S., & Mal, B. C. (2016). Effect of stocking density on water and soil quality, growth, production and profitability of farming Indian major carps. *Indian Journal of Fisheries, 63*(3). https://doi.org/10.21077/ijf.2016.63.3.31448-05

Banerjee, G., & Ray, A. K. (2017). The advancement of probiotics research and its application in fish farming industries. *Research in Veterinary Science, 115*, 66–77. https://doi.org/10.1016/j.rvsc.2017.01.016

Biswas, G., Jena, J. K., Singh, S. K., & Muduli, H. K. (2006a). Effect of feeding frequency on growth, survival and feed utilization in fingerlings of *Catla catla* (Hamilton), *Labeo rohita* (Hamilton) and *Cirrhinus mrigala* (Hamilton) in outdoor rearing systems. *Aquaculture Research, 37*(5), 510–514. https://doi.org/10.1111/j.1365-2109.2006.01457.x

Das, S., Mondal, K., Pal, A. K., & Sengupta, C. (2021). Evaluation of the probiotic potential of *Streptomyces antibioticus* and *Bacillus cereus* on growth performance of freshwater

catfish *Heteropneustes fossilis. Aquaculture Reports*, *20*, 100752. https://doi.org/10.1016/j.aqrep.2021.100752

Dash, G., Raman, R. P., Prasad, K. P., Marappan, M., Pradeep, M. A., & Sen, S. (2014). Evaluation of *Lactobacillus plantarumas* a water additive on host associated microflora, growth, feed efficiency and immune response of giant freshwater prawn, *Macrobrachium rosenbergii* (de Man, 1879). *Aquaculture Research*, *47*(3), 804–818. https://doi.org/10.1111/are.12539

Dawood, M. A., & Koshio, S. (2015). Recent advances in the role of probiotics and prebiotics in carp aquaculture: A review. *Aquaculture*, *454*, 243–251. https://doi.org/10.1016/j.aquaculture.2015.12.033

El-Kady, A. A., Magouz, F. I., Mahmoud, S. A., & Abdel-Rahim, M. M. (2021). The effects of some commercial probiotics as water additive on water quality, fish performance, blood biochemical parameters, expression of growth and immune-related genes, and histology of Nile tilapia (*Oreochromis niloticus*). *Aquaculture*, *546*, 737249. https://doi.org/10.1016/j.aquaculture.2021.737249

El-Saadony, M. T., Alagawany, M., Patra, A. K., Kar, I., Tiwari, R., Dawood, M. A., Dhama, K., & Abdel-Latif, H. M. (2021). The functionality of probiotics in aquaculture: An overview. *Fish & Shellfish Immunology*, *117*, 36–52. https://doi.org/10.1016/j.fsi.2021.07.007

Froese, R., Thorson, J. T., & Reyes, R. B. (2013). A Bayesian approach for estimating length-weight relationships in fishes. *Journal of Applied Ichthyology*, *30*(1), 78–85. https://doi.org/10.1111/jai.12299

Hai, N. (2015). The use of probiotics in aquaculture. *Journal of Applied Microbiology*, *119*(4), 917–935. https://doi.org/10.1111/jam.12886

Hansika, R. K. N., Withanage, M. P., Fouzi, M. N. M., Muneeb, M. M., & Rahmathullah, M. (2024). Development of an Efficient Fish Feed for *Catla catla* Post Larvae to Enhance the Survival Rates of Nursery Stages by Using Available Raw Materials. *Bulletin of University of Agricultural Sciences and Veterinary Medicine Cluj-Napoca Animal Science and Biotechnologies*, *81*(1), 14–21. https://doi.org/10.15835/buasvmcn-asb:2024.0007

Hassan, M. A., Fathallah, M. A., Elzoghby, M. A., Salem, M. G., & Helmy, M. S. (2022). Influence of probiotics on water quality intensified *Litopenaeus vannamei* ponds under minimum-water exchange. *AMB Express*, *12*(1). https://doi.org/10.1186/s13568-022-01370-5

Hossain, M. Y., Sayed, S. R. M., Rahman, M. M., Ali, M. M., Hossen, M. A., Elgorban, A. M., Ahmed, Z. F., & Ohtomi, J. (2015). Length-weight relationships of nine fish species from the Tetulia River, southern Bangladesh. *Journal of Applied Ichthyology*, *31*(5), 967–969. https://doi.org/10.1111/jai.12823

Jahangiri, L., & Esteban, M. Á. (2018). Administration of Probiotics in the Water in Fin Fish Aquaculture Systems: A review. *Fishes*, *3*(3), 33. https://doi.org/10.3390/fishes3030033

Kadhar, A., Kumar, A., Ali, J., & John, A. (2014). Studies on the Survival and Growth of Fry of *Catla catla* (Hamilton, 1922) Using Live Feed. *Journal of Marine Biology*, *2014*, 1–7. https://doi.org/10.1155/2014/842381

Kumar, R., Mukherjee, S. C., Ranjan, R., Vani, T., Brahmachari, R. K., & Nayak, S. K. (2015). Effect of dietary supplementation of *Bacillus subtilis* on haematological and immunological parameters of *Catla catla* (Hamilton). *Aquaculture International*, *23*(5), 1275–1292. https://doi.org/10.1007/s10499-015-9883-x

Manage, P. M. (2018). Heavy use of antibiotics in aquaculture: Emerging human and animal health problems – A review. *Sri Lanka Journal of Aquatic Sciences*, *23*(1), 13–27. https://doi.org/10.4038/sljas.v23i1.7543

Mishra, V., & Sharma, R. (2021). Impact of probiotic supplementation on water quality and behaviour parameters in *Cyprinus carpio. International Journal of Fisheries and Aquatic Studies*, *9*(1), 428–431. https://doi.org/10.22271/fish.2021.v9.i1e.2430

Mohanty, R. (2003). Feed intake pattern and growth performance of Indian major carps, common carp and freshwater prawn in a rice-fish integration system. *Asian Fisheries Science*, *16*(4). https://doi.org/10.33997/j.afs.2003.16.4.004

Nayak, S. K. (2020). Multifaceted applications of probiotic Bacillus species in aquaculture with special reference to *Bacillus subtilis. Reviews in Aquaculture*, *13*(2), 862–906. https://doi.org/10.1111/raq.12503

Olmos, J. (2014). *Bacillus subtilis* A Potential Probiotic Bacterium to Formulate Functional Feeds for Aquaculture. *Journal of Microbial & Biochemical Technology*, *06*(07). https://doi.org/10.4172/1948-5948.1000169

Pandiyan, P., Balaraman, D., Thirunavukkarasu, R., George, E. G. J., Subaramaniyan, K., Manikkam, S., & Sadayappan, B. (2013). Probiotics in aquaculture. *Drug Invention Today*, *5*(1), 55–59. https://doi.org/10.1016/j.dit.2013.03.003

Rathnachandra, S. D. D., Malkanthi, S. H. P., & Pothuwila, R. H. (2024). Forecasting of Inland Fish Production: Case of Catla (*Catla catla*) and Gift Tilapia (*Oreochromis niloticus*) Production in Udawalawa Reservoir in Sabaragamuwa Province, Sri Lanka. *Journal of Agriculture and Value Addition*, *7*(1), 66–83. https://doi.org/10.4038/java.v7i1.128

Sahu, M. K., Swarnakumar, N. S., Sivakumar, K., Thangaradjou, T., & Kannan, L. (2008). Probiotics in aquaculture: importance and future perspectives. *Indian Journal of Microbiology*, *48*(3), 299–308. https://doi.org/10.1007/s12088-008-0024-3

Samarawardane, T., Radampola, K., & Rathnapala, S. (2021). Effect of dietary probiotic supplementation on growth, survival, coloration and stress resistance in guppy (*Poecilia reticulata* Peters, 1859). *Tropical Agricultural Research and Extension*, *24*(3), 173. https://doi.org/10.4038/tare.v24i3.5520

Shah, S., Chesti, A., Rather, M., Hafeez, M., Aijaz, A., Yousuf, I., & Jan, S. (2021). Effect of Probiotics (*Bacillus subtilis*) on the Growth and Survival of Fingerlings of Grass Carp, *Ctenopharyngodon idella. Current Journal of Applied Science and Technology*, 31–37. https://doi.org/10.9734/cjast/2021/v40i1531411

Tabassum, T., Mahamud, A. G. M. S. U., Acharjee, T. K., Hassan, R., Snigdha, T. A., Islam, T., Alam, R., Khoiam, M. U., Akter, F., Azad, M. R., Al Mahamud, M. A., Ahmed, G. U., & Rahman, T. (2021). Probiotic supplementations improve growth, water quality, hematology, gut microbiota and intestinal morphology of Nile tilapia. *Aquaculture Reports*, *21*, 100972. https://doi.org/10.1016/j.aqrep.2021.100972

Wang, Y., Li, J., & Lin, J. (2008). Probiotics in aquaculture: Challenges and outlook. *Aquaculture*, *281*(1–4), 1–4. https://doi.org/10.1016/j.aquaculture.2008.06.002

Withanage, P. M., Rathnayaka, A. N. P., & Epa, U. P. K. (2022). Growth performance and survivability of *Catla catla* (*Cyprinidae*) fry fed with different levels of two cultivable mushrooms in Sri Lanka. *ResearchGate*. https://doi.org/10.13140/RG.2.2.33048.67843.

Yang, Z., Huang, S., Kong, W., Yu, H., Li, F., Khatoon, Z., Ashraf, M. N., & Akram, W. (2021). Effect of different fish feeds on water quality and growth of crucian carp (*Carassius carassius*) in the presence and absence of prometryn. *Ecotoxicology and Environmental Safety*, *227*, 112914. https://doi.org/10.1016/j.ecoenv.2021.112914

Zabidi, A., Yusoff, F. M., Amin, N., Yaminudin, N. J. M., Puvanasundram, P., & Karim, M. M. A. (2021). Effects of Probiotics on Growth, Survival, Water Quality and Disease Resistance of Red Hybrid Tilapia (*Oreochromis* spp.) Fingerlings in a Biofloc System. *Animals*, *11*(12), 3514. https://doi.org/10.3390/ani11123514

Zhou, X., Tian, Z., Wang, Y., & Li, W. (2009). Effect of treatment with probiotics as water additives on tilapia (*Oreochromis niloticus*) growth performance and immune response. *Fish Physiology and Biochemistry*, *36*(3), 501–509. https://doi.org/10.1007/s10695-009-9320-z

RESEARCH ARTICLE

Deep Learning

A comparison of optimizers in a PyTorch based artificial neural network to predict normal boiling points of alkanes

MZ Afzal* and SS Siddiqi
Department of Mathematics, University of Central Punjab, Lahore, Pakistan.

Abstract: In this study, we explore the effectiveness of various optimization algorithms for predicting the normal boiling points of alkanes using PyTorch-based neural network models. Alkane molecular structures were uniquely encoded into a machine-readable format and used to train both an artificial neural network (ANN) and a graph neural network (GNN) model. We compared the performance of three optimizers; Stochastic Gradient Descent (SGD), Adam, and Rprop, across two loss functions (L1Loss and MSELoss) and multiple learning rates (0.01, 0.001, and 0.0001). Our results indicate that Adam consistently yields the lowest mean squared error (MSE) values across both models, highlighting its robust performance. Notably, in the ANN framework, Rprop demonstrated rapid convergence and outperformed SGD, whereas in the GNN model, SGD showed superior performance compared to Rprop. The analysis of MSE values further corroborated these findings, emphasizing the critical role of optimizer selection in achieving both high accuracy and model stability. These insights provide valuable guidance for future applications of neural networks in chemical property prediction and underscore the importance of fine-tuning optimization parameters in machine learning workflows.

Keywords: Alkanes, boiling points of alkanes, neural network, optimizers, PyTorch.

INTRODUCTION

The (normal) boiling point of a substance is defined as the temperature at which it boils under standard atmospheric pressure. The common methods to determine the boiling points of substances are simple distillation, fractional distillation, reflux distillation, steam distillation, microscale boiling point determination, ebulliometry, and thermometric titration.

The boiling point of a substance holds significant importance in various fields of science and industry due to several reasons. It can be used to determine the purity of a substance. It is used to narrow down the possible identities of a compound. Knowledge of the boiling points of substances is crucial for controlling the separation and purification of chemical mixtures. The boiling point of a substance is indicative of its volatility and vapor pressure at a given temperature. Understanding the boiling points of substances helps in assessing the potential impacts of evaporation, condensation, and atmospheric dispersion on the environment in case of spills or releases. Knowledge of boiling points is essential for the handling and storage of chemicals safely.

Beside laboratory methods, quantitative structure-property relationship (QSPR) models became popular to predict normal boiling points after the seminal paper of Wiener (1947). In order to avoid an unusually long list of work in this direction, we are going to give references of papers that are published in the last twenty years. The normal boiling points of aldehydes, esters, and ketones were computed by Duchowicz *et al*. (2002). A wonderful review about predicting boiling point, melting point, and vapour pressure with QSPR models was published

* Corresponding author (l1f22phma0001@ucp.edu.pk; https://orcid.org/0009-0005-4472-2069)

by Dearden (2003). Using a QSPR technique, the boiling point of polycyclic aromatic hydrocarbons were studied by de Lima Ribeiro and Ferreira (2003). The normal boiling points of some organic molecules were computed by Gonz´alez et al. (2004). Using topological indices, the normal boiling points along with molar refractivities of a large set of organic compounds are found in the paper by Ghavami et al. (2009). SMILES-based optimal descriptors were used to find normal boiling points of acyclic and cyclic hydrocarbons by Toropov et al. (2010). Utilizing the electronegativity topological descriptor, Yi-min forecasted normal boiling points of alkanes, unsaturated hydrocarbons, and alcohols (Yi-min et al., 2013). With the help of semiempirical quantum chemistry, Saadi predicted the boiling points of amines (Saadi et al., 2015). The boiling points of n-alkanes were related to critical constants by Messerly et al. (2017). Using various topological indices, the normal boiling points of alcohols and phenols were predicted by Arjmand and Shafiei (2018). A new graph-based parameter, conduction, is introduced to develop a single-parameter model for accurately predicting alkane boiling points, offering a reliable alternative to experimental data (Mukwembi & Nyabadza, 2021). QSPRpred is an open-source Python toolkit for building, analyzing, and reproducing robust QSPR models, enabling seamless prediction of molecular properties from SMILES strings (van den Maagdenberg et al., 2024). A linear regression model accurately predicts thermochemical properties of alkanes (> C10) for studying hydro-isomerization equilibria in zeolites, outperforming traditional group contribution methods (Sharma et al., 2024).

Predicting boiling points using neural networks has evolved significantly over time, with advancements in both model architecture and data availability. It was Cherqaoui who first applied neural networks to find boiling points (Cherqaoui & Villemin, 1994; Cherqaoui et al., 1994). Using the molecular structure and a neural network, Goll predicted normal boiling points of some organic compounds (Goll & Jurs, 1999). A novel group contribution-based neural network model accurately predicts molecular boiling points across a wide temperature range, outperforming Joback's equation (Sumie & Umpei, 2010). Gharagheizi designed a three-layer feed-forward neural network along with the Levenberg–Marquardt optimization technique to predict normal boiling points of 17,768 chemical compounds (Gharagheizi et al., 2013). High-dimensional neural network (HDNN) potentials and systematic molecular fragmentation methods are compared for predicting alkane energies, with HDNN achieving higher accuracy against coupled cluster references (Gastegger et al.,

2016). By training an artificial neural network (ANN), Jin predicted normal boiling points of oxygen-containing and hydroxyl compounds (Jin & Bai, 2016a, 2016b, 2016c, 2016d). Neural networks trained on fragmented data predict physical properties of alkanes by leveraging property correlations, achieving high accuracy across various thermodynamic parameters (Santak & Conduit, 2019). By designing a multiple linear regression and a multi-layer perceptron neural network, Fissa predicted normal boiling points of pure hydrocarbons (Fissa et al., 2019). Using the Wang-Landau simulations and machine learning techniques, Groven predicted boiling points and critical points of polycyclic aromatic hydrocarbons (Groven et al., 2019). Using a graph convolutional neural network, Qu predicted normal boiling points of several organic compounds (Qu et al., 2022). A multi-layer perceptron model using molecular group descriptors accurately predicts thermophysical properties of fluorine/chlorine-containing refrigerants, with SHAP analysis confirming feature contributions (Li et al., 2022). Using an AI approach, Liu and Maryamto predicted normal boiling points of refrigerants (Liu et al., 2023). Lastly, A machine learning model was developed to accurately predict the boiling temperature of environmentally friendly insulation materials, aiding their screening and optimization (Tang et al., 2024).

We can efficiently train neural networks to discern the intricate relationships between molecular characteristics and boiling points, which ultimately enables us to predict the normal boiling points of alkanes with remarkable accuracy.

By leveraging PyTorch's robust framework and by using topological structures, this work predicts normal boiling points of 150 isomeric alkanes, which were extracted from NIST Chemistry Webbook https://webbook.nist.gov/ and analyzes the performance of several optimizers with different loss functions and learning rates.

MATERIALS AND METHODS

Data encoding

Consider an alkane isomer with a chain of at most 10 carbon atoms. We will represent this alkane isomer using a 10-digit number. First of all, carbon atoms in the straight chain are labelled, followed by branched ones. Each digit now corresponds to a number of carbon atoms connected to this carbon. The following example illustrates the encoding procedure for 2, 4-dimethyl-3-ethylpentane (Figure 1).
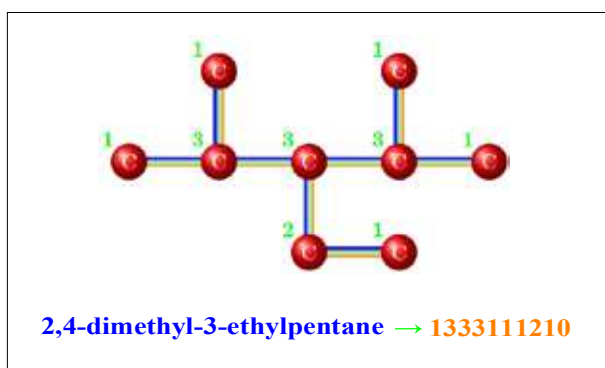
2,4-dimethyl-3-ethylpentane → 1333111210

Figure 1: Conversion of an alkane to a machine-readable code

Model architecture of ANN

Neural networks are computational models inspired by the human brain's structure, designed to recognize patterns and solve complex problems. They consist of interconnected layers of neurons that learn from data through training, enabling them to make predictions and decisions. This adaptive learning capability has led to significant advancements in fields such as image recognition, natural language processing, and predictive analytics. An example schematic of an ANN is depicted in Figure 2.
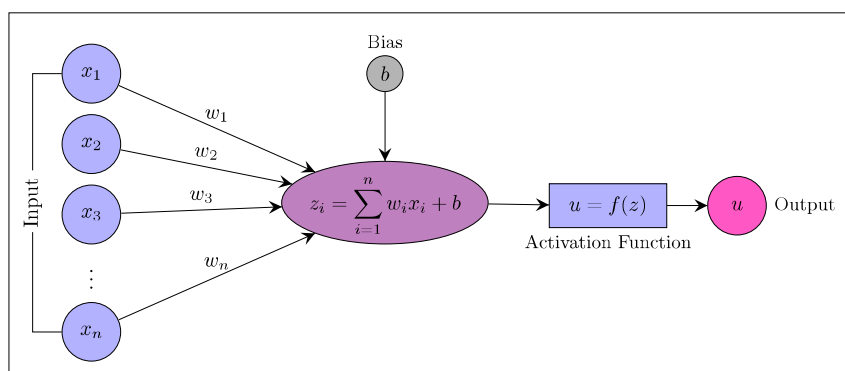

Figure 2: A schematic of a single artificial neuron, illustrating how the weighted sum of inputs plus bias is passed through an activation function to produce the output.

PyTorch to model a 3-layer ANN:

Input Layer: The input layer consists of 10 neurons, each representing one input feature. These neurons receive the input data and pass it to the next layer.

Hidden Layer: The hidden layer contains 7 neurons. Each neuron in the hidden layer receives inputs from all the neurons in the input layer. We used the sigmoid function as the activation function for each neuron in the hidden layer. This layer captures patterns and features in the input data.

Output Layer: The last layer of the network consists of a single neuron. It receives a weighted sum from all the neurons in the hidden layer. The output neuron predicts the normal boiling point of the corresponding alkane. The model is depicted in Figure 3.

Model architecture of graph neural network (GNN)

The GNN model used to predict the boiling point is depicted in Figure 4. This model is a GNN designed to predict the boiling points of chemical compounds using molecular structures represented as graphs. Each molecule is transformed into a graph where atoms serve as nodes with atomic number and degree as features, while bonds act as edges with bond type attributes. Additionally, molecular descriptors, as described in data encoding above, are included to enhance predictive accuracy. The GNN architecture comprises two graph convolutional layers (GCNConv) that extract relational features, followed by a fully connected layer that combines the graph embeddings with the molecular descriptors for final regression. The model is trained using both L1Loss and MSELoss loss functions and optimized using three optimizers: SGD, Adam, and Rprop over 3000 epochs. The best model is saved and used for inference, where predictions are exported to an Excel file.
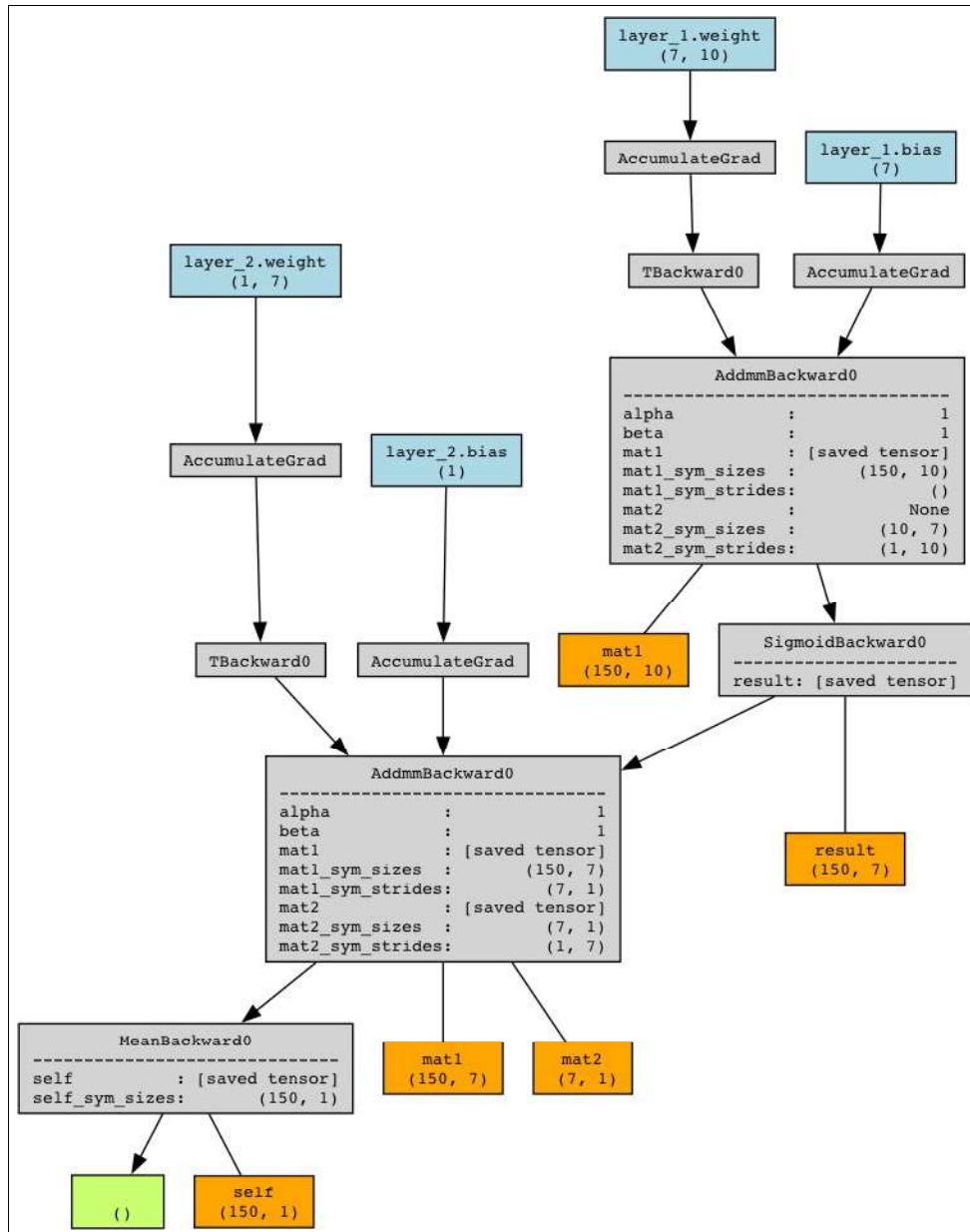
Figure 3: mat1 (input matrix) 150×10: 150-alkanes, each having 10-digit code; weight matrix (7×10) applied at the first layer. This results in a (150×7) matrix on which the sigmoid activation is applied. On the second layer weight matrix (1×7) is applied. This results in the final output matrix (150×1). The small grey rectangles store information about the operation applied at each layer, this helps the optimizer to keep track of the gradient descent operations. The α and β parameters are the values used by the optimizer during the backward pass. The stride parameter indicates that PyTorch inherently implements a convolution mechanism to perform matrix multiplications.

RESULTS AND DISCUSSION

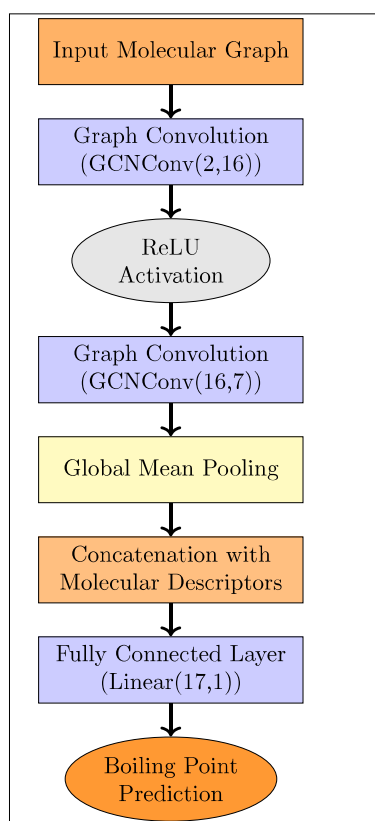In this section, we analyze the role of three optimizers, SGD, Adam, and Rprop, in the performance of our proposed models, ANN and GNN, in predicting the boiling points. The models were trained using each of the three optimizers and evaluated with two loss functions, L1Loss and MSELoss, across three learning rates (0.01, 0.001, and 0.0001). By systematically comparing these variations, we aim to assess the impact of different training configurations on prediction accuracy. The results provide insights into the effectiveness of ANN and GNN in capturing the underlying structure-property relationships in alkanes and highlight the most suitable model configurations for accurate boiling point prediction.

It can be seen in Figure 5 that Adam outperforms in both models. In the ANN model, Rprop proves more effective than SGD, while in the GNN model, SGD shows superior performance to Rprop. Note that Figure 5 compares only the validation dataset. Although the training loss continuously decreases, it is the validation performance that more accurately reflects potential overfitting, as improvements on the training data do not necessarily translate to better generalization.

Figure 4: GNN Boiling Point Flowchart

Table 1: MSE values for ANN and GNN under three optimizers (SGD, Adam, Rprop), two loss functions (L1Loss, MSELoss), and three learning rates (0.01, 0.001, 0.0001).

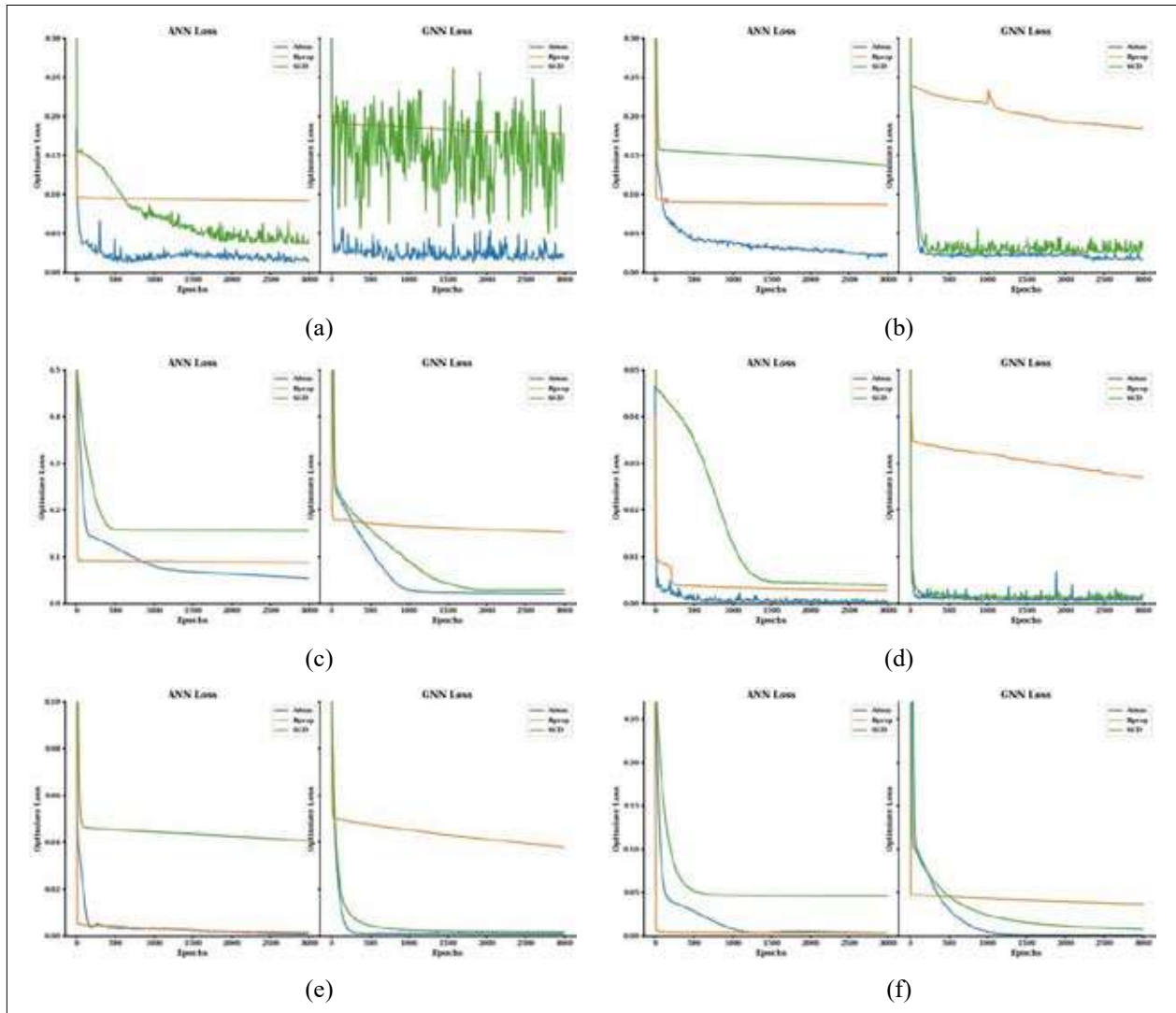| Loss Function	Learning Rate	ANN			GNN		
		SGD	Adam	Rprop	SGD	Adam	Rprop
	0.01	82.37	24.26	1322.45	109.69	12.91	1756.40
L1	0.001	2268.88	40.49	1180.48	67.68	19.59	1944.94
	0.0001	2541.31	235.00	1277.06	95.90	30.56	1825.25
	0.01	94.97	7.98	520.13	32.96	14.13	1372.73
MSE	0.001	2435.04	80.14	465.91	219.83	23.80	1382.61
	0.0001	2193.27	26.94	535.52	54.35	21.19	1579.77

(a)

(b)

(c)

(d)

(e)

(f)

Figure 5: (a)-(c) use L1Loss, while (d)-(f) use MSELoss, both with learning rates 0.01, 0.001, and 0.0001.

Statistical analysis

Table 1 presents the mean squared error (MSE) results obtained from the ANN and GNN models when trained using three optimizers (SGD, Adam, and Rprop) in combination with two loss functions (L1Loss and MSELoss) across three learning rates (0.01, 0.001, and 0.0001). Notably, these MSE values are calculated on the entire dataset—including the training, validation, and test sets—offering a comprehensive evaluation of model performance. Overall, Adam tends to yield lower MSE values compared to SGD and Rprop for both models, though the extent varies with the choice of loss function and learning rate. Rprop exhibits larger variability in some cases, while SGD occasionally achieves competitive performance, particularly in the GNN model. Furthermore, the trends observed in Table 1 align with those in the Figure 5, which focused solely on validation data, reinforcing the consistency of the observed optimizer performances. These findings underscore the importance of carefully selecting the optimizer, loss function, and learning rate to achieve optimal boiling point prediction accuracy.

CONCLUSION

This study demonstrates that neural networks, when effectively optimized using PyTorch, can accurately predict the normal boiling points of alkanes based on their molecular descriptors. Our experiments with both ANN and GNN architectures, trained with three optimizers (SGD, Adam, and Rprop), two loss functions (L1Loss and MSELoss), and various learning rates, reveal that overall, Adam consistently yields the lowest mean squared error. Notably, while Rprop outperforms SGD in the ANN model, the opposite trend is observed in the GNN model, where SGD shows superior performance over Rprop. For example, under MSELoss with a learning rate of 0.01, the ANN model achieved an MSE of 7.98 with Adam, compared to 94.97 with SGD and 520.13 with Rprop; similarly, the GNN model recorded an MSE of 14.13 with Adam, versus 32.96 with SGD and 1372.73 with Rprop. These findings underscore the potential of advanced neural network techniques in chemical property prediction, paving the way for their broader application in fields such as materials science and chemical engineering.

REFERENCES

Arjmand, F. & Shafiei, F. (2018). Prediction of the normal boiling points and enthalpy of vaporizations of alcohols and phenols using topological indices. *Journal of Structural Chemistry*, *59*, 748–754. Publisher: Springer. https://doi.org/10.1134/S0022476618030393

Cherqaoui, D. & Villemin, D. (1994). Use of a neural network to determine the boiling point of alkanes. *Journal of the Chemical Society, Faraday Transactions*, *90*(1), 97–102. Publisher: The Royal Society of Chemistry. https://doi.org/10.1039/ft9949000097

Cherqaoui, D., Villemin, D., Mesbah, A., Cense, J.-M., & Kvasnicka, V. (1994). Use of a neural network to determine the normal boiling points of acyclic ethers, peroxides, acetals and their sulfur analogues. *Journal of the Chemical Society, Faraday Transactions*, *90*(14), 2015–2019. https://doi.org/10.1039/ft9949002015

Dai, Y.-m., Zhu, Z.-p., Cao, Z., Zhang, Y.-f., Zeng, J.-l., & Li, X. (2013). Prediction of boiling points of organic compounds by QSPR tools. *Journal of Molecular Graphics and Modelling*, *44*, 113–119. Publisher: Elsevier. https://doi.org/10.1016/j.jmgm.2013.04.007

De Lima Ribeiro, F. A. & Ferreira, M. M. C. (2003). QSPR models of boiling point, octanol–water partition coefficient and retention time index of polycyclic aromatic hydrocarbons. *Journal of Molecular Structure: THEOCHEM*, *663*(1-3), 109–126. Publisher: Elsevier. https://doi.org/10.1016/j.theochem.2003.08.107

Dearden, J. C. (2003). Quantitative structure-property relationships for prediction of boiling point, vapor pressure, and melting point. *Environmental Toxicology and Chemistry: An International Journal*, *22*(8), 1696–1709. Publisher: Wiley Online Library. https://doi.org/10.1897/01-363

Duchowicz, P., Castro, E. A., & Toropov, A. (2002). Qspr Modeling of Normal Boiling Point of Aldehydes, Ketones and Esters by Means of Nearest Neighboring Codes Correlation Weighting. *Science Direct Working Paper*, (S1574-0331):04. https://ssrn.com/abstract=2969228

Fissa, M. R., Lahiouel, Y., Khaouane, L., & Hanini, S. (2019). QSPR estimation models of normal boiling point and relative liquid density of pure hydrocarbons using MLR and MLP-ANN methods. *Journal of Molecular Graphics and Modelling*, *87*, 109–120. Publisher: Elsevier. https://doi.org/10.1016/j.jmgm.2018.11.013

Gastegger, M., Kauffmann, C., Behler, J., & Marquetand, P. (2016). Comparing the accuracy of high-dimensional neural network potentials and the systematic molecular fragmentation method: A benchmark study for all-trans alkanes. *The Journal of chemical physics*, *144*(19). https://doi.org/10.1063/1.4950815

Gharagheizi, F., Mirkhani, S. A., Ilani-Kashkouli, P., Mohammadi, A. H., Ramjugernath, D., & Richon, D. (2013). Determination of the normal boiling point of chemical compounds using a quantitative structure–property relationship strategy: Application to a very large dataset. *Fluid Phase Equilibria, 354*, 250–258. Publisher: Elsevier. https://doi.org/10.1016/j.fluid.2013.06.034

Ghavami, R., Najafi, A., & Hemmateenejad, B. (2009). QSPR studies on normal boiling points and molar refractivities of organic compounds by correlation-ranking-based PCR and PC–ANN analyses of new topological indices. *Canadian Journal of Chemistry*, *87*(11), 1593–1604. https://doi.org/10.1139/V09-109

Goll, E. S. & Jurs, P. C. (1999). Prediction of the normal boiling points of organic compounds from molecular structures with a computational neural network model. *Journal of chemical information and computer sciences*, *39*(6), 974–983. Publisher: ACS Publications. https://doi.org/10.1021/ci9900711

Gonz´alez, M. P., Toropov, A. A., Duchowicz, P. R., & Castro, E. A. (2004). QSPR calculation of normal boiling points of organic molecules based on the use of correlation weighting of atomic orbitals with extended connectivity of zero- and first-order graphs of atomic orbitals. *Molecules*, *9*(12), 1019–1033. Publisher: MDPI. https://doi.org/10.3390/91201019

Groven, S. D., Desgranges, C., & Delhommelle, J. (2019). Prediction of the boiling and critical points of polycyclic aromatic hydrocarbons via Wang-Landau simulations and machine learning. *Fluid Phase Equilibria*, *484*, 225–231. https://doi.org/10.1016/j.fluid.2018.11.030

Jin, L. & Bai, P. (2016a). Modelling of normal boiling points of hydroxyl compounds by radial basis networks. *Mod. Chem.*, *4*(2), 24–29. https://doi.org/10.11648/j.mc.20160402.12

Jin, L. & Bai, P. (2016b). Prediction of the normal boiling point of oxygen containing organic compounds using quantitative structure–property relationship strategy. *Fluid Phase Equilibria*, *427*, 194–201. Publisher: Elsevier. https://doi.

org/10.1016/j.fluid.2016.07.015

Jin, L. & Bai, P. (2016c). QSPR study on normal boiling point of acyclic oxygen containing organic compounds by radial basis function artificial neural network. *Chemometrics and Intelligent Laboratory Systems*, *157*, 127–132. Publisher: Elsevier. https://doi.org/10.1016/j.chemolab.2016.07.007

Jin, L. & Bai, P. (2016d). QSPR study on normal boiling point of acyclic oxygen containing organic compounds by radial basis function artificial neural network. *Chemometrics and Intelligent Laboratory Systems*, *157*, 127–132. Publisher: Elsevier. https://doi.org/10.1016/j.chemolab.2016.07.007

Li, Q., Ren, J., Liu, Y., & Zhou, Y. (2022). Prediction of critical properties and boiling point of fluorine/chlorine-containing refrigerants. *International Journal of Refrigeration*, *143*, 28–36. https://doi.org/10.1016/j.ijrefrig.2022.06.024

Liu, B. & Nouroddin, M. K. (2023). Application of artificial intelligent approach to predict the normal boiling point of refrigerants. *International Journal of Chemical Engineering*, 2023. https://doi.org/10.1155/2023/6809569

Messerly, R. A., Knotts IV, T. A., Giles, N. F., & Wilding, W. V. (2017). Developing an internally consistent set of theoretically based prediction models for the critical constants and normal boiling point of large n-alkanes. *Fluid Phase Equilibria*, *449*, 104–116. https://doi.org/10.1016/j.fluid.2017.06.014

Mukwembi, S. & Nyabadza, F. (2021). A new model for predicting boiling points of alkanes. *Scientific reports*, *11*(1), 24261. https://doi.org/10.1038/s41598-021-03541-z

Qu, C., Kearsley, A. J., Schneider, B. I., Keyrouz, W., & Allison, T. C. (2022). Graph convolutional neural network applied to the prediction of normal boiling point. *Journal of Molecular Graphics and Modelling*, *112*, 108149. Publisher: Elsevier. https://doi.org/10.1016/j.jmgm.2022.108149

Saadi, S., Asrin, B., & Amin, R. (2015). Prediction the normal boiling points of primary, secondary and tertiary liquid amines from their molecular structure descriptors. *CMST*, *21*(4), 201–210. Publisher: PSNC, Poznan Supercomputing and Networking Center. https://doi.org/10.12921/

cmst.2015.21.04.004

Santak, P. & Conduit, G. (2019). Predicting physical properties of alkanes with neural networks. *Fluid Phase Equilibria*, *501*, 112259. https://doi.org/10.1016/j.fluid.2019.112259

Sharma, S., Sleijfer, J. J., Op de Beek, J., van der Zeeuw, S., Zorzos, D., Lasala, S., Rigutto, M. S., Zuidema, E., Agarwal, U., Baur, R., *et al.* (2024). Prediction of thermochemical properties of long-chain alkanes using linear regression: Application to hydroisomerization. *The Journal of Physical Chemistry B*, *128*(39), 9619–9629. https://doi.org/10.1021/acs.jpcb.4c05355

Sumie, T. & Umpei, N. (2010). Generation of a novel equation for molecular boiling point estimation using a neural network. *Journal of Computer Chemistry, Japan*, *9*(2), 73–78. https://doi.org/10.2477/jccj.H2128

Tang, N., Tan, J., Sun, D., Li, L., & Li, X. (2024). Boiling temperature prediction model of environmental friendly insulation molecules based on machine learning. In 2024 7th International Conference on Electric Power Equipment-Switching Technology (ICEPE-ST), pages 795–799. IEEE. https://doi.org/10.1109/ICEPE-ST61894.2024.10792464

Toropov, A., Toropova, A., & Benfenati, E. (2010). QSPR modelling of normal boiling points and octanol/water partition coefficient for acyclic and cyclic hydrocarbons using SMILES-based optimal descriptors. *Central European Journal of Chemistry*, *8*, 1047–1052. Publisher: Springer. https://doi.org/10.2478/s11532-010-0072-5

Van den Maagdenberg, H. W., Šícho, M., Araripe, D. A., Luukkonen, S., Schoenmaker, L., Jespers, M., B´equignon, O. J., Gonz´alez, M. G., van den Broek, R. L., Bernatavicius, A., *et al.* (2024). Qsprpred: a flexible open-source quantitative structure-property relationship modelling tool. *Journal of Cheminformatics, 16*(1), 128. https://doi.org/10.1186/s13321-024-00908-y

Wiener, H. (1947). Structural determination of paraffin boiling points. *Journal of the American Chemical Society*, *69*(1), 17–20. Publisher: ACS Publications. https://doi.org/10.1021/ja01193a005

RESEARCH ARTICLE

Food Processing Technology

Utilization of jackfruit seed flour (*Artocarpus heterophyllus* L.) as a thickening agent in tomato sauce production

CSDS Maduwage[1], SDN Kaushalya[2] and WAJP Wijesinghe[2*]
[1] *Department of Export Agriculture, Faculty of Animal Science and Export Agriculture, Uva Wellassa University, Sri Lanka.*
[2] *Department of Food Science and Technology, Faculty of Animal Science and Export Agriculture,Uva Wellassa University, Sri Lanka.*

Abstract: Starch-based thickening agents are widely used in the food industry, and corn flour (CF) is the most prominent in tomato sauce manufacturing. Jackfruit seeds which are highly abundant but underutilized source of flour, have very limited industrial applications. Jackfruit seed flour (JSF) which can be acquired from jackfruit seeds is a good option to meet different industrial applications. Hence, this study aims to investigate the thickening capacity of JSF in tomato sauce production. As functional properties of flour change with their drying techniques, two drying techniques: hot-air-drying (HAD-JSF) and freeze-drying (FD-JSF) were tried, and out of them, HAD-JSF was used for the further studies based on its functional properties and potential to be used in commercial level. According to the proximate analysis, ash, fat, crude protein, and crude fiber were significantly higher while moisture and total carbohydrate content were significantly lower in HAD-JSF than CF ($p < 0.05$). HAD-JSF incorporated tomato sauce showed incredible thickening properties with increased viscosity (1083 cP) with lower syneresis than CF- incorporated tomato sauce (1004 cP). During the 8 weeks of storage period, total soluble solids and titratable acidity of JSF- incorporated tomato sauce was significantly consistent ($p > 0.05$) while the pH and the water activity significantly increased ($p < 0.05$). The microbial counts were below the standard limits. JSF incorporated tomato sauce received the highest consumer acceptance on the sensory evaluations. This study proclaims the potential of JSF as a successful thickening agent in tomato sauce.

Keywords: Functional properties, jackfruit seed flour, thickening agent, underutilized source of flour.

INTRODUCTION

Thickening agents are widely used in the food industry to customize the consistencies of foods (Cho & Yoo, 2015). They are food additives that can improve the moisture binding capacity, alter flow properties, and help in structural modifications. Starches, proteins, gums, and seaweed extracts are some of the most used food thickeners in the food industry (Jayakody *et al*., 2023; Wedamulla & Wijesinghe, 2021). Considering starches, corn starch (CF) is the most prominent starch-based food thickener in use, mainly in food products such as sauces, soups, beverages, and purees.

Jackfruit (*Artocarpus heterophyllus* L.) seeds, a highly abundant source in Sri Lanka, are a rich source of starch and nutrients such as fiber, vitamins, minerals, and other phytonutrients (Amadi *et al*., 2018; Pushpakumara & Harris, 2007). It is a potential local food source where value addition is low. Most jackfruit seeds are discarded as waste reinforced by the short shelf life of fresh jackfruit seeds and sporadic uses and applications of jackfruit seeds. Jackfruit seed flour (JSF) which can be produced from jackfruit seeds, is a good option for different applications in the food industry and is also an alternate option to address the short shelf life of jackfruit seeds. Hence, this study was directed to investigate the potential of JSF to be used as a thickening agent.

* Corresponding author (jnkwijesinghe@yahoo.com; https://orcid.org/0000-0002-0621-534X)

Dehydration is a preservation technique used for fresh commodities where microbial and enzymatic activity is inhibited by reducing the water activity (Morais *et al.*, 2018). Dehydration is used to procure JSF from jackfruit seeds. There are different drying techniques in use, such as hot-air-drying, freeze-drying, microwave-assisted drying, ultrasound-assisted drying, high electric field drying, heat pump drying, and refractance window drying (Izli *et al.*, 2017; Moses *et al.*, 2014). The functional properties and physicochemical properties of the flour may be varied with the drying technique. Consequently, the applications of flour can be varied depending on the functional properties affected by the drying techniques. Considering this fact, the study aims to process JSF using two drying techniques: hot-air-drying and freeze-drying and assess the most suitable drying technique to produce JSF as a thickening agent while considering the practical and economical aspects of production.

Tomato (*Solanum lycopersicum*) is a key ingredient in worldwide cuisines where the production is going up day by day. Tomato sauce has been a rooted food product worldwide for many years, becoming the most consumed tomato-processed product in the world. Tomato sauce processing uses thickening agents to achieve the viscosity which is a vital quality parameter of tomato sauce. Traditionally, CF is used as the thickening agent, and in the present study, an effort was taken to replace CF with JSF as the thickening agent for tomato sauce. The physicochemical parameters of tomato sauces made using JSF and CF were investigated to examine the potential of JSF as a replacer for CF in tomato sauce production.

MATERIALS AND METHODS

Jackfruit seeds were collected from mature unripe and mature fully ripened jackfruits purchased from a local market in Pannipitiya, Sri Lanka, on the prior day of seed flour preparation. All other ingredients required for tomato sauce production were purchased from local supermarkets in Sri Lanka. All chemicals and reagents used during the study were of standard analytical grade.

Preparation of JSF

JSF was prepared using two main drying techniques.

Hot-air-dried JSF

Jackfruit seeds from mature, unripe and mature, fully ripe fruits were collected and rinds were removed. Lye peeling

was used to remove the seed coat (testa). Jackfruit seeds were soaked in sodium hydroxide (5% w/v) solution for 2 min and then soaked in citric acid (5% w/v) solution for 2 min. Then the seeds were thoroughly washed using tap water until the brown color seed coat was removed. Excess water was drained off. The cleaned seeds were sliced, steam blanched for 4-5 min and immediately dipped in cold water. Blanched seed slices were laid on clean white cloths in a way that cut surfaces were exposed to air. The slices were then dehydrated at 55°C for 20 h in a hot-air dehydrating oven. The dried jackfruit seeds of 8.32±0.09% moisture content were ground using an electric grinder and sieved through a standard 100 μm sieve to get a fine powder. The flour was packed in laminated pouches and stored in a dry place under room temperature (25°C).

Freeze-dried JSF

The same initial procedure was followed until steam blanching. Then the blanched seeds were immediately dipped in cold water, put into precleaned and dried petri dishes, and were frozen overnight. The frozen seeds were dried using the freeze drier at -40 °C for 20 h. The dried seeds of 4.98±0.43% moisture content were ground, sieved through a standard 100 μm sieve, packed in laminated pouches, and stored in a dry place under room temperature (25°C).

Determination of functional and physicochemical properties of JSF and CF

The functional properties and physicochemical properties of hot-air-dried JSF, freeze-dried JSF and CF were determined. The most suitable drying method out of hot-air drying and freeze drying to use JSF as a thickening agent was selected out of hot-air-dried and freeze-dried JSF in comparison to CF based upon their functional properties.

Bulk density

The bulk density was determined according to the method described by Chowdhury *et al.* (2012) with slight changes. A pre-weighed (w1) clean measuring cylinder was taken, and flour was filled up to a 5 mL level while tapping (where Chowdhury *et al.* (2012) had filled up to an unspecified level and recorded the volume). The weight of the measuring cylinder with flour (w2) was weighed and the density was calculated by using the below equation.

$$Bulk\ density\ (gmL^{-1}) = \frac{w2 - w1}{5}$$

Water absorption index (WAI) and water solubility index (WSI)

The WAI and WSI were determined according to Ahmed *et al*. (2016). 1.0 g of fully dried flour was dissolved in 6 mL of distilled water in a pre-weighed centrifuge tube and heated at 80°C for 30 min in the shaking water bath. It was then centrifuged at 2500 rpm for 10 min. After centrifugation, the supernatant was poured into a pre-weighed dry petri dish and oven-dried at 105°C for 10 h. The dried sample was weighed. The weight of the wet sediment was measured. The test was done in triplicates. The WAI and WSI were calculated using the following equations.

$$WAI = \frac{Weight\ of\ wet\ sediment}{Dry\ weight\ of\ flour}$$

$$WSI = \frac{Weight\ of\ dried\ supernatant}{Dry\ weight\ of\ flour} \times 100\%$$

Oil absorption capacity

Oil absorption capacity was determined as per Chowdhury *et al*. (2012) with minor modifications. 1g of JSF was measured into a pre-weighed centrifuge tube, and 25 mL of refined oil (vegetable oil, Marina brand) was added to it. It was vortexed thoroughly for 5 min and centrifuged at 4000 rpm for 30 min. The centrifuged tubes were kept resting for another 30 min at room temperature (25°C). The volume of the supernatant was measured. The oil absorption capacity was calculated as a percentage and expressed as mL of oil absorbed by 1g of flour (v/w).

Swelling power

Swelling power was determined according to Ahmed *et al*. (2016) with slight modifications. 0.5 g of fully dried flour was measured into a pre-weighed centrifuge tube. 15 mL of distilled water was decanted into the centrifuge tube. Then it was heated at 80 °C for 30 min in a shaking water bath. Afterward, the sample was centrifuged at 4000 rpm for 20 min. The supernatant was collected in a pre-weighed dry petri dish and oven-dried at 105°C until a constant weight was acquired. The dried supernatant

was weighed. The weight of wet sediment together with the centrifuge tube was measured. The swelling power was calculated by using the below-given equation. The result was taken as the average of triplicates.

$$Swelling\ power$$
$$= \frac{Weight\ of\ sediment}{Weight\ of\ flour - Weight\ of\ dried\ supernatant}$$

Least gelation capacity

The least gelation capacity was determined as per Aremu *et al*. (2008) and Chowdhury *et al*. (2012). Flour suspensions of 1-15% were prepared in test tubes using distilled water as each test tube contains 10 mL. The test tubes were heated in boiling water until gels were formed. Next, test tubes were cooled immediately to 4 °C under refrigerated conditions (4 °C) and kept for 2 h. Then the test tubes were inverted and checked for the falling or slipping nature of suspensions. The least gelation concentration was determined as the concentration when the sample from the inverted test tube did not fall or slip.

Emulsifying activity and stability

Both emulsifying activity and stability were determined according to Elkhalifa *et al*. (2005) with slight modifications. 1g of flour was measured into a beaker and 50 mL of distilled water at 4 °C and 50 mL of refined oil (vegetable oil, Marina brand) were added into the beaker. The mixer was stirred at high speed for 5 min using the magnetic stirrer. 50 mL of the stirring mixture was pipetted out while stirring and filled into a centrifuge tube. The remaining 50 mL was filled into another centrifuge tube. One centrifuge tube was directly centrifuged at 4000 rpm for 10 min while the other centrifuge tube was heated at 80°C for 30 min, cooled to room temperature (25°C), and then centrifuged under the same conditions. Afterwards, the height of the emulsion layer was measured in centimeters using a graduated transparent ruler and expressed as a percentage of the total height of the material in the centrifuge tube. The height of the emulsion layer of the heated and centrifuged sample was used to determine the emulsion stability while the rest was used to determine the emulsion capacity of the flour. The test was performed in triplicates.

$$\text{Emulsion activity (\%)} = \frac{\text{Height of the emulsion layer}}{\text{Height of the total material content}} \times 100\%$$

$$\text{Emulsion stability (\%)} = \frac{\text{Height of the emulsion layer of heated sample}}{\text{Height of the total material content}} \times 100\%$$

Foaming capacity and Foaming stability

The foaming capacity and stability were determined as per Aremu *et al.* (2008) with slight modifications. One gram (1 g) of flour was measured into a calibrated 100 mL measuring cylinder and 50 mL of distilled water was added. The volume was noted. Then the resulting solution was homogenized using a linear shaker at high speed for 5 min. The volume of foam was noted. The total volume of foam remaining over time at intervals of 0.00, 0.5, 1, 2, 3, and 4 up to the 24th was noted to determine the foam stability. The foaming capacity and stability were calculated using the equation given below. The test was done in triplicates.

$$\text{Foaming capacity (\%)} = \frac{\text{Volume after homogenization} - \text{Volume before homogenization}}{\text{Volume before homogenization}} \times 100\%$$

$$\text{Foaming stability (\%)} = \frac{\text{Volume of foam after time (t)}}{\text{Volume before homogenization}} \times 100\%$$

The most preferable drying technique to produce JSF as a thickening agent was selected based on their functional properties and carried forward to determine proximate composition and use as a thickening agent in tomato sauce.

Determination of gelatinization properties using Rapid Viscosity Analyzer (RVA)

The gelatinization properties of the selected HAD-JSF sample were determined by using the RVA (RVA; TechMaster, PerkinElmer Co., Ltd, Austria) according to the pre-described method with increased sample weight (Zhang *et al.*, 2023). Three grams (3 g) of flour were filled into the metal canister and 25 mL of deionized water was added. The plastic paddle of the RVA mixed the flour and water rotating at a speed of 960 rpm at the start and then maintained at 160 rpm during the rest of the analysis. The sample was heated at 50 °C for 1 min and then increased to 95°C at a rate of 12 °C/min. The system was maintained at 95°C for 2.5 min and was decreased to 50°C at the rate of 12°C/min which maintained for the next 2 min. The RVA curve was generated by using the data and the peak viscosity (PV), trough viscosity (TV), breakdown (BD = PV – TV), final viscosity (FV), and setback (SB = FV – TV) were calculated. The test was done in triplicates.

Determination of proximate composition of JSF and corn flour

The moisture content, crude ash, crude protein, crude fat, and crude fiber content of JSF and CF were determined as per standard AOAC, 2016 methods (925.10, 900.02, 930.25, 920.39, and 978.10 respectively). The digestible carbohydrate content was determined according to the method described by Akande *et al.* (2020) by using the below equation.

Digestible carbohydrate content (%) = 100 - (% moisture + % ash + % protein + % fat + % fiber content)

Preparation of tomato sauce

Tomato sauce, more specifically ketchup was prepared according to the specifications given by Sri Lanka Standards for tomato sauce (ketchup) (SLS 260:1989). Three sauce samples were prepared using JSF and CF as the thickening agents and the control without any thickening agent. 37.5 g of thickening agents were used for 1 kg of tomato pulp.

The glass bottles were cleaned using detergent and tap water and sterilized by boiling in hot water for 30-40 min

for ketchup storage. Fully mature, ripened tomatoes were selected, cleaned using tap water, and blanched for 8-10 min to remove the peel. The tomato pulp was then extracted using a sieve. The pulp was concentrated by heating at medium heat. Garlic, ginger, onion, cardamom, and cinnamon were ground into a paste and a spice bag was prepared. The spice bag was dipped in tomato extract concentrate. Sugar, chilli powder, and salt were added to the pulp and stirred for 10 min while supplying medium heat. The thickening agent and vinegar were added and stirred until the Brix value reached 25-30°Bx. The sauce was then filled into sterilized glass bottles, sealed, and stored for further studies.

Determination of physicochemical properties of tomato sauce

The physicochemical properties given below were determined throughout the storage period of 8 wks.

pH

Five grams of tomato sauce was measured into a beaker (100 mL) and diluted up to 50 mL level by using distilled water. The sample was well mixed using a magnetic stirrer to homogenize the sample. The pH was then measured using a calibrated digital pH meter. Three replicates were determined, and the probe of the digital pH meter was washed with distilled water and wiped with a paper towel prior to each measurement.

Total soluble solids (TSS)

A handheld refractometer was used to determine the TSS of sauce samples. The refractometer was calibrated using distilled water and wiped off. A drop of sauce was placed on the glass plate and the Brix reading was taken. Three replicates were performed for each treatment.

Titratable acidity

One gram of sauce was weighed into a conical flask and diluted with 10 mL of distilled water. 2 to 3 drops of phenolphthalein were added into the conical flask and titrated against 0.1N NaOH solution. The burette reading was taken at the endpoint where the orange color turned into a permanent pink color. Three replicates were done for each sample. The acidity of the sample was calculated based on the volume of 0.1N NaOH used to neutralize the acids available in tomato sauce using the below-given equation.

$$Titratable \ acidity \ (\%) = \frac{V \times N \times 60 \times 100}{W \times 1000}$$

Where,
V = Volume of NaOH required for the titration
W = Weight of the sample
N = Molarity of NaOH (moldm^{-3})
60 = Equivalent weight of the acid

Serum separation

The serum separation of the tomato sauce samples was determined by pipetting out the separated serum and measuring the volume. Serum separation was determined initially for 8 wks with 4-wk intervals.

Viscosity

The viscosity of the samples was determined using a Brookfield DVDTLV TJO viscometer fitted with model LV spindles. LV-2 (62), LV-3 (63), and LV-4 (64) spindles were used to measure the viscosity of control, CF-added tomato sauce, and JSF-added tomato sauce samples, respectively. The sauce samples were stirred well before measuring the viscosity. All measurements were done in triplicates.

Determination of microbial properties

The total plate count and the yeast and mold count of prepared tomato samples were determined according to the SLS 516: Part 1 and SLS 516: Part 2 with slight modifications. During the total plate count determination, the incubation period was extended (24 h) as no colonies appeared after the recommended incubation period (72 h). Both the tests were carried out after one month and two months of preparation. Tomato sauces were stored in sealed glass bottles under room temperature (25 °C) during the period. All the microbial analyses were performed in triplicates.

Sensory evaluation

The consumer acceptability and sensory perception were evaluated using a sensory evaluation. Color, aroma, flavor, mouthfeel, and overall acceptability of sauce samples were evaluated using the 9-point hedonic scale, where 9 represents extremely like and 1 represents extremely dislike. Fifty untrained panelists equally representing males and females in the age of 20-40 years, with no deprivations in sensory functions, were chosen. All the

sensory evaluations were done on the next day of tomato sauce preparation and samples coded using a 3-digit code were presented at room temperature (25°C) under normal lighting conditions. Potato chips were provided as the carrier for the tomato sauce and cream crackers were provided to remove lingering tastes in the mouth. A cup of potable water was provided for oral rinsing between sensory attribute evaluations (Jayamali *et al.*, 2022).

Statistical analysis

Data on the functional properties of JSF were analyzed using Excel 2018. Proximate analysis of JSF and CF, physicochemical properties, microbial properties, and sensory properties of sauce samples were analyzed using MINITAB 16 statistical software.

RESULTS AND DISCUSSION

Physicochemical and functional properties of JSF and CF

The physicochemical properties and the functional properties of hot air-dried JSF (HAD-FSF), freeze-dried JSF (FD-JSF), and CF were determined. The functional properties of flours vary with their drying techniques. Hence, the functional properties of HAD-JSF and FD-JSF were compared with the functional properties of CF to select the most suitable drying technique to use JSF as a thickening agent. The results are presented in Table 1.

Table 1: Physicochemical and functional properties of JSF and CF

Property	HAD-JSF	FD-JSF	CF
Moisture content (%)	8.77 ± 0.12^b	5.17 ± 0.59^c	12.95 ± 0.15^a
Bulk density (gcm⁻³)	0.95 ± 0.03^a	0.85 ± 0.04^b	0.57 ± 0.02^c
Water absorption capacity (mLg⁻¹)	2.05 ± 0.05^b	2.52 ± 0.13^a	1.53 ± 0.15^c
Water solubility index (%)	22.68 ± 4.04^b	3.84 ± 1.03^c	43.54 ± 0.88^a
Oil absorption capacity (mLg⁻¹)	0.24 ± 0.05^c	2.51 ± 0.13^a	1.43 ± 0.11^b
Swelling power	5.09 ± 0.18^c	6.37 ± 0.34^b	12.63 ± 0.63^a
Least gelation capacity (%)	2.0 ± 0.0^b	2.0 ± 0.0^b	7.0 ± 0.0^a
Emulsifying capacity (%)	1.49 ± 0.01^b	0.49 ± 0.00^c	3.20 ± 0.36^a
Emulsifying stability (%)	1.9 ± 0.1^a	1 ± 0.01^c	1.36 ± 0.24^b
Foaming capacity (%)	20.3 ± 2^a	7.17 ± 1.04^b	0.00 ± 0.00^c
Foaming stability (%)	20.2 ± 2^a	0.00 ± 0.00^b	0.00 ± 0.00^b

Values are average of triplicate analysis ± standard deviation. [a–c] Values in rows with different letters are significantly different at p < 0.05.

Moisture content is a crucial parameter of flour that ensures its storability and marketability. The moisture content of flour should lie within the admissible limits recommended by the WHO, which is 15% to ensure a longer shelf-life (Kaushalya & Wijesinghe, 2024). The moisture levels of all studied flour types were below the recommended level. The moisture content of FD-JSF was significantly lower than the moisture content of HAD-JSF ($p < 0.05$) after drying for an equal time. The moisture content of the CF purchased had the highest moisture content.

Bulk density is defined as the heaviness of flour, which is specifically the mass of particles per unit volume (Alam *et al.*, 2023; Sasanka *et al.*, 2024). In comparison, HAD-JSF had an aggregated granule-like nature and had the highest bulk density. FD-JSF had a small, individual, and uniform granule-like nature with a bulk density lower than HAD-JSF. However, the bulk densities of both HAD-JSF and FD-JSF were significantly higher than that of CF ($p < 0.05$). The lower the bulk density of flour, the flour absorbs water more efficiently. In regards to FD-JSF, it can be identified as more appealing than HAD-

JSF with its lower bulk density value and neither of them were appealing than CF with higher bulk densities.

High water absorption capacity of a flour characterizes its potential of thickening (Nwosu, 2012). The water absorption capacities of both HAD-JSF and FD-JSF were significantly higher than the water absorption capacity of CF ($p < 0.05$). FD-JSF marked the highest water holding capacity. Water absorption capacity of flour is regulated by the structural properties of starch polymers. The small, individual granule-like nature of FD-JSF starch may offer a great surface for hydration, rooting for the higher water absorption capacity. Freeze-drying as a technique that operates at very low temperatures supports more protein retention where higher amounts of proteins offer rich hydrophilic properties to the flour (Alam *et al.*, 2023). The higher fiber content of JSF (Table 3) may act as one possible reason for higher water binding capacity than CF where the fiber content is very low (Jakobek & Matić, 2019).

The water solubility index of CF was significantly higher than JSF ($p < 0.05$) while HAD-JSF had significantly higher water solubility index than FD-JSF ($p < 0.05$). A higher water solubility index is an indicator of lower water absorption capacity and swelling power (Alam *et al.*, 2023). Accordingly, FD-JSF marks a perk of being an efficient thickening agent over HAD-JSF.

Oil absorption capacity is a crucial property in the bakery industry that is regulated by the hydrophilic or hydrophobic properties of proteins (Godswill *et al.*, 2019). The oil absorption capacities of three flour samples were significantly different ($p < 0.05$) and that of FD-JSF was significantly higher than HAD-JSF and CF ($p < 0.05$). The low temperature and high vacuum used during the production of FD-JSF prevent the collapse of protein molecules which can be considered as the most plausible cause.

Swelling power is the ability to absorb water where a rigid structure is given through water retention (Ulfa *et al.*, 2020). The swelling power of CF was significantly higher than JSF and that of FD-JSF was significantly higher than HAD-JSF ($p < 0.05$). Consistency and cohesiveness of the microstructural network of uniform granules with larger amounts of carbohydrates and proteins in FD-JSF allow more absorption and expansion.

The lowest concentration of starch at which gel develops and does not migrate in an inverted manner down the test tube walls is called the least gelation concentration (Maria, 2017). The least gelation concentrations of JSF and CF were significantly different, whereas the least gelation concentration of CF was significantly higher than that of JSF ($p < 0.05$). However, the least gelation concentrations of HAD-JSF and FD-JSF were similar ($p > 0.05$).

Emulsion activity and emulsion stability are functions of proteins that are regulated by their hydrophobic properties (Godswill *et al.*, 2019). CF was found to possess the highest emulsion activity and stability over JSF at 95% significance level ($p < 0.05$). HAD-JSF possessed a significantly higher emulsion activity and stability than FD-JSF ($p < 0.05$).

The amount of interfacial area that can be created by proteins when shaken with water is the foaming capacity, and the stability of those interfacial areas over time is measured as foaming stability. These properties are regulated by the amount of protein and are influenced by starch. Both foaming capacity and foaming stability were significantly higher in HAD-JSF than FD-JSF and CF. CF didn't show any foaming properties while FD-JSF reported no foaming stability.

Based upon the above findings, both drying techniques (hot air-drying and freeze-drying) share their own advantages and disadvantages in producing JSF as a thickening agent. In comparison, FD-JSF shares the most favorable functional properties as a thickening agent over HAD-JSF, such as lower bulk density, higher water absorption capacity, and lower water solubility index. However, HAD-JSF also shared advantageous properties such as higher emulsifying ability and stability over FD-JSF. Freeze-drying, being an expensive technique restricts its commercial applications in the food industry while challenging commercial application of FD-JSF as a thickening agent in tomato sauce. Hence, hot-air drying was selected to proceed with the study as commercial application of the findings is crucial.

Gelatinization properties of JSF

The RVA parameters, including peak viscosity (PV), trough viscosity (TV), breakdown (BD), final viscosity (FV) and setback viscosity (SB) of JSF are as in Table 2.

Upon the increase of temperature from 50°C to 95°C, the viscosity of JSF increased and reached the PV, which is characterized by the gelatinization of starch. During the time, starch granules swell, and amylose chains leach out due to rupturing of starch granules. The pasting temperature was reported to be 92.95±1.12°C. The TV

shows how intact starch granules are following significant swelling and how resistant the starch is to being harmed by high temperatures and shearing pressures. With the resultant TV, JSF indicates a higher integrity of starch granules under the pre mentioned conditions. JSF reported

a lower BD (16.00±1.16 cP) which indicates a lesser degree of damage to starch granules and steadiness of the starch paste after heating. During the cooling process, the viscosity increased reaching FV (1463.00±9.58 cP), resulted from the retrogradation phenomenon of starch.

Table 2: RVA parameters of JSF

	PV (cP)	TV (cP)	BD (cP) (BD = PV – TV)	FV (cP)	SB (cP) (SB = FV – TV)
JSF	951.00 ± 6.04	935.00 ± 5.24	16.00 ± 1.16	1463.00 ± 9.58	528.00 ± 3.23
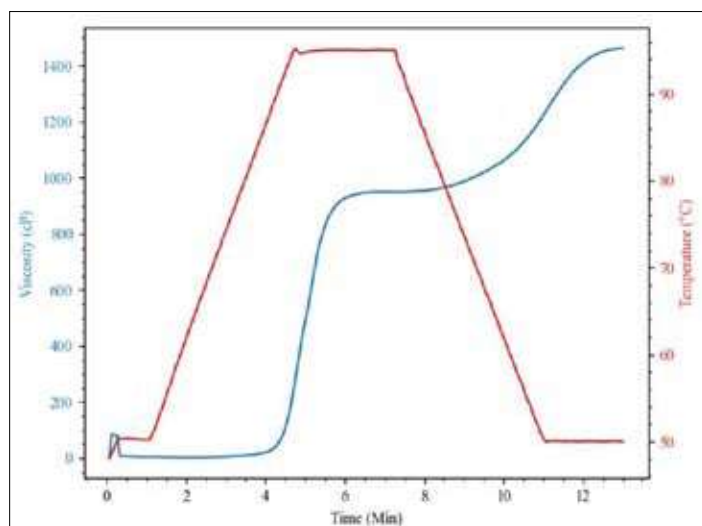
Figure 1:   RVA curve for JSF

Table 3:   Proximate composition of JSF and CF

Constituent	HAD-JSF	CF
Moisture content (%)	8.53 ± 0.19[b]	12.94 ± 0.15[a]
Crude ash (%)	2.39 ± 0.37[a]	0.44 ± 0.04[b]
Crude protein (%)	13.4 ± 0.09[a]	0.53 ± 0.00[b]
Fat (%)	2.77 ± 0.05[a]	0.22 ± 0.01[b]
Crude fiber (%)	2.93 ± 0.15[a]	0.02 ± 0.00[b]
Total carbohydrate (%)	69.96 ± 0.31[b]	85.83 ± 0.11[a]

Values are average of triplicate analysis ± standard deviation. [a–b] Values in rows with different letters are significantly different at $p < 0.05$.

Proximate composition of JSF and corn flour

The proximate composition of HAD-JSF and CF are as in Table 3. JSF holds significantly ($p > 0.05$) higher amounts of crude ash, crude protein, fat, and crude fiber than CF, while the moisture content and the total carbohydrate content were significantly ($p > 0.05$) higher in CF than JSF. The moisture content of both JSF and CF was within the admissible limits as mentioned before. The higher ash content of JSF indicates higher contents of inorganic constituents such as minerals than CF (Lawal *et al*., 2022). The higher protein content of JSF can impart the functional properties of JSF, such as water absorption capacity, swelling power, emulsifying activity, and foaming capacity. The potential of JSF as a food thickening agent is supported by its higher protein content and its total carbohydrate content. The significantly higher total carbohydrate content of CF proves its mastery as a starch-based thickening agent (Carcelli *et al*., 2020).
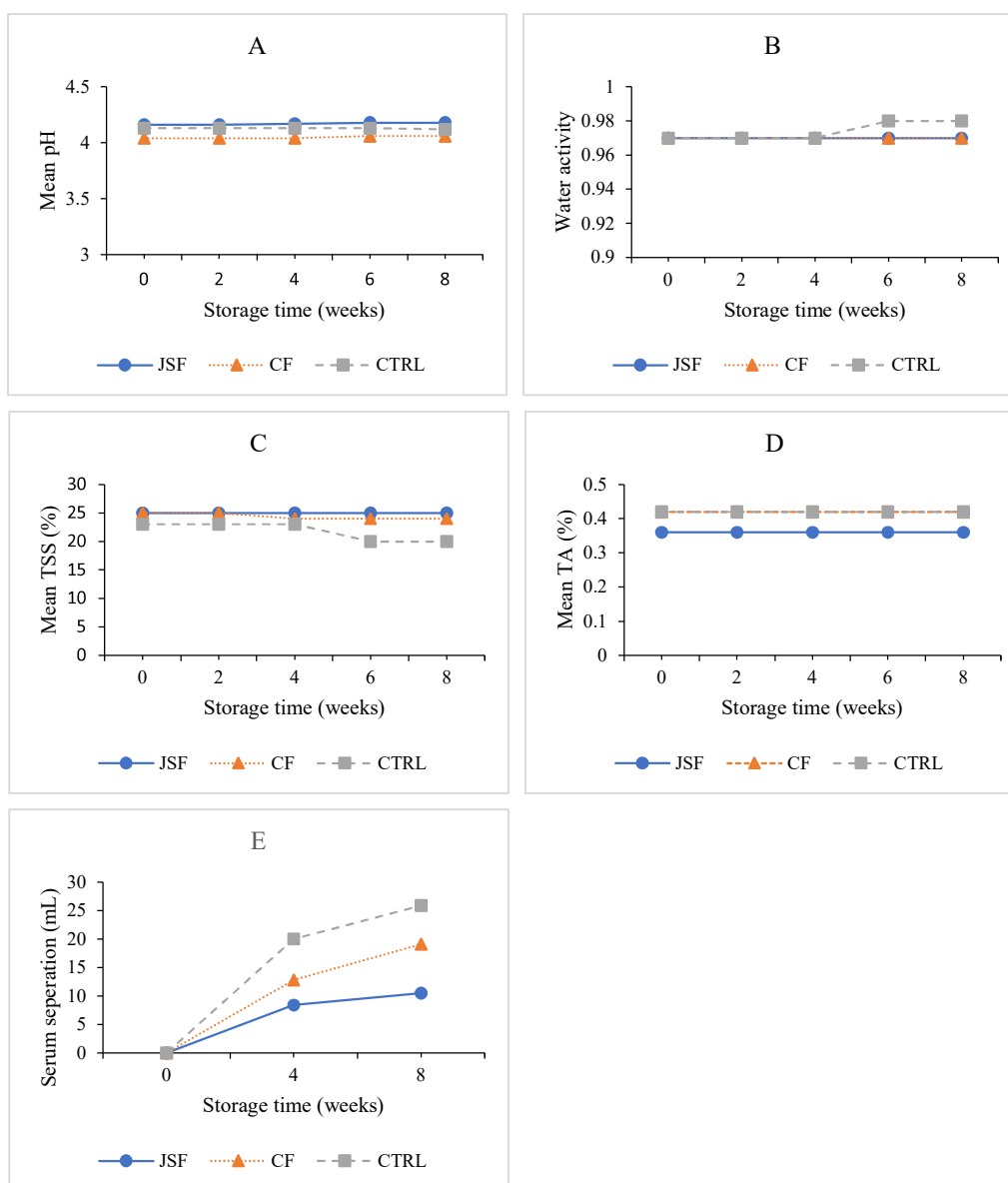

Figure 2: Variation of physicochemical properties of tomato sauce during storage period; A: Variation of mean pH, B: Variation of water activity, C: Variation of mean total soluble solids (TSS), D: Variation of titratable acidity (TA), E: Serum separation; JSF: Jackfruit seed flour, CF: Corn flour, CTRL: Control

Physicochemical properties of tomato sauce

pH

pH is one crucial factor influencing the quality of tomato sauce. Acetic acid in vinegar supports to attain the acidic pH values of tomato sauces along with the original acidity of tomato. The change of pH of tomato sauce over 8-week storage period is as illustrated in Figure 2A. The pH values of the three treatments were not significantly ($p < 0.05$) different at all time periods. The tomato sauce with JSF had the highest pH value followed by the control sample continuously. However, tomato sauce with CF reported the lowest pH value out of the three treatments over the whole storage period. Although the pH of all tomato sauces did not change significantly ($p < 0.05$) over time, an increasing trend of pH of JSF and CF- added tomato sauces could be observed.

Water activity (a_w)

The variation of water activity of tomato sauce over 8-week storage period is in Figure 2B. There was not any significant change in water activity among JSF and CF-added tomato sauces and the control tomato sauce during the first four weeks of storage time which reported a value of 0.97 continuously in all samples. Although tomato sauces with JSF and CF continued to be the same ($a_w = 0.97$) up until the 8th week, the control tomato sauce showed an increased water activity after the 4th week ($a_w = 0.9$).

Total soluble solids (TSS)

TSS is an important parameter in tomato sauce production where TSS affects the final quality of tomato sauce. Other than TSS from the tomato pulp, the addition of other ingredients such as sugar, vinegar, thickening agents and spices acts on the final TSS of tomato sauces. The initial TSS percentages of both JSF and CF added tomato sauces were 25% which had reached the minimum permissible level (25%) defined by Sri Lanka Standards 260:2008 – Specification for tomato sauce (Sri Lanka Standards Institution). Figure 2C presents the variation of TSS over the 8-week storage period.

JSF incorporated tomato sauce didn't show any change of TSS during the 8 weeks of storage. A decreasing trend was observed for TSS in CF-added tomato sauce and the control sample. TSS of CF-added tomato sauce remained the same at 25% until the 2nd week and slightly decreased afterwards. The control sample kept its TSS % constant until the 4th week, decreased by the 6th week, and remained unchanged by the 8th week. Regardless, the TSS of JSF and CF added tomato sauces were always significantly higher than the control sample.

Titratable acidity (TA)

The TA was expressed as a percentage of acetic acid. TA of tomato sauce samples are presented in Figure 2D. TA of tomato sauce with JSF was significantly ($p > 0.05$) lower than that of CF-added tomato sauce and the control tomato sauce. Both CF-added tomato sauce, and the control sample shared the same TA value (0.42%). However, none of the treatments reported any deviation of TA throughout the storage time.

Serum separation

Serum separation or syneresis indicates the inability of tomato sauce to hold the water during storage time (Román *et al.*, 2018). JSF-added tomato sauce showed the least serum separation along 8 weeks of storage, and this proved the potential of JSF as a better thickening agent than CF. The highest serum separation was observed in the control sample where no thickening agent is used. The variations of serum separation are shown in Figure 2E.

Viscosity

The texture is one of the most outstanding parameters of foods that determine their quality, and viscosity is the measure of the texture of sauces (Wang *et al.*, 2016). The use of a thickening agent remarkably affects the viscosity of the tomato sauce. The general viscosity of tomato sauce is 1000 cP. The highest viscosity was reported by JSF-added tomato sauce (1086 cP) followed by the CF-added tomato sauce (1004 cP). The least was reported by the control sample (142.5 cP) which had a watery consistency. The increase of viscosity of tomato sauce demonstrates the thickening potential of JSF evenly matching with CF in tomato sauce. The viscosities of the three treatments are presented in Table 4.

The physicochemical stability of JSF-incorporated tomato sauce, together with the lowest syneresis and highest viscosity, makes it a competing viable thickening agent.

Table 4: Viscosities of tomato sauce samples

Tomato sauce sample	Viscosity (cP)	Torque (%)	Spindle speed (rpm)
JSF	1086	18.1	100
CF	1004	17.9	100
CTRL	142.5	47.5	100

Table 5: Microbial properties of tomato sauce during storage

Weeks	Test	JSF	CF	CTRL
2	Total plate count	Not detected	Not detected	Not detected
	Yeast and mold count	Not detected	Not detected	Not detected
4	Total plate count	< 1 CFUg^{-1}	< 1 CFUg^{-1}	< 1 CFUg^{-1}
	Yeast and mold count	< 1 CFUg^{-1}	< 1 CFUg^{-1}	< 1 CFUg^{-1}
6	Total plate count	< 1 CFUg^{-1}	< 1 CFUg^{-1}	< 1 CFUg^{-1}
	Yeast and mold count	< 1 CFUg^{-1}	< 1 CFUg^{-1}	< 1 CFUg^{-1}
8	Total plate count	< 1 CFUg^{-1}	< 1 CFUg^{-1}	< 1 CFUg^{-1}
	Yeast and mold count	< 1 CFUg^{-1}	< 1 CFUg^{-1}	< 1 CFUg^{-1}

Microbial properties

Total plate count and yeast and mold count were determined by standard methods (SLS 516: Part 1 and SLS 516: Part 2) throughout the storage period of 8 weeks and the results are presented in Table 5. Microbial counts of both tests at every instance were below the standard maximum limits described by the Sri Lanka Standards 260:2008 – Specification for tomato sauce (Sri Lanka Standards Institution).

The above microbial counts manifested the microbial stability of all the tomato sauces along with their storage stability and safety of the tomato sauces. Several causes of lower microbial counts can be identified. Antimicrobial properties of acetic acid are another underlying reason for lower total plate counts (Kadhum Wali & Mohammed Abed, 2019). Heating during the processing of tomato sauce destroys the microbes in the product itself and the use of sterilized bottles for storage minimizes external contaminations. Hot filling of sterilized glass bottles which subsequently sealed minimized them further.

Sensory evaluations

Two sensory evaluations were held. Sensory evaluation 1 analyzed the organoleptic acceptability of JSF-added tomato sauce in comparison to CF-added and control tomato sauces. There was no significant difference in color and aroma of three tomato sauce samples at the 95% significance level ($p > 0.05$). The JSF added tomato sauce scored the highest for flavor, mouthfeel, and overall acceptability with an estimated median of 8.0 for every parameter while the control sample scored the lowest. The web diagram for the respective sensory evaluation is as in Figure 3A.

Another sensory evaluation (Sensory evaluation 2) was done to compare JSF-added tomato sauce with a commercially available tomato sauce where CF is used as the thickening agent. In regard to color of the tomato sauce, the majority liked the color of the commercial tomato sauce over JSF-added tomato sauce with an estimated median of 8.0 at a 95% significance level ($p < 0.05$). There was a significant difference between flavor and mouthfeel where the JSF-added tomato sauce had scored over commercial tomato sauce with an 8.0 estimated median ($p < 0.05$). No significant difference was noted among the two samples with respect to the aroma ($p > 0.05$). However, the overall acceptability for the JSF incorporated tomato sauce was higher than the commercial product at a 95% significance level ($p < 0.05$) with the highest estimated median (8.0) and the highest sum of rank. Figure 3B presents the web diagram for the second sensory evaluation.
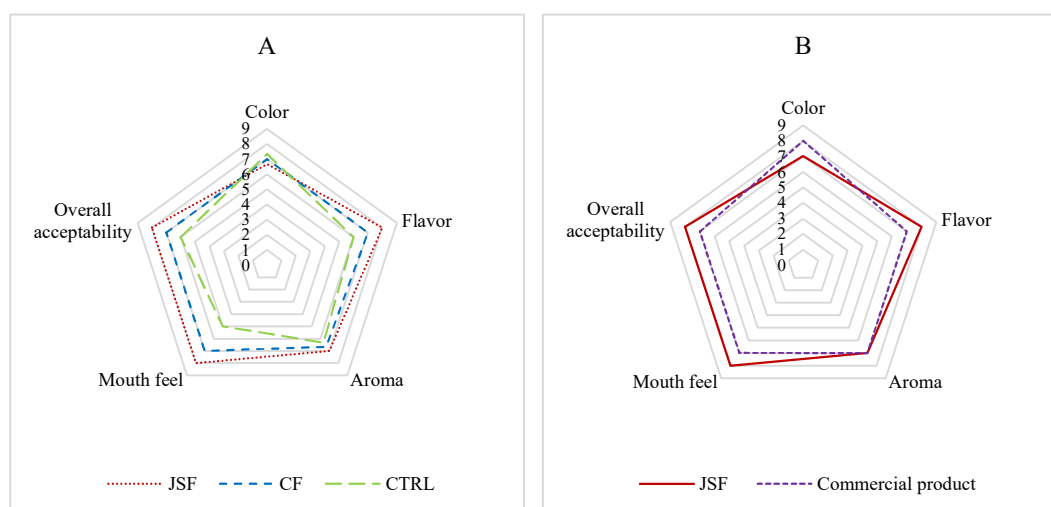
Figure 3: Web diagrams of sensory evaluations; A: Web diagram for sensory evaluation 1 conducted to evaluate three treatments of tomato sauce; B: Web diagram for sensory evaluation 2 conducted to compare JSF incorporated tomato sauce and a commercial product; JSF: Jackfruit seed flour, CF: Corn flour, CTRL: Control

CONCLUSION

The present study investigated the potential of using JSF as a thickening agent in tomato sauce as a replacer for CF. JSF produced using two drying techniques: hot-air drying (HAD-JSF) and freeze-drying (FD-JSF) shared favorable functional properties more or less to be used as a thickening agent. Considering the practical aspects, such as cost and constraints of commercial-level production of freeze-drying technique, HAD-JSF was selected to continue with further investigations. Analysis of physicochemical and sensory properties of hot air dried JSF-added tomato sauce during the 8-week storage, showed impressive results compared to CF-added tomato sauce. The study proved that JSF is a great thickening agent and a viable replacer for CF in tomato sauce production.

Acknowledgement

REFERENCES

Ahmed, I., Qazi, I. M., & Jamal, S. (2016). Assessment of Proximate Compositions and Functional Properties of Blends of Broken Rice and Wheat Flours. *Sarhad Journal of Agriculture*, *32*(3), 142–150. https://doi.org/10.17582/journal.sja/2016.32.3.142.150

Akande, A. O., Jolayemi, O. S., Adelugba, V. A., & Akande, S. T. (2020). Silkworm pupae (*Bombyx mori*) and locusts as alternative protein sources for high-energy biscuits. *Journal of Asia-Pacific Entomology*, *23*(1), 234–241. https://doi.org/10.1016/j.aspen.2020.01.003

Alam, M., Biswas, M., Hasan, M. M., Hossain, M. F., Zahid, M. A., Al-Reza, M. S., & Islam, T. (2023). Quality attributes of the developed banana flour: Effects of drying methods. *Heliyon*, *9*(7). https://doi.org/10.1016/j.heliyon.2023.e18312

Amadi, Joy A C, Austin, & Afam-Anene. (2018). Nutrient and Phytochemical Composition of Jackfruit (*Artocarpus heterophyllus*) Pulp, Seeds and Leaves. *International Journal of Innovative Food, Nutrition & Sustainable Agriculture*, *6*(3), 27–32. https://www.researchgate.net/publication/350710287

Aremu, M. O., Olaofe, O., Akintayo, E. T., & Adeyeye, E. I. (2008). Foaming, Water Absorption, Emulsification and Gelation Properties of Kersting's Groundnut (*Kerstingiella geocarpa*) and Bambara Groundnut (*Vigna*

subterranean) Flours as Influenced by Neutral Salts and Their Concentrations. *Pakistan Journal of Nutrition*, *7*(1), 194–201.

Carcelli, A., Masuelli, E., Diantom, A., Vittadini, E., & Carini, E. (2020). Probing the functionality of physically modified corn flour as clean label thickening agent with a multiscale characterization. *Foods*, *9*(8). https://doi.org/10.3390/foods9081105

Cho, H. M., & Yoo, B. (2015). Rheological characteristics of cold thickened beverages containing xanthan gum-based food thickeners used for dysphagia diets. *Journal of the Academy of Nutrition and Dietetics*, *115*(1), 106–111. https://doi.org/10.1016/j.jand.2014.08.028

Chowdhury, A. R., Bhattacharyya, A. K., & Chattopadhyay, P. (2012). Study on functional properties of raw and blended Jackfruit seed flour (a non-conventional source) for food application. *Indian Journal of Natural Products and Resources*, *3*(3), 347–353. https://www.researchgate.net/publication/285983474

Elkhalifa, A. E. O., Schiffler, B., & Bernhardt, R. (2005). Effect of fermentation on the functional properties of sorghum flour. *Food Chemistry*, *92*(1), 1–5. https://doi.org/10.1016/j.foodchem.2004.05.058

Godswill, C., Somtochukwu, V., & Kate, C. (2019). The functional properties of foods and flours. *International Journal of Advanced Academic Research | Sciences*, *5*(11), 2488–9849.

Izli, N., Izli, G., & Taskin, O. (2017). Influence of different drying techniques on drying parameters of mango. *Food Science and Technology (Brazil)*, *37*(4), 604–612. https://doi.org/10.1590/1678-457x.28316

Jakobek, L., & Matić, P. (2019). Non-covalent dietary fiber - Polyphenol interactions and their influence on polyphenol bioaccessibility. *Trends in Food Science and Technology*, *83*, 235–247. https://doi.org/10.1016/j.tifs.2018.11.024

Jayakody, M. M., Kaushani, K. G., Vanniarachchy, M. P. G., & Wijesekara, I. (2023). Hydrocolloid and water soluble polymers used in the food industry and their functional properties: a review. *Polymer Bulletin*, *80*(4), 3585–3610. https://doi.org/10.1007/s00289-022-04264-5

Kadhum Wali, M., & Mohammed Abed, M. (2019). Antibacterial activity of Acetic acid against different types of bacteria causes food spoilage. *Plant Archives*, *19*(1), 1827–1831.

Kaushalya, S. D. N., & Wijesinghe, W. A. J. P. (2024). Gluten-free biscuit prepared using jackfruit (*Artocarpus heterophyllus* L.) seed flour: An approach towards utilization of unexploited food source. *Tropical Agricultural Research and Extension*, *27*(4), 225–235. https://doi.org/10.4038/tare.v27i4.5720

Lawal, H. Z., Madu, P. C., Opaluwa, A. D., Mohammed, Y., & Shuaibu, B. S. (2022). Proximate and mineral content of selected condiments used as thickeners in soup preparation. *Bayero Journal of Pure and Applied Sciences*, *13*(1), 60–66. https://doi.org/10.4314/bajopas.v13i1.11S

Maria, S. (2017). Evaluation of the functional properties of mung bean protein isolate for development of textured vegetable protein. *International Food Research Journal*, *24*(4), 1595–1605.

Morais, R. M. S. C., Morais, A. M. M. B., Dammak, I., Bonilla, J., Sobral, P. J. A., Laguerre, J. C., Afonso, M. J., & Ramalhosa, E. C. D. (2018). Functional Dehydrated Foods for Health Preservation. *Journal of Food Quality*, *2018*. https://doi.org/10.1155/2018/1739636

Moses, J. A., Norton, T., Alagusundaram, K., & Tiwari, B. K. (2014). Novel Drying Techniques for the Food Industry. *Food Engineering Reviews*, *6*(3), 43–55. https://doi.org/10.1007/s12393-014-9078-7

Nwosu, J. N. (2012). The Rheological and Proximate Properties of some Food thickeners ("Ukpo", "Achi" and "Ofo") as affected by processing. *International Journal of Basic and Applied Sciences*, *4*, 304–312. www.crdeep.com

Pushpakumara, D. K. N. G., & Harris, S. A. (2007). Potential of RAPD markers for identification of fruit types of *Artocarpus heterophyllus* Lam. (jackfruit). *Journal of National Science Foundation of Sri Lanka*, *35*(3), 175–179. https://doi.org/10.4038/jnsfsr.v35i3.2016

Román, L., Reguilón, M. P., & Gómez, M. (2018). Physicochemical characteristics of sauce model systems: Influence of particle size and extruded flour source. *Journal of Food Engineering*, *219*, 93–100. https://doi.org/10.1016/j.jfoodeng.2017.09.024

Sasanka, I., Wijewardane, N. A., Wijesinghe, W. A. J. P., Jeewanthi, W., & Priyadarshana, I. B. (2024). Development of Banana Flour Incorporated Biscuit and Evaluation of its Physicochemical Properties. *Advances in Technology*, *2024*(1), 10–23. https://doi.org/https://doi.org/10.31357/ait.v4i01.7858

Ulfa, G. M., Putri, W. D. R., Fibrianto, K., Prihatiningtyas, R., & Widjanarko, S. B. (2020). The influence of temperature in swelling power, solubility, and water binding capacity of pregelatinised sweet potato starch. *IOP Conference Series: Earth and Environmental Science*, *475*(1). https://doi.org/10.1088/1755-1315/475/1/012036

Wang, T., Zhang, M., Fang, Z., Liu, Y., & Gao, Z. (2016). Rheological, Textural and Flavour Properties of Yellow Mustard Sauce as Affected by Modified Starch, Xanthan and Guar Gum. *Food and Bioprocess Technology*, *9*(5), 849–858. https://doi.org/10.1007/s11947-016-1673-6

Zhang, H. Y., Sun, H. N., Ma, M. M., & Mu, T. H. (2023). Dough rheological properties, texture, and structure of high-moisture starch hydrogels with different potassium-, and calcium-based compounds. *Food Hydrocolloids*, *137*. https://doi.org/10.1016/j.foodhyd.2022.108337

RESEARCH ARTICLE

Environmental Science

Annual and seasonal trends in extreme precipitation events in the dry zone of Sri Lanka

KC Kaushalya[1*], JBDAP Kumara[2], AD Ampitiyawatta[2] and EM Wimalasiri[2]
[1] *Faculty of Graduate Studies, Sabaragamuwa University of Sri Lanka, Belihuoya, Sri Lanka.*
[2] *Faculty of Agricultural Sciences, Sabaragamuwa University of Sri Lanka.*

Abstract: Extreme precipitation events can be devastating, especially in countries heavily reliant on agriculture. In Sri Lanka, where agriculture is predominantly influenced by the dry zone, studying trends in precipitation extremes is crucial for enhancing resilience and mitigating adverse impacts. The objective of this study is to examine the annual and seasonal trends in extreme precipitation events within the dry zone of Sri Lanka. Daily precipitation data from 19 selected locations within the dry zone, spanning 38 years from 1981 to 2019, were analyzed. Thirteen extreme precipitation indices were computed using the RClimDex software package and Microsoft Excel, following the guidelines established by the expert team on climate change detection and indices (ETCCDI). Regression analysis and Mann-Kendall tests were conducted to assess trends in annual and seasonal extreme precipitation events. This study, which utilized more recent data, identified significant ($p < 0.05$) trends in both annual and seasonal precipitation indices. Seven locations exhibited a significant ($p < 0.05$) positive trend in annual total precipitation (PRCPTOT), mainly attributed to variations in the number of rainy days. While precipitation during the *Yala* season remained consistent in many locations, a decrease in drought events was observed. During the *Maha* season, Anuradhapura, Batticaloa, Okkampitiya, Wellaway Trincomalee and Polonnaruwa showed significant positive trends for flood-related indices indicating a decrease in drought occurences during the season.

Keywords: Dry zone of Sri Lanka, extreme precipitation, *Maha* season, Mann Kendal, RClimDex, *Yala* season.

INTRODUCTION

Climate change (CC) refers to a change in the state of the climate that can be identified by changes in the long-term mean or the short-term variability of its properties and that persists for an extended period, typically decades or longer (IPCC, 2014). It has caused changes in the frequency and severity of climate extremes such as heat waves, droughts, floods, and tropical cyclones (Jayadas & Ambujam, 2019). Therefore, CC has been identified as a significant threat to both natural and human ecosystems in the 21st century (De Costa, 2008). The impacts of climate change can either be beneficial or detrimental to natural and man-made ecosystems, particularly affecting ecosystem services and human well-being (Solomon, 2007). Changes in the frequency, intensity, spatial extent, duration, and timing of weather attributes can result in climate-related disasters (IPCC, 2014). The occurrence of weather attributes beyond their threshold limits is known as 'climate extremes' (Field *et al*., 2012).

Numerous studies conducted in the recent past have shown a growing tendency of precipitation variability at sub-regional, regional, and global scales (Collins *et al*., 2000, Zhang *et al*., 2000, Groisman *et al*., 2005, Griffiths & Bradley, 2007, Pendergrass *et al*., 2017). In

the last few decades, the Asian region has experienced significant changes in the occurrence of extreme climate events (Griffiths *et al*., 2005, Choi *et al*., 2009, Caesar *et al*., 2011). Many Asian countries are classified as highly vulnerable to extreme climate events based on their economic status and other related limiting factors. A study by Sheikh *et al*. (2015) in South Asia revealed that changes in extreme precipitation indices are less coherent. However, on average, most extreme precipitation indices show increases in South Asia.

Sri Lanka, a South Asian island, has a diverse geography, including mountains rising up to 2500 m amidst flat terrain. The country's altitude delineates three zones: low country (< 300m), mid country (300-900m), and up country (> 900m). Sri Lanka experiences Southwest (SWM) and Northeast (NEM) monsoons, which determine its precipitation patterns leading to two main seasons (SWM: May-Sept, NEM: Dec-Feb) and two inter-monsoon periods [first inter-monsoon (FIM): Mar-Apr, second inter-monsoon (SIM): Oct-Dec] (Domroes 1974; Suppiah, 1996). Based on the precipitation climate, the country has traditionally been classified into Dry (<1750mm), Intermediate (1750-2500mm), and Wet (>2500mm) zones. The seasonal variation of monsoon precipitation delineates two distinct agricultural (cropping) seasons, the major *Maha* and the minor *Yala* across the dry zone of the country.

Climate change has caused significant changes in precipitation trends in Sri Lanka over the last few decades (Naveendrakumar *et al*., 2018). Studies in Sri Lanka have documented numerous extreme precipitation events, resulting in catastrophic floods, and droughts (Jayawardena *et al*., 2018, Naveendrakumar *et al*., 2019, Thevakaran *et al*., 2019). Moreover, it has been reported that high-intensity precipitation-driven flash floods in urban areas are becoming more frequent in recent years. The number of deaths due to flash floods has increased during the past decade in Sri Lanka (Ministry of Disaster Management, 2016). In addition, about five million people were affected between 2000 and 2013 due to 25 large-scale floods in Sri Lanka (Ministry of Disaster Management, 2018).

An increasing trend in annual total precipitation was reported from 1980 to 2015 (Karunathilaka *et al*., 2017, Sanjeewani & Manawadu, 2017, Jayawardene *et al*., 2018). Sanjeewani & Manawadu (2017) emphasized that extraordinary precipitation extremes are mainly concentrated in the southwestern part of Sri Lanka. In contrast, Thevakaran et al. (2019) reported that in the

last 50 years, large-scale climate change resulted in increasing trends in the number of dry days in the wet zone.

Previous studies on the long-term trends of most precipitation indices in Sri Lanka, covering various periods from 1870 to 2007, have shown spatially and temporally variable trends - both positive and negative (Suppiah, 1986; 1996; Senevirathna *et al*., 1997, Wickramagamage, 1998, Malmgren *et al*., 2003, Madduma & Wickramagamage, 2004, Eriyagama & Smakhtin, 2006, Ampitiyawatta & Guo 2009). Malmgren *et al*. (2003) found a decrease in the average monthly precipitation at higher elevations and an increase in precipitation in the lowlands in the southwestern sector of Sri Lanka during the southwest monsoon. According to Sanjeewani & Manawadu (2014), some of the dry zone locations (Batticaloa, Hambantota, and Trincomalee) showed a significant increase in annual maximum consecutive five-day precipitation events. Sheikh *et al*. (2015) found declining precipitation trends in the southern part of Sri Lanka from 1961 to 2000. Owing to these contradictory findings Jayawardena *et al*., (2005) concluded that a coherent increase or decrease in precipitation in the wet or dry zones is apparent in the last 100 years (1895-1996).

Extreme climate events such as high intensity precipitation and long duration droughts are more significant and cause more catastrophic disasters than small changes in the climate. Understanding climate change and how these changes can impact extreme climate events would provide insights into future courses of action. Therefore, analyzing extreme precipitation events in different climatic regions and seasons in Sri Lanka is crucial for policymakers to plan adaptation strategies and minimize the impact from extreme events such as flash floods and droughts. Additionally, it will provide valuable information for the planning and management of water resources to ensure peoples livelihoods and food security. Although many research studies are available on climate change and climate variability in Sri Lanka, less attention has been given to the study of extreme climate events, especially in various climatic zones and monsoon seasons. Since the different climatic zones are not uniform, distinct studies are necessary. Therefore, the objective of this study is to identify annual and seasonal trends in precipitation extremes in the dry zone of Sri Lanka.

The dry zone covers almost three-quarters of the island's land surface (Punyawardena *et al*., 2003). This

area receives less than 1750 mm of annual precipitation and the main agricultural practices in this region are rain-fed. The dry zone contributes the most to the national paddy production, which is the major food crop in Sri Lanka. Therefore, identifying precipitation extremes over the dry zone of Sri Lanka will be beneficial for planning adaptation strategies and sustaining agriculture in the future.

MATERIALS AND METHODS

Data and study Area

From the long-term daily precipitation records available at the Department of Meteorology in Sri Lanka, 19 gauging stations were selected to cover geographical areas in the dry zone. The locations (Figure 1) and elevation details of all selected stations are given in Table 01.

Figure 1: Selected gauging stations in the Dry Zone, Sri Lanka

Table 1: Latitude, longitude and altitude of selected locations

Location	Latitude	Longitude	Altitude(m)
Batticaloa	7.72	81.70	5
Jaffna	9.68	80.03	5
Puttalam	8.03	79.83	6
Pottuvil	6.88	81.83	7
Mannar	8.98	79.92	8
Trincomalee	8.58	81.25	8
Allai tank	8.40	81.32	9
Hambantota	6.12	81.13	16
Akkarayankulam	9.30	80.35	28
Amparai tank	7.28	81.67	40
Polonnaruwa	7.87	81.05	51
Yala	6.37	81.53	67
Giritale	8.00	80.93	77
Anuradhapura	8.35	80.38	81
Vavuniya	8.75	80.50	99
Bandagiriya	6.23	81.15	100
Okkampitiya	81.3	6.75	100
Mahailuppallama	8.12	80.46	113
Wellawaya	6.73	81.10	189

Long-term data records are essential for detecting trends (Westmacott & Burn, 1997). Therefore, daily observed precipitation data from all selected locations were collected from 1981 to 2019. According to Keggenhoff *et al*. (2014), trends can be successfully observed when missing values are less than 20%. All selected stations satisfied this condition and had a minimum of 30 years of data. The length of the data set meets the minimum requirement to investigate evidence of climate change in hydro-climatic time series as proposed by Burn and Elnur (2002) and Kahya and Kalayci (2004). The annual data was rearranged into the two cultivation seasons (*Yala* and *Maha*), considering the two monsoons (SWM and NEM). Data covering six months from March to August (*Yala* season), and six months from September to February (*Maha* season) were analyzed seasonally (Chithranayana and Punyawardene, 2008).

Data and quality control

Data quality control was done using the RClimDex (version 4.0.2.) software to identify missing and

unrealistic values. During this process, all user-defined missing and unrealistic values were replaced by a default missing marker. Since the focus of the study is on extreme events, no attempt was made to reconstruct the missing daily precipitation records.

Selection of extreme indices

Researchers have utilized various threshold values and indices to study extreme climate events, depending on the region of interest and the season (Sanjeewani and Manawadu, 2017, Mekonen and Berlie, 2020, Huo *et al*., 2021). In this study, extreme precipitation indices defined by the Expert Team on Climate Change

Detection and Indices (ETCCDI) (Table 2) were used. The RClimDex software calculates 27 extreme climate indices as described by ETCCDI. For this study, 11 extreme precipitation indices were selected based on their relevance to the dry zone of Sri Lanka. Further, two indices, R95p* and R99p*, were defined by the authors (Table 3) to better explain the conditions in Sri Lanka according to the ETCCDI definitions.

Annual extreme precipitation events were calculated using the RClimDex software package (version 4.0.2.) while both the RClimDex software package (version 4.0.2.) and Excel software package were used for seasonal analysis.

Table 2: Precipitation indices recommended by Expert Team on Climate Change Detection and Indices

Index	Descriptive name	Definition	Unit
PRCPTOT	Annual total wet days precipitation	Annual/seasonal total precipitation on wet days (precipitation >=1 mm)	mm
R10	Heavy precipitation days	Annual/seasonal count of days when precipitation is greater than 10 mm	days
R20	Very heavy precipitation Days	Annual/seasonal count of days when precipitation is greater than 20 mm	days
R25	Extreme precipitation Days	Annual/seasonal count of days when PRCP >= 25 mm; 25 mm is the user-defined threshold	days
R95p	Very wet days	Annual/seasonal total precipitation when precipitation is greater than the 95th percentile	mm
R99p	Extremely wet days	Annual/seasonal total precipitation when precipitation is greater than the 99th percentile	mm
RX1day	Maximum 1-day precipitation amount	Annual/seasonal maximum 1-day precipitation	mm
RX5day	Max 5-day precipitation amount	Annual/seasonal maximum of consecutive 5-day precipitation	mm
SDII	Simple daily intensity index	Annual/seasonal total precipitation divided by the number of wet days (defined as precipitation >= 1.0 mm) in the year	mm/day
CWD	Consecutive wet days	Annual/seasonal maximum number of consecutive days with precipitation >=1 mm	days
CDD	Consecutive dry days	Annual/seasonal maximum number of consecutive days with precipitation <1 mm	days

Table 3: User-defined precipitation indices derived from the indices recommended by the Expert Team on Climate Change Detection and Indices

Index	Descriptive name	Definition	Units
R95p*	Number of very wet days	Annual/seasonal count of days when precipitation is greater than 95th percentile	days
R99p*	Number of extremely wet days	Annual/seasonal count of days when precipitation is greater than 99th percentile	days

Trend analysis

The annual and seasonal trends of extreme events were detected by the Mann-Kendall (MK) test and regression analysis. The Mann-Kendall test is widely used in climatological and hydrological time series trend analysis because it is a non-parametric test and does not require the data to be normally distributed (Mann, 1945, Kendall, 1975).

$$Z_{mk} = \begin{cases} \dfrac{S-1}{\sqrt{\text{var}(S)}} & S > 0 \\ 0 & S = 0 \\ \dfrac{S+1}{\sqrt{\text{var}(S)}} & S < 0 \end{cases}$$

In which,

$$S = \sum_{i=1}^{n-1} \sum_{k=i+1}^{n} \text{sgn}(x_k - x_i)$$

Where Z_{mk}, is the Mann-Kendall statistic, x_k, and x_i are the sequential data values, n is the length of the data set, and sgn $(x_k - x_i)$ is equal to 1,0, -1. If $(x_k - x_i)$ is greater than, equal to, or less than zero, respectively. e_i is the extent of any given tie and $\sum$ denotes the summation of all ties. The null hypothesis, H_o, of no trend is accepted if the computed p-value is greater than the significance level ($\alpha = 0.05$). A positive value of Kendall's tau indicates an 'upward trend' while a negative value indicates a 'downward trend'.

RESULTS AND DISCUSSION

This study analyzes the trend of annual and seasonal extreme precipitation over the past 38 years (from 1981 to 2019) in the dry zone of Sri Lanka. Annual and seasonal (*Yala* and *Maha*) trends of extreme precipitation indices are described separately within this section. The significance of the trends was determined at the 95% confidence level.

Annual trends of the precipitation extremes in the dry zone

Annual total precipitation

During the study period, the dry zone received an average of 1359±188 mm of annual precipitation. The highest (1871±149 mm) and lowest (902±96mm) mean values were observed in Wellawaya and Bandagiriya, respectively. The highest variability of inter-annual precipitation was observed in Batticaloa (inter-quartile value of 652 mm) and the lowest in Mannar (inter-quartile value of 231 mm). The annual precipitation at seven locations (Anuradhapura, Akkarayankulam, Batticaloa, Mahailuppallama, Pottuvil, Polonnaruwa, and Wellawaya) showed significant positive trends (Figure 2), which is consistent with Jayawardene *et al*. (2018).
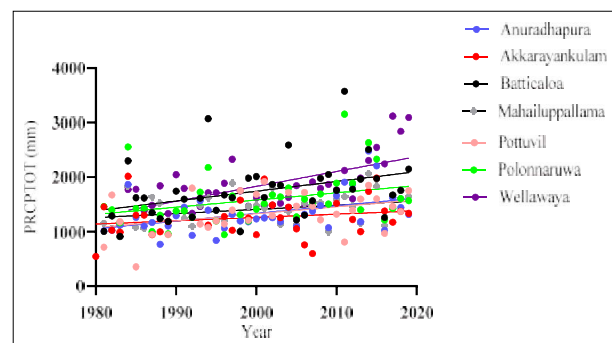

Figure 2: Locations with significant increasing trends for annual total wet days precipitation

Table 4: Correlation of total precipitation to higher intensity rainfall events R10, R20, R25, R99p, RX1day, RX5day in locations with positive precipitation trends

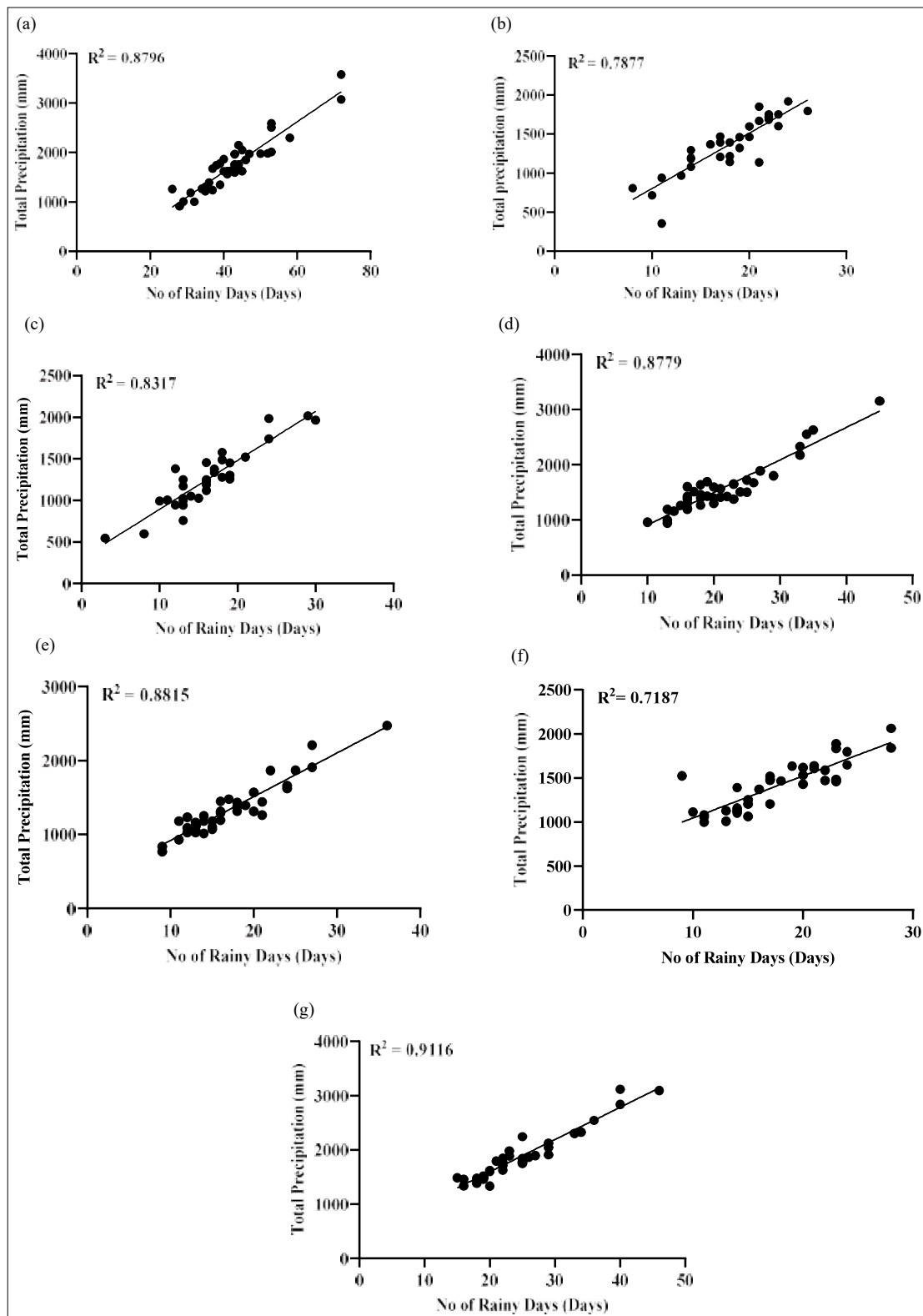| Location	R10	R20	R25	R95p	R99p	RX1day	RX5day
Anuradhapura	0.88	0.93	0.94	0.73	0.32	0.39	0.60
Akkarayankulam	0.77	0.88	0.90	0.30	-0.02	0.51	0.66
Batticaloa	0.94	0.93	0.93	0.81	0.74	0.67	0.72
Mahailuppallama	0.78	0.80	0.85	0.52	0.13	0.39	0.38
Pottuvil	0.81	0.88	0.89	0.34	0.01	0.46	0.58
Polonnaruwa	0.87	0.93	0.94	0.74	0.67	0.44	0.71
Wellawaya	0.85	0.93	0.96	0.66	0.39	0.16	0.47

Figure 3: Correlations among the indices explaining number of rainy days (R10/R20/R25) with the total precipitation (PRCPTOT) at (a)Batticaloa (b) Pottuvil (c) Akkarayankulam (d)Polonnaruwa (e) Anuradhapura (f) Mahailuppallama and (g) Wellawaya.
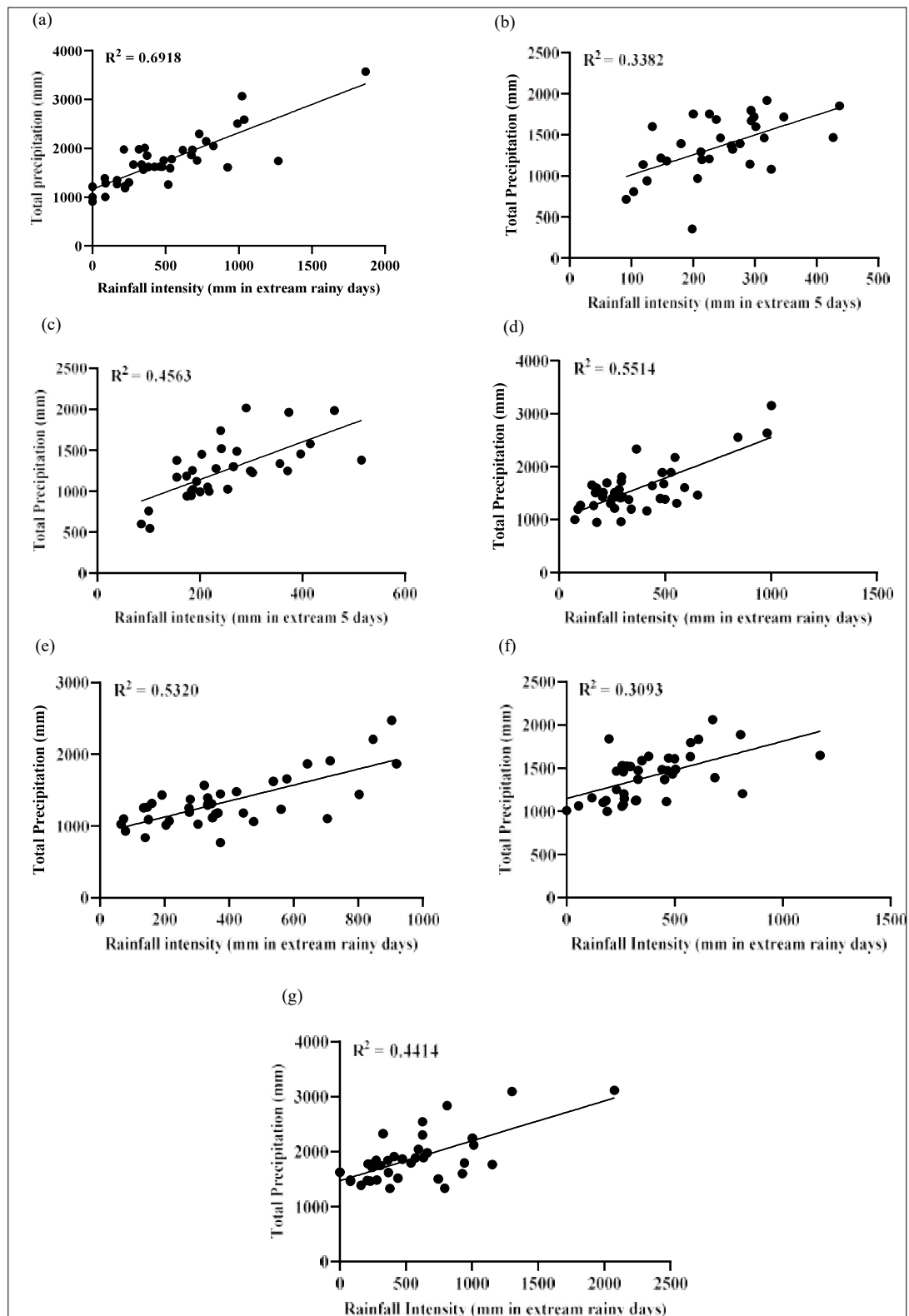
Figure 4: Correlations among the indices explaining rainfall intensity (R95p/Rx5day) with the total precipitation (PRCPTOT) at (a)Batticaloa (b) Pottuvil (c) Akkarayankulam (d)Polonnaruwa (e) Anuradhapura (f) Mahailuppallama and (g) Wellawaya.

The total precipitation is governed by two factors: the number of rainy days and the intensity of precipitation. In RClimDex, "extreme rainy days" are further classified into R10, R20 and R25 based on daily precipitation. The precipitation intensity is explained by the indices, R95p and R99p. The most extreme precipitation event for each calendar year is identified as RX1day and RX5day.

The locations that show positive annual precipitation trends are strongly correlated with R10, R20 and R25 indices (Figures). However, R95p, R99p, RX1day and RX5day did not show a strong correlation with variations in total precipitation. Furthermore, the Simple Daily Intensity Index (SDII) for Anuradhapura, Batticaloa, Mahailuppallama, Okkampitiya, Giritale and Wellawaya showed positive trends over the study period. Therefore, variations in total precipitation are primarily due to changes in extreme rainy days (i.e., R25 and SDII).

Variation in extreme precipitations

The fixed threshold base indices, R10, R20 and R25, represent the number of days with heavy (≥10 mm), very heavy (≥20 mm) and extreme (≥25 mm) daily precipitation, respectively. According to this study, the dry zone receives 13-20 days of very heavy precipitation per year. The highest median number of very heavy precipitation was recorded in the Amparai tank (25 days) and the lowest in Hambanthota, Bandagiriya and Yaala (12 days). The extreme precipitation index, R10, showed a significant positive trend at 4 locations (Anuradhapura, Batticoloa, Amparai tank, Polonnaruwa). The R20 index similarly showed significant positive trends at six locations (Anuradhapura, Mahailuppallama, Batticoloa, Amparai tank, Wellawaya, Okkampitiya), and the R25 index showed positive trends at seven locations (Anuradhapura, Mahailuppallama, Batticoloa, Amparai tank, Wellawaya, Polonnaruwa, Giritale). All three indices showed positive trends in Anuradhapura, Batticaloa and Amparai tank (Table 4). Both R20 and R25 showed positive trends in Mahailuppallama and Wellawaya, while Polonnaruwa showed positive trends for R10 and R25 indices. Okkampitiya and Giritale showed positive trends for R20 and R25, respectively. This is in agreement with Jayawardene et al., (2018) who reported increases of 10, 20 and 30 mm rainy days in Sri Lanka.

The absolute indices RX1day and RX5day (Annual maximum one day precipitation and Annual maximum five consecutive days precipitation) showed positive trends at three locations (Anuradhapura, Mahailuppallama, Giritale) and four locations

(Anuradhapura, Mahailuppallama, Batticoloa, Wellawaya), respectively. Both indices had significant positive trends in Anuradhapura and Mahailuppallama, while Giritale showed a positive trend for RX1day precipitation. Batticaloa and Wellawaya showed positive trends for RX5day precipitation. The mean RX1day precipitation for the dry zone was 115±8mm and that for RX5day precipitation was 221±19mm.

The percentile indices, R95p and R99p (precipitation on very wet days and extremely wet days), exhibited positive trends in Anuradhapura, Mahailuppallama and Wellawaya. In contrast, Mannar showed a significant negative trend for R95p. The mean of the simple daily intensity index (SDII) for the dry zone was 19.1±1.6 mm/day. The highest mean SDII was recorded at the Allai Tank (23.8 mm/day) and the lowest at Hambanthota (12.4 mm/day). The SDII showed significant positive trends at six locations (Anuradhapura, Batticaloa, Mahailuppallama, Wellawaya, Okkampitiya and Giritale) and was negative at three locations (Mannar, Bandagiriya and Yaala).

The annual number of consecutive wet days (CWD) indicates the probability of floods. Five stations (Anuradhapura, Hambantota, Pottuvil, Trincomalee, and Polonnaruwa) showed significant positive trends for CWD (Figure 5). None of the stations showed significant negative trends for CWD. The probability of the occurrence of drought can be identified from consecutive dry days (CDD). The CDD decreased significantly at four locations (Pottuvil, Wellawaya, Bandagiriya, and Yaala). However, Mannar showed a significant increasing trend of CDD (Figure 6).
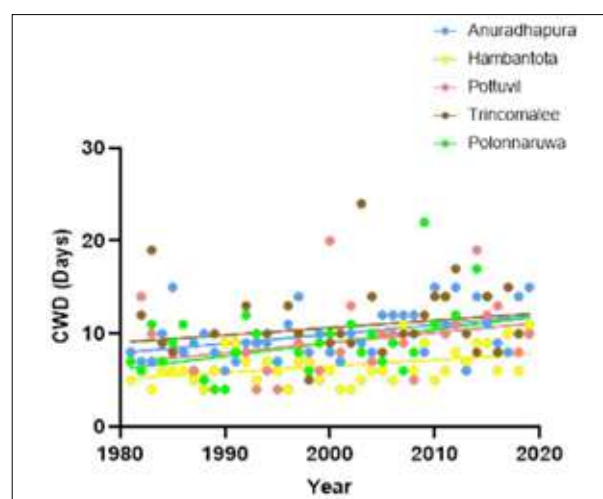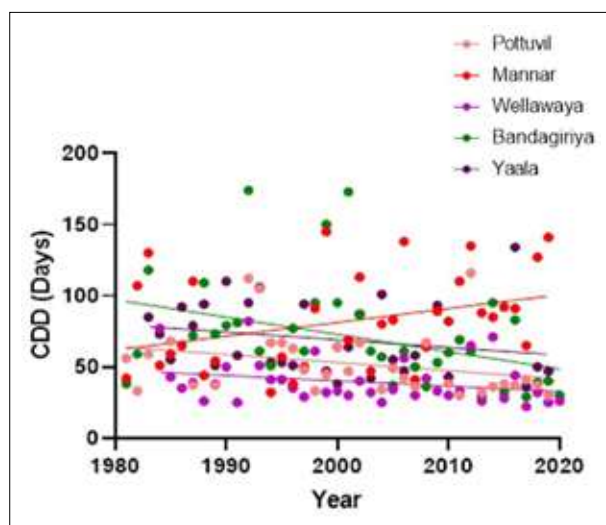

Figure 5: Locations with significant increasing trends for CWD

Extreme indices showed significant trends (positive or negative) at 12 locations: Anuradhapura (12 indices), Wellawaya (10 indices), Mahailuppallama (9 indices), Batticaloa (8 indices), Polonnaruwa (5 indices), Pottuvil (4 indices), Amparai tank (3 indices), Giritale (3 indices), Mannar (3 indices), Bandagiriya (2 indices), Okkampitiya (2 indices), and Yaala (2 indices).

Mannar, the trends were negative for R95p and SDII, and positive for CDD. The flood risk in Mannar decreased due to the reduced intense precipitation and increased CDDs. Further Bandagiriya and Yaala also showed negative trends for SDII. In contrast, all other locations showed positive trends for precipitation intensity, heavy precipitation and consecutive rainy days indicating a higher flood risk in those areas. Therefore, widespread areas of the dry zone are expeiencing increasing total annual precipitation, higher intensity of precipitation and flood risk. The probability of flood risks was higher in Anuradhapura, Mahailuppallama, Wellawaya and Batticaloa. Basnayake *et al*., (2002) and Malmgren *et al*., (2003) reported there was no clear trend or pattern in precipitation indices within Sri Lanka. However, present study, with more recent data, shows significant trends in annual precipitation indices.

Number of extreme rainy days

In the period 1981-2019, significant positive trends in the number of extreme rainy days were identified in Anuradhapura (R95p*, R99p*), Mahailuppallama (R95p*), Batticaloa (R95p*, R99p*), Pottuvil (R99p*), Wellawaya (R95p*, R99p*), Polonnaruwa (R95p*), and Giritale (R99p*) (Figure 7). Allai tank (R99p*) displayed a significant negative trend for number of extreme rainy days.
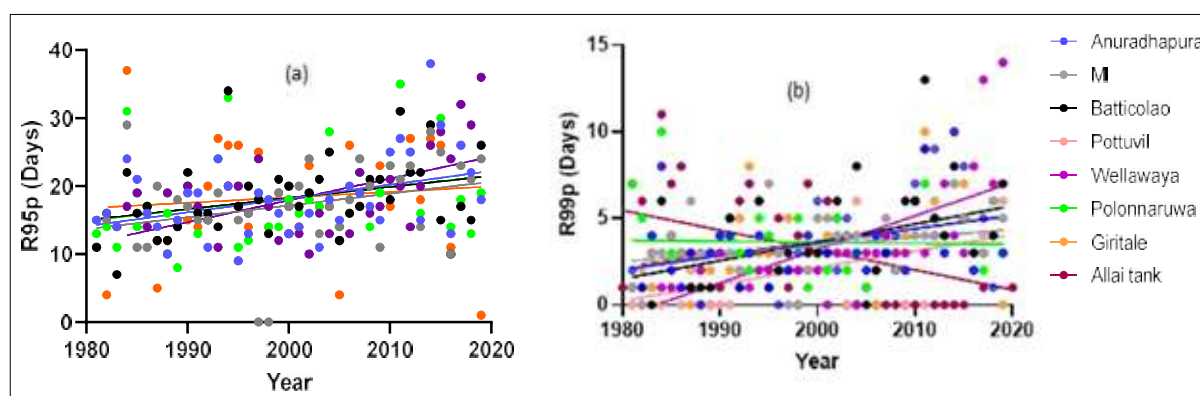

Figure 7: Locations with significant trends in (a) the number of very wet days (R95p), and (b) the number of extremely wet days (R99p)

Seasonal trend analysis - *Yala* season

Seasonal total precipitation

Yala is relatively a dry season in the dry zone of Sri Lanka. During the study period, the mean *Yala* precipitation in

the dry zone was 350±25 mm. Precipitation was highest in Wellawaya (661±46 mm) and lowest in Yaala (223±16 mm). The highest variability in *Yala* precipitation was observed in Wellawaya (inter-quartile value 354 mm) and the lowest in Hambanthota (inter-quartile value 99 mm). Only Wellawaya showed a significant increase in

precipitation during the study period. Based on mean values, Wellawaya recorded the highest values for nine indices including highest mean precipitation (661.5mm), maximum one day precipitation (RX1DAY, 83.9mm), maximum five consecutive days precipitation (RX5DAY, 156.1mm), very wet days precipitation (R95p, 430.1mm), extremely wet days precipitation (R99p, 160.9mm), number of heavy precipitations (R10, 18 days), number of very heavy precipitations (R20, 10 days), number of extreme precipitations (R25, 7 days) and consecutive wet days (CWD, 6days). In contrast Allai tank had the highest value for consecutive dry days (69 days) followed by Mannar (66 days). Most locations in the dry zone received 3 (1st Quartile) - 7 (3rd Quartile) extreme precipitations (R25) in the *Yala* season. *Yala* seasons with precipitation Beyond this range (i.e., greater than Q3) were considered extreme.

The mean maximum *Yala* season RX1day and RX5day precipitation were in the range 51-83 mm and 86-156 mm, respectively. These absolute indices RX1day and RX5day showed positive trends at two locations (Mahailuppallama and Wellawaya) and three locations (Anuradhapura, Mahailuppallama and Wellawaya) locations, respectively. The increasing trends of R25, RX1day and RX5day in Anuradhapura, Mahaillupplallama, Vauniya, Amparai tank and Wellawaya indicate a potential flood risk in these dry zone areas.

The percentile indices R95p had positive trends in Anuradhapura and Wellawaya, and R99p in Trincomalee and Wellawaya. The mean of the simple daily intensity index (SDII) for the dry zone was 17.1±1.1 mm/day. The highest mean for SDII was recorded in Mannar (33.5 mm/day) and the lowest in Hambanthota (10.5 mm/day).
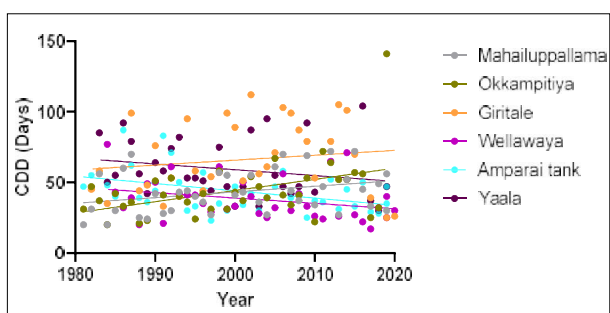

Figure 8: Locations with significant trends for CDD in the *Yala* season

SDII had significant positive trends at three locations (Mahailuppallama, Wellawaya and Okkampitiya) and was negative at two locations (Bandagiriya and Yaala). Wellawaya showed significant positive trends for CWD while Mahailuppallama, Okkampitiya and Giritale showed significant positive trends for CDD. The trend was negative for Wellawaya, Yaala and Amparai tank (Figure 8).

In conclusion, the precipitation during the *Yala* season did not change for many locations in the dry zone. However, Anuradhapura, Mahailluplallama, Vauniya, Amparai tank and Wellawaya showed significant positive trends for flood-related indices and negative trends for drought indices. Positive trends in drought indices suggest a potential for drought in Mahailuppallama, Okkampitiya and Giritale areas. This aligns with the findings of Thevakaran *et al*., (2019), on the behaviour of dry days during the *Yala* season. However, Chithranayana & Punyawardene (2008) concluded that all Agroecological regions of the dry zone are highly vulnerable to drought conditions during the *Yala* seasons. Therefore, the present study and that of Thevakaran *et al*., (2019) using more recent data concludes a reduction in drought events in the dry zone during the *Yala* season. In contrast to the present study, Wikramagamage (2015) reported a decrease in precipitation across Sri Lanka's dry zone regions during the *Yala* season from 1981 to 2010. The Southwest monsoon serves as the primary moisture source for the country during the *Yala* season. Karunathilaka *et al*., (2017) found a downward trend in precipitation records during the Southwest monsoon season across most parts of the country, based on data from 1966 to 2015.

Number of extreme rainy days - Yala Season

Both the R95p* and R99p* indices of Wellawaya showed significant positive trends in the number of extreme rainy days during the *Yala* season throughout the study period. Thevakaran *et al*., (2019) found no consistent statistically significant trends in heavy precipitation events during the two cropping seasons in Sri Lanka from 1961 to 2010. This study also detected a statistically significant upward trend in Jaffna, determined by the 99th percentile within the *Yala* season of the year. However, no significant trends were found in Jaffna for both indices (R95p*, R99p*) from our study using the most recent data for the *Yala* season.

Seasonal trend analysis - *Maha* **season**

Seasonal total precipitation

Maha is the major cropping season in Sri Lanka. During the study period the mean *Maha* seasonal precipitation in the dry zone was 1014±57 mm. The highest *Maha* seasonal precipitation was observed in Batticaloa (1441±88 mm) and the lowest in Bandagiriya (628±43 mm). The variability of the *Maha* seasonal precipitation was highest in Allai tank (inter-quartile value of 657 mm) and the lowest in Mannar (inter-quartile value of 188 mm). During the study period, the *Maha* seasonal precipitation increased significantly only in Wellawaya. Most locations in the dry zone received 9-16 (1st and 3rd Quartile) extremely heavy precipitation events (R25) in the *Maha* season. Beyond this range (greater than Q3) was considered an extreme M*aha* season. The R25 showed significant increasing trends in Wellawaya. Mean maximum *Maha* season RX1day and RX5days precipitation were in the range of 76-129 mm and 151-241 mm, respectively. The above absolute indices (RX1day and RX5days) showed positive trends in one (Anuradhapura) and two (Anuradhapura and Batticaloa) locations, respectively.

The percentile index R95p showed positive trends in Batticaloa and Wellawaya, and R99p in Wellawaya. The mean of the simple daily intensity index (SDII) for the dry zone was 19.1±1.0 mm/day. The highest mean SDII was recorded in Allai tank (24.9 mm/day) and the lowest in Hambanthota (6.1 mm/day). The SDII had significant positive trends at three locations (Anuradhapura, Okkampitiya and Giritale) and negative trends in Bandagiriya. Wellawaya, Trincomalee and Polonnaruwa showed significant positive trends for CWD (Figure 9) and Bandagiriya showed significant negative trends for CDD.
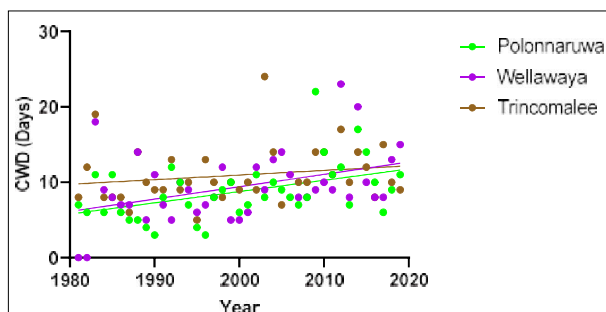

Figure 9: Locations with significant trends for CWD in the *Maha* season

In conclusion, precipitation in the *Maha* season did not change at many locations in the dry zone of Sri Lanka. However, Anuradhapura, Batticaloa, Okkampitiya, Wellawaya Trincomalee and Polonnaruwa had significant positive trends for flood related indices. This is in agreement with the findings of Chithranayana & Punyawardene (2008) that drought in dry zone is less likely to be experienced during the *Maha* season.

Number of extreme rainy days Maha **season**

A general increasing trend was detected in the number of extreme rainy days in the *Maha* season during the study period. Out of the 19 selected locations, 16 showed increasing trends for R95p* while 3 showed decreasing trends. The R99p* index showed increasing trends at 11 locations while 8 locations showed a decreasing trend. Most importantly the eastern coastal part of the country had a clear increasing pattern in the number of extreme rainy days; however, the trend was significant only in Batticaloa (R95*). All other trends were non-significant during the study period.

CONCLUSION

This study attempted to investigate annual and seasonal trends in the occurrence of extreme precipitation events in the dry zone of Sri Lanka. Trend analysis revealed significant positive trends in both annual and seasonal total precipitation within the dry zone throughout the study period. The rise in total precipitation was mainly driven by the number of rainy days. Moreover, an expanded area of the dry zone showed an increase in higher-intensity precipitation events, elevating the risk of floods. The probability of flood risk was greater in Anuradhapura, Mahailuppallama, Wellawaya and Batticaloa. Changes in atmospheric moisture resulting from warming oceans and intensified monsoonal circulation may contribute to an increased frequency of rain-bearing systems reaching the dry zone. Increases in atmospheric water vapor may lead to warming temperatures, which in turn fuels intense rainfall when condensation occurs.

Although some previous studies have concluded no significant changes in precipitation patterns within the dry zone, our study reveals significant changes in extreme precipitation indices, including both increasing and decreasing significant trends. Among the locations examined in this study, Wellawaya and Mannar showed significant deviations from the typical behavior of precipitation indices. Wellawaya demonstrated a significant positive trend in extreme precipitation,

whereas Mannar exhibited a significant occurrence of extreme drought indices. Overall, the majority of locations within the dry zone displayed a wetting trend during the study period.

Acknowledgment

REFERENCES

Ampitiyawatta, A. D., & Guo, S. (2009). Precipitation trends in the Kalu Ganga basin in Sri Lanka. *The Journal of Agricultural Sciences, 4*(1), 10–18. https://doi.org/10.4038/jas.v4i1.1641

Basnayake, B. R. S. B., Fernando, T. K., & Vithanage, J. C. (2002). Variation of air temperature and rainfall during Yala and Maha agricultural seasons. *Proceedings of the 58th Annual Session of Sri Lanka Association for the Advancement of Science (SLASS)*, Section E1 (p. 212).

Burn, D. H., & Elnur, M. A. H. (2002). Detection of hydrologic trends and variability. *Journal of Hydrology, 255*(1–4), 107–122. https://doi.org/10.1016/S0022-1694(01)00514-5

Caesar, J., Alexander, L. V., Trewin, B., Tse-Ring, K., Sorany, L., Vuniyayawa, V., ... Jayasinghearachchi, D. A. (2011). Changes in temperature and precipitation extremes over the Indo-Pacific region from 1971 to 2005. *International Journal of Climatology, 31*(6), 791–801. https://doi.org/10.1002/joc.2118

Chithranayana, R. D., & Punyawardena, B. V. R. (2008). Identification of drought-prone agro-ecological regions in Sri Lanka. *Journal of the National Science Foundation of Sri Lanka, 36*(2). https://doi.org/10.4038/jnsfsr.v36i2.143

Choi, G., Collins, D., Ren, G., Trewin, B., Baldi, M., Fukuda, Y., Lias, N. (2009). Changes in means and extreme events of temperature and precipitation in the Asia-Pacific Network region, 1955–2007. *International Journal of Climatology, 29*(13), 1906–1925. https://doi.org/10.1002/joc.1979

Collins, D. A., Della-Marta, P. M., Plummer, N., & Trewin, B. C. (2000). Trends in annual frequencies of extreme temperature events in Australia. *Australian Meteorological Magazine, 49*(4), 277–292.

De Costa, W. A. J. M. (2008). Climate change in Sri Lanka: Myth or reality? Evidence from long-term meteorological data. *Journal of the National Science Foundation of Sri Lanka, 36*. https://doi.org/10.4038/jnsfsr.v36i0.8048

Disaster Management Center. (2016). Annual report Sri Lanka, 26th May 2016. Ministry of Public Administration and Disaster Management.

Eriyagama, N., & Smakhtin, V. (2006). Observed and projected climate changes: A review. In A. Evans & K. Jinapala (Eds.), *National Conference on Water, Food Security and Climate Change in Sri Lanka*: 2, 1–10. International Water Management Institute.

Field, C. B., Barros, V., Stocker, T. F., & Dahe, Q. (2012). *Managing the risks of extreme events and disasters to advance climate change adaptation* (Special report of the Intergovernmental Panel on Climate Change). Cambridge University Press.

Griffiths, G. M., Chambers, L. E., Haylock, M. R., Manton, M. J., Nicholls, N., Baek, H. J., Zhai, P. (2005). Change in mean temperature as a predictor of extreme temperature change in the Asia-Pacific region. *International Journal of Climatology, 25*, 1301–1330. https://doi.org/10.1002/joc.1194

Griffiths, M. L., & Bradley, R. S. (2007). Variations of twentieth-century temperature and precipitation extreme indicators in the northeast United States. *Journal of Climate, 20*(21), 5401–5417. https://doi.org/10.1175/2007JCLI1594.1

Groisman, P. Y., Knight, R. W., Easterling, D. R., Karl, T. R., Hegerl, G. C., & Razuvaev, V. N. (2005). Trends in intense precipitation in the climate record. *Journal of Climate, 18*(9), 1326–1350. https://doi.org/10.1175/JCLI3339.1

Huo, R., Li, L., Chen, H., Xu, C. Y., Chen, J., & Guo, S. (2021). Extreme precipitation changes in Europe from the last millennium to the end of the twenty-first century. *Journal of Climate, 34*(2), 567–588. https://doi.org/10.1061/(ASCE)HE.1943-5584.0002122

Intergovernmental Panel on Climate Change (IPCC). (2014). AR5 synthesis report: *Climate change* 2014. https://www.ipcc.ch/report/ar5/syr/

Jayadas, A., & Ambujam, N. K. (2019). Observed trends in indices for daily rainfall extremes specific to the agriculture sector in Lower Vellar River sub-basin, India. *Journal of Earth System Science, 128*(3), 61. https://doi.org/10.1007/s12040-019-1074-0

Jayawardene, H. K. W. I., Sonnadara, D. U. J., & Jayewardene, D. R. (2005). Trends of rainfall in Sri Lanka over the last century. *Sri Lankan Journal of Physics, 6*. https://doi.org/10.4038/sljp.v6i0.197

Jayawardena, I. S. P., Darshika, D. T., & Herath, H. R. C. (2018). Recent trends in climate extreme indices over Sri Lanka. *American Journal of Climate Change, 7*(4), 586–599. https://doi.org/10.4236/ajcc.2018.74036

Karunathilaka, K. L. A. A., Dabare, H. K. V., & Nandalal, K. D. W. (2017). Changes in rainfall in Sri Lanka during 1966–2015. Engineer: *Journal of the Institution of Engineers, Sri Lanka, 50*(2). https://doi.org/10.4038/engineer.v50i2.7251

Keggenhoff, I., Elizbarashvili, M., Amiri-Farahani, A., & King, L. (2014). Trends in daily temperature and precipitation extremes over Georgia, 1971–2010. *Weather and Climate Extremes, 4*, 75–85. https://doi.org/10.1016/j.wace.2014.05.001

Kahya, E., & Kalayci, S. (2004). Trend analysis of streamflow in Turkey. *Journal of Hydrology, 289*(2), 128–144. https://doi.org/10.1016/j.jhydrol.2003.11.006

Kendall, M. G. (1975). Rank correlation methods. Charles Griffin.

Madduma, B. C. M., & Wickramagamage, P. (2004). Climate change and its impact on upper watershed of the hill country

of Sri Lanka. In S. Herath *et al.* (Eds.), Proceedings of the International Conference on Sustainable Water Resources Management in the Changing Environment of the Monsoon Region (pp. 17–19). Colombo, Sri Lanka.

Malmgren, B. A., Hulugalla, R., Hayashi, Y., & Mikami, T. (2003). Precipitation trends in Sri Lanka since the 1870s and relationships to El Niño–Southern Oscillation. *International Journal of Climatology, 23*(10), 1235–1252. https://doi.org/10.1002/joc.921

Mann, H. B. (1945). Non-parametric test against trend. *Econometrica, 13*, 245–259. https://doi.org/10.2307/1907187

Mekonen, A. A., & Berlie, A. B. (2020). Spatiotemporal variability and trends of rainfall and temperature in the Northeastern Highlands of Ethiopia. *Modeling Earth Systems and Environment, 6*, 285–300. https://doi.org/10.1016/j.sciaf.2023.e01635

Naveendrakumar, G., Vithanage, M., Kwon, H. H., Iqbal, M. C. M., Pathmarajah, S., & Obeysekera, J. (2018). Five decadal trends in averages and extremes of rainfall and temperature in Sri Lanka. Advances in Meteorology, 2018, Article 4217917. https://doi.org/10.1155/2018/4217917

Naveendrakumar, G., Vithanage, M., Kwon, H. H., Chandrasekara, S. S. K., Iqbal, M. C. M., Pathmarajah, S., Obeysekera, J. (2019). South Asian perspective on temperature and rainfall extremes: A review. *Atmospheric Research, 225,* 110–120. https://doi.org/10.1016/j.atmosres.2019.03.021

Pendergrass, A. G., Knutti, R., Lehner, F., Deser, C., & Sanderson, B. M. (2017). Precipitation variability increases in a warmer climate. *Scientific Reports, 7,* 17966. https://doi.org/10.1038/s41598-017-17966-y

Punyawardena, B. V. R., Bandara, T. M. J., Munasinghe, M. A. K., Jayaratne Banda, M., & Pushpakumara, S. M. V. (2003). Agro-ecological regions of Sri Lanka (Map). Natural Resources Management Center, Department of Agriculture.

Sanjeewani, R. M. S. S., & Manawadu, L. (2017). Dynamic trends of intensity of precipitation extremes in Sri Lanka.

Colombo Arts Journal of Social Sciences and Humanities, 2(1).

Senavirathna, A. G. C., Sumathipala, W. L., Dias, P., & Weerakoon, S. (1997). Annual and seasonal trend in precipitation in Sri Lanka. In Proceedings of the 53rd Annual Session of the Sri Lanka Association for the Advancement of Science (Part I, p. 322).

Sheikh, M. M., Manzoor, N., Ashraf, J., Adnan, M., Collins, D., Hameed, S., Islam, N. (2015). Trends in extreme daily rainfall and temperature indices over South Asia. International *Journal of Climatology, 35*, 1625–1637. https://doi.org/10.1002/joc.4081

Suppiah, R. (1986). Trends and periodicities in the seasonal rainfall fluctuations of Sri Lanka. *The Indian Geographical Journal, 61*(2), 1–14.

Suppiah, R. (1996). Spatial and temporal variations in the relationships between the Southern Oscillation phenomenon and the rainfall of Sri Lanka. *International Journal of Climatology, 16*(12), 1391–1407. https://doi.org/10.1002/(SICI)1097-0088(199612)16:12<1391::AID-JOC94>3.0.CO;2-X

Solomon, S., Qin, D., Manning, M., Chen, Z., Marquis, M., Averyt, K., Tignor, M., & Miller, H. (Eds.). (2007). Climate change 2007: The physical science basis (IPCC fourth assessment report). Cambridge University Press.

Westmacott, J. R., & Burn, D. H. (1997). Climate change effects on the hydrologic regime within the Churchill–Nelson River Basin. *Journal of Hydrology, 202*(1–4), 263–279. https://doi.org/10.1016/S0022-1694(97)00073-5

Wickramagamage, P. (1998). Large-scale deforestation for plantation agriculture in the hill country of Sri Lanka and its impacts. *Hydrological Processes, 12*(13–14), 2015–2028. https://doi.org/10.1002/(SICI)1099-1085(19981030)12:13/14<2015::AID-YP716>3.0.CO;2-

Zhang, X., Vincent, L. A., Hogg, W. D., & Niitsoo, A. (2000). Temperature and precipitation trends in Canada during the 20th century. *Atmosphere-Ocean, 38*(3), 395–429. https://doi.org/10.1080/07055900.2000.964

RESEARCH COMMUNICATION

Food Biochemistry

The first report on the *in-vitro* HDAC inhibitory potential of Sri Lankan traditional rice varieties

MK Ediriweera[1*] and JM Anandappa[2]
[1] *Department of Biochemistry & Molecular Biology, Faculty of Medicine, University of Colombo, Colombo, Sri Lanka.*
[2] *Department of Advanced Convergence Science and Technology, Jeju National University, South Korea.*

Abstract: The objective of this investigation is to study, for the first time, the histone deacetylase (HDAC) inhibitory potential of ethanol extracts obtained from selected traditional Sri Lankan rice varieties to highlight their biochemical significance. HDACs play a key role in epigenetic-mediated gene expression. Dysregulations in the expression and activity of HDACs are seen in a wide range of diseases. The ethanolic extracts of seven rice varieties demonstrated HDAC inhibitory effects in the order of *Madathawalu > Pachchaperumal > Hangimuttan > Maa-wee > Kalu Heenati > Kurulu Thuda > Suwandel*. Our findings support the use of Sri Lankan traditional rice varieties in epigenetic research. To fully elucidate the HDAC inhibitory effects of rice extracts, profiling the composition of secondary metabolites in active extracts is crucial. This preliminary investigation demonstrates that Sri Lankan rice varieties possess the potential to inhibit the activity of HDAC in vitro.

Keywords: Enzyme assays, Epigenetics, HDAC, histone-modifying enzymes, rice.

INTRODUCTION

Rice is the main staple food in Sri Lanka and other Asian countries (Samaranayake *et al*., 2022, Suresh *et al*., 2021). It is a rich source of carbohydrates, proteins, fatty acids, B vitamins and minerals such as magnesium, phosphorus and calcium (Verma & Srivastav, 2017). Studies have demonstrated that the consumption of rice is linked to a decreased risk of developing diseases and conditions such as diabetes mellitus, cancer, hypertension, cardiovascular disease, obesity and allergies (Rathna Priya *et al*., 2019). The Plant Genetics Resource Center in Gannoruwa Sri Lanka has a collection of over 2000 traditional rice varieties (Kariyawasam *et al*., 2016). Compared to improved rice varieties, the traditional Sri Lankan rice varieties are nutritionally significant and possess promising bioactivities (Goonathilaka *et al*., 2023). Research by Premakumara *et al*. (2013) found that traditional rice varieties like *Goda Heeneti*, *Masuran*, *Sudu Heeneti* and *Dik Wee* have anti-amylase and anti-glycation effects. Recent studies have characterized the fatty acid and amino acid compositions of selected traditional Sri Lankan rice varieties (Samaranayake *et al*., 2021; Liyanaarachchi *et al*., 2022;).

In epigenetics-mediated gene expression, HDACs play a key role in modifying chromatin structures. There are 18 different types of HDACs categorized into four major classes (I, II - IIa and IIb, III, and IV) identified in humans (Ediriweera *et al*., 2019). Dysregulation in the activity or expression of HDACs has been implicated in a wide range of human diseases (Ediriweera *et al*., 2019). HDAC inhibitors (such as benzamide derivatives, short and long-chain fatty acids, hydroxamic acid derivatives, and cyclic peptides) are a class of small-molecules that can reverse HDAC activity, leading to increased acetylation of histones and altered gene expression (Ediriweera *et al*., 2019).

* Corresponding author (meran@bmb.cmb.ac.lk; https://orcid.org/0000-0001-9393-9516)

Food items such as broccoli, garlic, eggs, turmeric and grapes have been identified to exert epigenetic effects (Ediriweera, 2023; Stefanska *et al*., 2012). There is growing recognition of the nutritional and functional value of traditional Sri Lankan rice varieties, particularly due to their unique biochemical profile. However, no studies have assessed their HDAC inhibitory effects. This research gap motivated us to investigate the HDAC inhibition potential of selected traditional rice varieties (Figure 1). We anticipate that our findings will provide substantial additional evidence to the existing body of knowledge regarding the biochemical and nutritional significance of traditional Sri Lankan rice varieties.

Figure 1:   Dehusked rice seeds of Sri Lankan traditional rice varieties used in this study

MATERIALS AND METHODS

Chemicals and kits

The chemicals and organic solvents used in this study were purchased from Sigma-Aldrich (St. Louis, MO, USA) unless otherwise specified. The total colorimetric HDAC assay kit was purchased from Abcam, Massachusetts, USA (ab1432).

Collection of rice samples

Seeds of the seven Sri Lankan traditional rice varieties (*Pachchaperumal, Kurulu Thuda, Madathawalu, Kalu Heenati, Suwandel, Maa-wee* and *Hangimuttan*) were purchased from a reputed vendor (*Sanstha Kulubadu* shops) and transferred to the laboratory. Rice seeds were oven dried and stored in sealed plastic bags. Each variety was given a specimen number: *Pachchaperumal* (TR-1), *Kurulu Thuda* (TR-2), *Madathawalu* (TR-3),

Kalu Heenati (TR-4), *Suwandel* (TR-5), *Maa-wee* (TR-6), and *Hangimuttan* (TR-7). The selection of these rice varieties was based on their availability and ease of access.

Extraction of rice seeds with ethanol

Dehusked rice seeds were ground and 3 g of flour was used for extraction with 6 mL of 99 % (v/v) ethanol at room temperature. The extracts were filtered using Whatman filter papers (grade 1) and speed-vacuumed. Stock solutions were prepared in ethanol by dissolving the dried extracts, corresponding to the seeds of each rice variety. The final concentration of each stock solution was 400 mg/mL.

HDAC inhibitory activity assay

The HDAC colorimetric activity assay was conducted according to the protocol supplied by the kit (ab1432). For the HDAC inhibitor assay, 1 mg/mL of each rice extract was used. The absorbance was recorded at 405 nm using a microplate reader (Bioevopeak, China, MPR-A9600/MPR-A9600T) and Trichostatin A was used as the positive control. The results were presented as the percentage of enzyme activity for each rice sample tested.

Statistical analysis

Experiments were carried out in triplicate and the results are expressed as the mean ± standard deviation (SD). GraphPad Prism version 5 (GraphPad Software, Inc., San Diego, CA, USA) software was used for statistical analysis. One-way analysis of variance (ANOVA) was used with Dunnett's post hoc test for group comparisons (control vs treated) to analyze HDAC assay results statistically. The control refers to a no-extract control containing only the enzyme. The treated groups received both the enzyme and the extract.

RESULTS AND DISCUSSION

As shown in Figure 2, the ethanol seed extracts of the seven traditional Sri Lankan rice varieties showed HDAC inhibitory potential *in vitro*. The ethanol extracts of all rice varieties exhibited HDAC inhibition at a concentration of 1 mg/mL in the following order: *Madathawalu > Pachchaperumal > Hangimuttan> Maa-wee >Kalu Heenati > Kurulu Thuda > Suwandel.* The results from this investigation highlight the HDAC inhibitory potential of selected traditional Sri Lankan

rice varieties, paving the way for further investigations into their epigenetic effects, including their impact on DNA methylation and various HDAC isoforms.
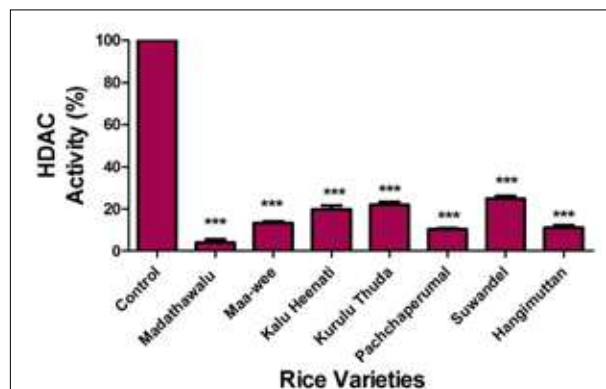

Figure 2: The histone deacetylase (HDAC) inhibitory potential of ethanol extracts from selected traditional rice varieties. The extracts showed HDAC inhibitory effects in the order of *Madathawalu > Pachchaperumal > Hangimuttan> Maa-wee >Kalu Heenati > Kurulu Thuda > Suwandel*. ***P<0.001 vs. control. The control refers to a no-extract control containing only the enzyme.

HDAC dysfunction is associated with various diseases (Ediriweera *et al*., 2019). This study demonstrates the HDAC inhibitory effects of specific traditional rice varieties found in Sri Lanka. Among the tested rice samples, the variety *Madathawalu* showed a high HDAC inhibitory potential (Figure 2). This investigation opens new opportunities for identifying and isolating specific secondary metabolites responsible for the observed HDAC inhibition. Benzamide derivatives, short and long-chain fatty acids, hydroxamic acid derivatives, and cyclic peptides have demonstrated encouraging clinical and pre-clinical outcomes as histone deacetylase inhibitors (HDACi) (Ediriweera *et al*. 2019). Rice contains a diverse range of phytochemicals such as phenolic compounds, flavonoids, terpenoids, steroids, fatty acids, amides, amino acids, and their derivatives, which may collectively contribute to its potent HDAC inhibitory activity (Pereira-Caro *et al*. 2013; Ravichanthiran *et al*. 2018). Fatty acids, in particular, have already been established as effective HDAC inhibitors (Ediriweera *et al*. 2019). In addition, secondary metabolites, such as ferulic acid, p-coumaric acid, and quercetin found in rice have been reported to possess HDAC inhibitory activity, further enhancing the overall HDAC inhibitory potential of these rice varieties (Apea-Bah *et al*., 2014; Uba *et al*., 2023).

It is worth noting that *Madathawalu* has been reported to contain higher levels of polyunsaturated fatty acids/saturated fatty acids (Samaranayake *et al*., 2022), which could significantly impact its HDAC inhibitory potential as fatty acids have been shown to inhibit HDACs (Ediriweera, 2023a; Ediriweera 2023b). However, the HDAC inhibitory potential is believed to be influenced by the synergistic activity of multiple phytochemicals present in the extract, including fatty acids.

CONCLUSION

The findings of this preliminary study demonstrate that traditional Sri Lankan rice varieties possess the ability to inhibit the activity of HDAC enzymes. Further experimental evidence is required to validate its classification as an 'epigenetic diet'. To fully elucidate the HDAC inhibitory effects of rice extracts, it is crucial to profile the composition of secondary metabolites in the active extracts.

Funding

Availability of the data and materials

The datasets used and/or analyzed during the current study are available from the corresponding author upon reasonable request.

REFERENCES

Apea-Bah F. B., Li X., & Beta T. (2021). Phenolic composition and antioxidant properties of cooked rice dyed with sorghum-leaf bio-colorants. *Foods*, *10*(9), 2058. doi.org/10.3390/foods10092058

Ediriweera M. K., Tennekoon K. H., & Samarakoon S. R. (2019). Emerging role of histone deacetylase inhibitors as anti-breast-cancer agents. *Drug discovery today*, *24*(3), 685-702. doi.org/10.1016/j.drudis.2019.02.003

Ediriweera M. K. (2023). Fatty acids as histone deacetylase inhibitors: old biochemistry tales in a new life sciences town. *Drug Discovery Today*, 103569. doi.org/10.1016/j.drudis.2023.103569

Ediriweera M. K. (2023). The Histone Deacetylase Inhibitory Potential of Chicken Egg Yolk Fat and Their Fatty Acid Composition. *Scientifica*, 2023. doi.org/10.1155/2023/6360487

Goonathilaka P. D. S. A., Abeysundara P. D. A., & Jayasinghe

M. A. (2023). Development of a value added rice milk by utilizing selected traditional and improved rice varieties in Sri Lanka. *Food Chemistry Advances*, *2*, 100319. doi.org/10.1016/j.focha.2023.100319

Kariyawasam T. I., Godakumbura P. I., Prashantha M. A. B., & Premakumara G. A. S. (2016). Proximate composition, calorie content and heavy metals (As, Cd, Pb) of selected Sri Lankan traditional rice (*Oryza sativa* L.) varieties. *Procedia food science*, *6*, 253-256. doi.org/10.1016/j.profoo.2016.02.036

Liyanaarachchi G. V. V., Mahanama K. R. R., Somasiri H. P. P. S., Punyasiri P. A. N., Ranatunga, M. A. B., Wijesena K. A. K., & Weerasinghe W. D. P. (2022). Impact of seasonal, geographical and varietal variations on amino acid profile of Sri Lankan rice varieties (*Oryza sativa* L.). *Journal of Food Composition and Analysis*, *109*, 104494. doi.org/10.1016/j.jfca.2022.104494

Pereira-Caro G., Watanabe S., Crozier A., Fujimura T., Yokota T., & Ashihara H. (2013). Phytochemical profile of a Japanese black–purple rice. *Food Chemistry*, *141*(3), 2821-2827. doi.org/10.1016/j.foodchem.2013.05.100

Premakumara G. A. S., Abeysekera W. K. S. M., Ratnasooriya W. D., Chandrasekharan N. V., & Bentota A. P. (2013). Antioxidant, anti-amylase and anti-glycation potential of brans of some Sri Lankan traditional and improved rice (Oryza sativa L.) varieties. *Journal of cereal science*, *58*(3), 451-456. doi.org/10.1016/j.jcs.2013.09.004

Rathna Priya T. S., Eliazer Nelson A. R. L., Ravichandran K., & Antony U. (2019). Nutritional and functional properties of coloured rice varieties of South India: a review. *Journal of Ethnic Foods*, *6*(1), 1-11. doi.org/10.1186/s42779-019-0017-3

Ravichanthiran K., Ma Z. F., Zhang H., Cao Y., Wang C. W., Muhammad S., ... & Pan B. (2018). Phytochemical profile of brown rice and its nutrigenomic implications. *Antioxidants*, *7*(6), 71. doi.org/10.3390/antiox7060071

Samaranayake M. D. W., Abeysekera W. K. S. M., Hewajulige I. G. N., Somasiri H. P. P. S., Mahanama K. R. R., Senanayake D. M. J. B., & Premakumara G. A. S. (2022). Fatty acid profiles of selected traditional and new improved rice varieties of Sri Lanka. *Journal of Food Composition and Analysis*, *112*, 104686. doi.org/10.1016/j.jfca.2022.104686

Stefanska B., Karlic H., Varga F., Fabianowska-Majewska K., & Haslberger A. G. (2012). Epigenetic mechanisms in anti-cancer actions of bioactive food components—the implications in cancer prevention. *British journal of pharmacology*, *167*(2), 279-297. doi.org/10.1111/j.1476-5381.2012.02002.x

Suresh K., Wilson C., Khanal U., Managi S., & Santhirakumar S. (2021). How productive are rice farmers in Sri Lanka? The impact of resource accessibility, seed sources and varietal diversification. *Heliyon*, *7*(6). doi.org/10.1016/j.heliyon.2021.e07398

Uba A. I., & Zengin G. (2023). Phenolic compounds as histone deacetylase inhibitors: binding propensity and interaction insights from molecular docking and dynamics simulations. *Amino Acids*, *55*(5), 579-593. doi.org/10.1007/s00726-023-03249-6

Verma D. K., & Srivastav P. P. (2017). Proximate composition, mineral content and fatty acids analyses of aromatic and non-aromatic Indian rice. *Rice Science*, *24*(1), 21-31. doi.org/10.1016/j.rsci.2016.05.005

JOURNAL OF THE NATIONAL SCIENCE FOUNDATION OF SRI LANKA

GUIDANCE TO CONTRIBUTORS

GENERAL INFORMATION

Scope

The Journal of the National Science Foundation of Sri Lanka publishes the results of research in all aspects of Science and Technology. It is open for publication of Research Articles, Reviews, Research Communications and Correspondence.

Use of AI Tools in Manuscript Preparation

To ensure transparency and uphold scholarly standards, authors must disclose any use of Artificial Intelligence (AI) tools during the research and manuscript preparation process.

- The use of AI tools (e.g., for language editing, summarization, data analysis, or figure generation) must be declared in the manuscript, typically before the Acknowledgements.
- AI tools must not be credited as authors. Human authors remain fully responsible for the integrity, accuracy, and originality of the submitted work.
- AI-generated content must be critically reviewed by the authors to ensure quality and ethical compliance, including data privacy and bias mitigation.
- AI must not be used to fabricate or manipulate original research data, unless it is part of the approved research methodology and explicitly described.
- Non-compliance with these guidelines may lead to rejection of the manuscript or post-publication corrective actions.

IT related and other non-empirical articles

The JNSF is a journal primarily devoted to natural sciences. It also considers for publication significant and novel contributions from formal sciences. Authors of emerging sub-disciplines of Computing and related areas such as Machine Learning, Artificial Intelligence and Data Sciences are requested to carefully adhere to the following guidelines when submitting manuscripts for this journal.

- Clear formulation of outcome-oriented **Research Objective/s** for targeted knowledge (sub)domain/s or (sub)discipline/s.
- Selection and comprehensive summarization of **appropriate Research Method/s** adopted to achieve the stated Research Objective/s.
- Reporting a sound **(Empirical) Evaluation** of the research finding/s thereby arguing reliability, validity, and generalizability of research claim/s.

Categories of manuscripts

Research Articles: Research Articles are papers that present complete descriptions of original research. Research Articles should include an Abstract, Keywords, Introduction, Methodology, Results and Discussion, Conclusion and Recommendations where relevant. References should be prepared according to the "Guidelines for the preparation of manuscripts". Maximum length of the article should be limited to 30 pages with a word count less than 10,000 including references, figures and tables. Any articles above this limit will be returned. Please refer author guidelines for further details (https://jnsfsl.sljol.info/about/submissions#author-guidelines)

Reviews: Reviews are critical presentations on selected topics of Science or Technology. They should be well focused and organized and avoid general "textbook" style. As reviews are intended to be critical presentations on selected topics, the author (or the principal author in a multi-author review) need to have had substantial leadership in research supported by a publication track record in the areas covered by the review. A person/s wishing to submit a Review Article should obtain prior approval from the Editorial Board by submitting a concise summary of the intended article, along with a list of the author's publications in the related area (jnsf@nsf.gov.lk). Maximum length of the article should be limited to 40 pages with a word count of 12,000 including references, figures and tables. Any articles beyond this limit will be returned.

Research Communications: Research Communications are intended to communicate important new findings in a specific area of limited scope that are worthy of rapid dissemination among the scientific community. Authors are required to provide a statement justifying the suitability of the submission for a Research Communication. The article should include an Abstract, Keywords, Introduction, Methodology, Results & Discussion, Conclusion and References. Maximum length of the article should be limited to 10 pages with a word count of 2,500 including references, figures and tables. Any articles beyond this limit will be returned.

Correspondence: Correspondence will be accepted regarding one or more articles in the preceding four issues of the Journal, as well as Letters to the Editor. Articles covering important scientific events or any other news of interest to scientists, reviews of books of scientific nature, articles presenting views on issues related to science and scientific activity will also be considered. Publication will be made at the discretion of the Editor-in-Chief. Maximum length of the article should be limited to 05 pages with a word count of 2,000 including references, figures and tables. Any articles beyond this limit will be returned.

SUBMISSION OF MANUSCRIPT

Authors submitting articles to the JNSF should first create an account in the Sri Lanka Journals Online System (https://jnsfsl.sljol.info/). All manuscripts should be in MS Word format and must be electronically submitted to the journal's online platform at https://jnsfsl.sljol.info/about/submissions. Submissions via email are not encouraged. Please make sure that no author information is mentioned in the article other than in the title page submitted. Names with initials, emails and affiliations of all the authors must be fed into the system during the online submission process.

Authors are required to provide their personal, validated ORCID ID (by obtaining an ORCID ID from https://orcid.org/) when submitting the manuscript. No change to the authors or order of authors will be accepted after the submission. All those who have made significant contributions should be listed as co-authors. The corresponding author should ensure that all contributing co-authors are included in the author list and have approved the final version of the paper and have agreed to its submission for publication.

All submissions should be in English. If the manuscript conforms to the guidelines specified, the date received will be the date that the manuscript was submitted to the online system.

Submissions are accepted for processing on the understanding that they will be reviewed and that they have not been submitted for publication elsewhere (including publication as a full paper or extended abstract as a part of Conference Proceedings).

Suggesting potential reviewers by authors
The authors are requested to suggest three names of referees when submitting their manuscript, in the Cover Letter space provided at the bottom of the page in the first stage of online submission. Referees should not be from the institution where the work was carried out and should not have been co-authors in previous publications. The address, institutional affiliation and e-mail of the suggested referees should be provided. Please note that the JNSF is not bound to select all or any of the suggested referees for sending the manuscript for reviewing

Authorship
All authors designated as authors should be eligible for authorship. Those who have made a substantial contribution to the concept or design of the work; or acquisition, analysis or interpretation of data are recognized as Authors.
The corresponding author should be prompt and ensure adherence to timelines when responding to requests, queries and recommendation of reviewers conveyed by or on behalf of the Editor-in Chief and Editorial Board.

Avoiding predatory references in manuscripts
Authors of the manuscripts should identify and not include predatory journal articles in the reference list.

If any paper that is cited is published in an Open Access journal, the authors are advised to ensure that the journal is listed in the DOAJ (Directory of Open Access Journals) or by the COPE (Committee on Publication Ethics). Please note that authors should check with DOAJ and COPE by themselves, and not assume that the statements given in the journal websites are accurate.

If the journal is included either in DOAJ or COPE, it can be presumed as legitimate. If not, authors need to review the journal website and published articles for characteristics of predatory journals. At the same time, authors can check whether the journal or relevant publisher is included in the directory of predatory journals and publishers.

If it is revealed that the manuscript is supported by articles published in predatory journals, it could be rejected by the JNSF at any stage of the publication process.

Supplementary materials
Any experimental data necessary to evaluate the claims made in the paper but not included in the paper should be provided as supplementary materials. Supplementary materials will be sent to the reviewers and published online with the manuscript if accepted. The supplementary materials should conform to Journal guidelines and should be uploaded as separate files. Authors should number Supplementary Tables and Figures as, for example, 'Supplementary Table S1'. Refer to each piece of supplementary material at the appropriate point(s) in the main article. Supplementary Materials may include description of the materials and methods, controls, or tabulated data presented in Tables or Figures, and programming codes.

Peer review
The manuscripts submitted to the JNSF will initially be screened by the Editorial Board and, if suitable, will be referred to at least two subject experts in the relevant field. The peer-review process of the JNSF is double-blind.
When revision of a manuscript has been requested, the revised manuscript should be submitted on or before the stated deadline. The authors' response to the comments of referees should be tabulated with the comment and response. The decision of the Editorial Board shall be final.
Accepted papers are subject to editing. The date of acceptance will be the date the Editorial Board accept the paper for publication.

Article processing fee
Article processing fee of US$ 250 will be levied for each manuscript in two stages, except when the corresponding author is affiliated with a Sri Lankan institution,
  • An initial processing fee of US$ 20 will be levied for each manuscript at the peer-review stage.
  • The remaining US$ 230 will be charged for accepted articles at the time of publication.

Payments can be made online via NSF Payment Portal (http://pg.nsf.gov.lk/)

Authors' declaration
The authors are required to accept the conditions indicated in the online author declaration statement.

Copyright
Articles in JNSF are published under the Creative Commons License CC-BY-ND. This license permits use, distribution and reproduction of articles for commercial and non-commercial purposes, provided that the original work is properly cited and is not changed in anyway. The copyright of the article is with the National Science Foundation of Sri Lanka. Therefore, authors are requested to check with institution's copyright and publication policy before submitting an article to the JNSF. Authors secure the right to reproduce any material that has already been published or copyrighted elsewhere. When an article is accepted for publication, the authors are required to submit the Transfer of Copyright document signed by all the authors.

Post-publication corrections
The Editorial Board reserves the right to take action on publishing an erratum or corrigendum. If serious errors are identified in a published article, the Journal may consider a retraction or publishing a correction.

STRUCTURE OF MANUSCRIPT

Manuscript
The manuscript should be free of errors and prepared in single column, using 1.5 line spaced text of Times New Roman 12 font leaving 1 inch margins. Pages should be numbered consecutively.

a. Style
The paper should be written clearly and concisely. The style of writing should conform to scholarly writing. Slang, jargon, unauthorized abbreviations, abbreviated phrasings should not be used. In general, the impersonal form should be used. Poor usage of language will result in rejection of the manuscript during initial screening.

b. Layout
Manuscripts other than review articles should be generally organized as follows: Title, Abstract, Keywords, Introduction, Methodology, Results and Discussion, Conclusion and Recommendations (where relevant), Acknowledgements and References. Pages should be arranged in the following order:

Title page (First page) should include the **title of manuscript**, and **complete author information** (name and affiliation). The author information **should not be mentioned anywhere in the manuscript** other than in the title page . If a major part of the research has been published as an abstract in conference proceedings, it should be cited as a footnote on the title page. Authors must also indicate the **general and specific research area** of the manuscript and a running title in the title page.

Title: Should accurately and concisely reflect the contents of the article.

Running title: Should be a shortened title (limited to a maximum of 50 characters) that could be printed at the top of every other page of the Journal article.

Abstract: Should be between 200 - 250 for research articles and 200 - 300 for reviews. It should not contain any references and should be able to stand on its own. It should outline objectives and methodology together with important results and conclusions.
Keywords: Include a maximum of six keywords, which may include the names of organisms (common or scientific), methods or other important words or phrases specific to the study.

Introduction: This should state the reasons for performing the work with a brief review of related research studies in the context of the work described in the paper. Objectives of the study should be clearly stated.

Materials and Methods: This section should give the details of how you conducted your study. New methods may be described in detail with an indication of their limitations. Established methods can be mentioned with appropriate references. Sufficient details should be included to allow direct repetition of the work by others. Where human subjects are involved, they should be referred to by numbers or fictitious names. A paper reporting the results of investigations on human subjects or on animals must include a statement to the effect that the relevant national or other administrative and ethical guidelines have been adhered to, and a copy of the ethical clearance certificate should be submitted. Methods of statistical analyses used should be mentioned where relevant.

Results and Discussion
Results: the results should be concisely and logically presented. Repetition of the same results in figures, tables or text should be avoided.
Discussion: data essential for the conclusions emerging from the study should be discussed. Long, rambling discussions should be avoided. The discussion should deal with the interpretation of results. It should logically relate new findings to earlier ones. Unqualified statements and conclusions not completely supported by data should be avoided.
Molecular sequence data, such as gene or rDNA sequences, genome sequences, metagenomic sequences etc. must be deposited in a public molecular sequence repository, such as GenBank, that is part of the International Nucleotide Sequence Database Collaboration (INSDC). The accession numbers obtained must be cited in the text, Table or on Figures of phylogenetic trees of the manuscript.

Conclusion: The conclusion should be brief, highlight the outcomes of the study and should be aligned with the objectives of the study. It should not contain references.

Competing Interest statement: The authors should include a statement on conflict of interest disclosing any financial or other substantive conflicts of interest that may influence the results or interpretation of the research in the space provided in the online article submission form. All sources of financial support for the project should also be disclosed.

Acknowledgement: Should be brief and made for specific scientific, financial and technical assistance only. If a significant part of the research was performed in an institution other than the authors' affiliations should be acknowledged. All those who have made substantial contribution to the research but do not qualify to be authors should be acknowledged.

References :
The JNSF uses APA (7th Edition) reference style
All research work of other authors, when used or referred to or cited, should be correctly acknowledged in the text and in the References.
All the references in the text should be in the list and vice versa

Citing references in the text:
- References to the literature must be indicated in the text and tables as per the Author-Year System, by the author's last name and year, in parenthesis (i.e. Able, 1997) or (Able & Thompson, 1998).
- Citation to work by more than two authors should be abbreviated with the use of et al. (i.e. Able *et al*., 1997).
- Multiple publications by the same first author in the same year should be coded by letters, (i.e. Thompson, 1991a, 1991b,1992,1993).
- Multiple citations of different authors should be made in chronological order and separated by a semicolon, (i.e. Zimmerman *et al*., 1986; Able *et al*., 1997).

Citing references in the List of references:
- The list of References should be arranged in alphabetical order based on the last name of the first author.
- In APA 7th ed., **up to 20 authors** should be included in a reference list entry. Write out the last name and first initial(s) for each contributor.

Example for 2–20 authors:

Wright, A., Komal, G., Siddharth, D., Boyd, G., Cayson, N., Beverley, K., Travers, K., Begum, A., Redmond, M., Mills, M., Cherry, D., Finley, B., Fox, M., Ferry, F., Almond, B., Howell, E., Gould, T., Berger, B., Bostock, T., & Fountain, A. (2020). Styling royalty. London Bridge Press.

- For references with more than 20 authors, after listing the 19th author replace any additional author names with an ellipsis (…) followed by the final listed author's last name and first initial(s).

Example for 21+ authors:

Kalnay, E., Kanamitsu, M., Kistler, R., Collins, W., Deaven, D., Gandin, L., Iredell, M., Saha, S., White, G., Woolen, J., Zhu, Y., Chelliah, M., Ebisuzaki, W., Higgins, W., Janowiak, J., Mo, K.C., Ropelewski, C., Wang, J., Leetmaa, A., … Joseph, D. (1996). The NCEP/NCAR 40-year reanalysis project. Bulletin of the American Meteorological Society, 77(3), 437-471. http://doi.org/fg6rf9

- All the initials of the author must be given after the last name and the year of publication should follow in parentheses.
- This should be followed by the full title of the referred publication.
- When journal articles are listed, the journal name should be given in full and in italics and followed by the volume number, issue number in parentheses and then the inclusive pages.
- Where there are several publications by the same author(s) and published in the same year they should be differentiated by adding a lower-case letter after the year.

Example

Clarke, P. N., & Fawcett, J. (2014a). Life as a mentor. *Nursing Science Quarterly*, 27(3), 213-215. https://doi.org/10.1177/0894318414534492

Clarke, P. N., & Fawcett, J. (2014b). Life as a nurse researcher. *Nursing Science Quarterly*, 27(1), 37-41. https://doi.org/10.1177/0894318413509708

- Digital object identifiers (DOIs) should be included for all references where available.

Details about this reference style can be obtained from below links
- https://apastyle.apa.org/style-grammar-guidelines/references
- https://apastyle.apa.org/style-grammar-guidelines/references/examples
- https://libguides.jcu.edu.au/apa

Abbreviations and Symbols: Unless common, these should be defined when first used, and **not included in the abstract**. The SI System of units should be used wherever possible. lf measurements were made in units other than SI, the data should be reported in the same units followed by SI units in brackets, e.g. 5290 ft (1610 m).

Formulae and Equations: Equations should be typewritten and quadruple spaced. They should be started on the left margin and the number placed in parentheses to the right of the equation.

Nomenclature: Scientific names of plants and animals should be printed in italics. In the first citation, genus, species and authority must be given. e.g. *Borassus flabellifer* Linn. In latter citations, the generic name may be abbreviated, for example, *B. flabellifer* L.

Tables and figures: Tables and Figures should be clear and intelligible and kept to a minimum, and should not repeat data available elsewhere in the paper. Any reproduction of illustrations, tabulations, pictures etc. in the manuscript should be acknowledged.

Tables: Tables should be numbered consecutively with Arabic numerals and placed at the appropriate position in the manuscript. If a Table must be continued, a second sheet should be used and all the headings repeated. The number of columns or rows in each Table should be minimized. Each Table should have a title, which makes its general meaning clear, without reference to the text. All Table columns should have explanatory headings. Units of measurement, if any, should be indicated in parentheses in the heading of each column. Vertical lines should not be used and horizontal lines should be used only in the heading and at the bottom of the table. Footnotes to Tables should be placed directly below the Table and should be indicated by superscript lower case italic letters ([a], [b], [c], etc.).

Figures: All illustrations are considered as figures, and each graph, drawing or photograph should be numbered consecutively with Arabic numerals and placed at the appropriate position in the manuscript. Any lettering to appear on the illustrations should be of a suitable size for reproduction and uniform lettering should be used in all the Figures of the manuscript. Scanned figures or photographs should be of high quality (**300 dpi**), to fit the proportions of the printed page (12 × 17 cm). Each figure should carry a legend so that the general meaning of the figure can be understood without reference to the text. Where magnifications are used, they should be stated.

Units of measurement

Length: km, m, mm, μm, nm
Area: ha, km^2, m^2
Capacity: kL, L, mL, μL
Volume: km^3, m^3, cm^3
Mass: t, kg, g, mg, μg

Time: year(s), month(s), week(s), day(s), hour(s), minute(s), second(s)
Concentration: M, mM, N, %, g/L, mg/L, ppm
Temperature: °C, K
Gravity: x g

Molecular weight: mol wt
Others: Radio-isotopes: 32P
Radiation dose: Bq
Oxidation-reduction potential: rH
Hydrogen ion concentration: pH